IMPROVED STEM CELL RETENTION AND MECHANICAL STABILITY IN A CHITOSAN-GELATIN HYDROGEL

BY

CHRISTIAN JOSE TORMOS

Bachelor of Science in Chemical Engineering
Iowa State University
Ames, Iowa
2012

Submitted to the Faculty of the
Graduate College of the
Oklahoma State University
In partial fulfillment of
The requirements for
The degree of
DOCTOR OF PHILOSPHY
July, 2016

IMPROVED STEM CELL RETENTION AND MECHANICAL STABILITY IN A CHITOSAN-GELATIN HYDROGEL

Dissertation Approved:

Dr. Sundar Madihally

Dissertation Adviser

Dr. Heather Fahlenkamp

Dr. AJ Johannes

Dr. Yolanda Vasquez

Dr. Veronique Lacombe

ACKNOWLEDGEMENTS

It is my pleasure to thank each and every one who helped make this dissertation possible. I would like to express my deepest and sincerest gratitude to my family, especially my wife and my daughter, for their love and support throughout my life and the course of this dissertation. I would like to thank my advisor Dr. Sundar Madihally for his guidance and support throughout my research, studies, and time at Oklahoma State University. His passion and enthusiasm for research has been a great motivator, he has been a great mentor and role-model. I really appreciate his time and effort in reviewing and providing input to not only improve this dissertation but countless other manuscripts and abstracts.

Additionally, I would like to extend my thanks to my colleagues Jimmy Walker, Abdu Kalf, Carrie German, Kevin Roehm, and Carol Abraham for their direct and indirect help with this research. Thanks to my committee members, Dr. AJ Johannes, Dr. Heather Fahlenkamp, Dr. Yolanda Vasquez, and Dr. Veronique Lacombe for their guidance, assistance, and feedback. I would like to thank my friends for the wonderful graduate school experience. I would like to thank Kar-Ming Fung and Louisa J. Williams from the Stephenson Cancer Center at the University of Oklahoma Health Sciences Center for their help with the preparation of cryosectioned samples. Lastly, I would like to thank Oklahoma State University, the Ronald E. McNair Program, and the School of Chemical Engineering for providing a great learning opportunity.

Name: CHRISTIAN JOSE TORMOS

Date of Degree: JULY, 2016

Title of Study: IMPROVED STEM CELL RETENTION AND MECHANICAL STABILITY IN A CHITOSAN-GELATIN HYDROGEL

Major Field: CHEMICAL ENGINEERING

Abstract:

Due to the heart's poor regenerative ability, new treatments need to be developed in order to repair damaged cardiac tissue after cardiac arrest. A common approach is to deliver adult stem cells combined with injectable hydrogels using minimally invasive surgery to the affected area. However, these studies have shown significant attrition of injected cells, attributed to hydrogel instability, nutrient and oxygen deficiency, and poor mechanical strength of the hydrogel. In addition, the injectable hydrogel must be able to support stem cell differentiation and long term survival of stem cells. An injectable chitosan-gelatin hydrogel has been developed to combat these challenges. To increase stability, gelatin was crosslinked with transglutaminase, an enzyme commonly used as meat glue in the food industry. To address the nutrient and oxygen deficiency, growth medium (nutrient source during *in vitro* culture) and oxygen releasing molecules have been added to the hydrogel. The mechanical strength of the hydrogel was manipulated to match cardiac tissue by varying the concentrations of the different polymers present in the hydrogel. This injectable hydrogel was seeded with human adipocyte stem cells and evaluated for viability of these cells. This hydrogel was able to retain cells inside the hydrogel without killing a significant population of the embedded cells for 21 days. Differentiation of human adipocyte stem cells did not occur for cells embedded in the hydrogel. Chemical stimulants and mechanical properties were not enough to induce differentiation. However, if this hydrogel were to be used for *in vivo* studies, the cardiac tissue mechanical and electrical cues may induce differentiation.

TABLE OF CONTENTS

LIST OF TABLES

LIST OF FIGURES

CHAPTER I

INTRODUCTION

Americans are newly diagnosed with a heart attack every 34 seconds (Members et al., 2012). A heart attack, myocardial infarction (MI), occurs when the blood flow to the heart is blocked. This causes the cardiac cells to undergo a series of events that end in cell death due to the hypoxic environment (Konstantinidis et al., 2012). The remaining viable cells enlarge to make up for the work of the dead cells (Cleutjens et al., 1999, Konstantinidis et al., 2012). When cells enlarge, they experience more stress and increases the risk of the patient experiencing another heart attack. The life expectancy of a heart attack patient is 5-10 years. If the patient arrives at the hospital and doctors diagnose the patient with a heart attack, they will administer different treatments to restore blood flow and prevent any further damage (Page, 1999). After the heart attack occurs, the "treatments" urge the patient to live a healthier life style by losing weight, eating a more nutritional diet, exercising regularly, eliminating alcohol and tobacco consumption; but do nothing to repair the actual damage in the cardiac tissue (Page, 1999). Researchers are working on developing cell based therapies to repair the damage using stem cells (Behfar et al., 2014, Campbell and Suzuki, 2012, Garbern and Lee, 2013, Segers and Lee, 2008). However, stem cells

alone cannot repair the tissue. Studies have shown that an injection of stem cells to the damaged region is not successful because the majority of the implanted cells (~90%) die within 1 week (Behfar et al., 2014, Menasche, 2011a, Segers and Lee, 2008). Cell death is hypothesized to be caused by lack of distribution, nutrients, and oxygen. With this knowledge, researchers are using biomaterials to deliver the stem cells to the damaged region in order to improve the chances of repairing the cardiac tissue. However, even with the addition of biomaterials, improvement in cell survival upon delivery was minimal (Hong et al., 2007). While the addition of biomaterials resolved the issue of distribution, it brought upon new obstacles. Obstacles that are associated with the addition of biomaterials include: stability of material, immune reaction by the host, and mechanical property compatibility. The focus of this dissertation was to develop a cell based therapy that addresses the issues of lack of nutrients, lack of oxygen, material stability, mechanical property compatibility, and immune reaction by the host. To address these challenges, the project was divided into three aims.

1.1 Aim 1: Develop hydrogel that can withstand wound healing environment and improve cell survival

The purpose of this aim was to develop a hydrogel with mechanical properties similar to cardiac tissue and that is mechanically stable when exposed to a wound healing environment. To simulate a wound healing environment, hFF-1 were cultured for seven days in a chitosan-gelatin hydrogel. Previously, hFF-1 have been shown to release a significant amount of MMP-2 and MMP-9 when cultured on gelatin scaffolds. In order to address the challenges presented above, additional components such as growth medium, transglutaminase, and PLGA nanoparticles encapsulating doxycycline hyclate were

added to the hydrogel and their effects on mechanical properties and cell retention and viability were assessed. The formulation that most resemble cardiac tissue, in terms of compressive modulus, was found to have a compressive modulus of 41.65 ± 4.07 kPa. Cell viability experiments showed a 2.5 times improvement in cell retention and viability in DOX with TG cross-linked CG hydrogels after seven days. Stability of the hydrogel improved by adding TG and doxycycline encapsulated in PLGA. Levels of MMP-2 and MMP-9 activity decreased after exposure to hydrogels containing DOX nanoparticles.

1.2 Aim 2: Improve the survival of hASCs after application and evaluate 3D differentiation.

For regeneration of functional cardiac patch, cardiomyocytes are needed to repair the cardiac tissue. Using autologous sources would help minimize complications related to immunotherapy related to allogeneic cells. Using adult stem cells harvested from specific patients would help in this regard. Liposuction is used to remove excess adipose tissue which used to be discarded until identification of useful hASCs using collagenase and other chemicals (Zuk et al., 2001). The hASCs extracted from the adipose tissue should differentiate into cardiomyocytes. There are many factors that affect the differentiation process (Hwang et al., 2008). Current methodologies differentiate hASCs in a 2-D environment using 5-azacytidine and laminin (Chang et al., 2012, van Dijk et al., 2008). To test whether differentiation can occur in a 3D environment, cardiomyogenic growth medium and laminin were incorporated into the hydrogel and hASCs differentiation was tested. First, differentiation of hASCs was assessed in 2-D cultures using i) phorbolmyristate acetate (PMA), a protein kinase C activator for in nine days (Chang et al., 2012), and ii) a combination of 5-azacytidine and laminin for 21 days.

Expression of genetic markers present in hASCs and not in cardiomyocytes (CD105 and CD144) after hASCs were assessed either by flow cytometry, immunohistochemistry, or qPCR. This suggests that differentiation was successful in 2-D environment containing 5-azacytidine and laminin. Next, hASCs were cultured in the hydrogel containing 5-azacytidine and laminin for up to three weeks and viability and retention was assessed similar to Aim 1. Addition of 5-azacytidine and laminin to the hydrogel decreased the viability to nearly 70% after 21 days. This could be attributed to the long term exposure to 5-azacytidine. In any case, the presence of hASCs markers were confirmed by immunohistochemistry at the end of 21 days, suggesting differentiation was not successful in 3-D environment. In summary, this hydrogel is able to support stem cell culture for three weeks but does not induce differentiation of adipocyte stem cells into cardiomyocytes.

1.3 Aim 3: Addition of oxygen releasing component in hydrogel formulation and investigate hydrogel's differentiation ability and mechanical properties.

When hydrogels along with cells are injected into the cardiac tissue, they are in a hypoxic environment. In order to address oxygen requirement and improve viability, oxygen releasing molecule, calcium peroxide (CaO_2), was added during the hydrogel preparation. However, CaO_2 is alkaline and alters the pH of the solution. Since the injectable hydrogel preparation is pH sensitive, hydrogel formulation needs to be adjusted in order to maintain the characteristics of temperature sensitive gelation. In this aim, first I optimized the hydrogel preparation methodology with the inclusion of CaO_2. Measured mechanical properties (compressive, tensile, cyclical and relaxation) showed significant improvement compared to hydrogels without CaO_2. However, release of oxygen

appeared to be quicker relative to the culture duration of stem cells. Also, amount of CaO_2 that could be added to the hydrogel is limited by i) solubility and ii) pH change. In order to increase the amount of CaO_2 to prolong the release of oxygen, different methods of encapsulation were tested. Encapsulation of calcium peroxide was unsuccessful, but addition of CaO_2 despite improved the mechanical properties. Viability studies showed that addition of CaO_2 resulted in a decrease in cell viability. Differentiation studies showed the presence of hASCs markers were confirmed by immunohistochemistry at the end of 21 days, suggesting differentiation was not successful in 3-D environment. In summary, this hydrogel is able to support stem cell culture for three weeks but does not induce differentiation of adipocyte stem cells into cardiomyocytes.

1.4 Summary

This investigation is focused on developing an injectable hydrogel for use in conjunction with hASCs to repair large cardiac necrotic regions. Several obstacles were addressed in order to increase the probability of success when this treatment is used *in vivo*. The hydrogel formulation was optimized to mimic the mechanical properties of cardiac tissue. To avoid immune rejection by the host, I propose using the patient's own adipocyte stem cells. According to Iacobellis, obese people are more likely to experience a heart attack and to survive the attack (Iacobellis, 2009). Therefore, there is a high probability that the patient receiving this treatment will benefit from liposuction surgery and the waste adipose tissue can be used to obtain adipocyte stem cells that will not be rejected by the patient's immune system. If treatment is successful, the quality of life may improve for patients with existing cardiac necrotic regions.

CHAPTER II

BACKGROUND

2.1 The biology of the heart and heart attack

Cardiac tissue regeneration has been investigated for more than 150 years (Laflamme and Murry, 2011), because the heart is responsible for the transportation of blood throughout the body; without proper function death is imminent. Heart disease is the number one cause of death in the world, approximately 17.3 million deaths per year with 600,000 deaths in the United States alone (Mendis et al., 2011, Kochanek et al., 2011). Latinos and Hispanics, unfortunately, have even higher risks compared to the average American because of high blood pressure, obesity and diabetes (Go et al., 2013). According to the American Heart Association (AHA), in 2008 coronary heart disease accounted for 50% of heart disease related deaths and the cost of coronary heart disease (including hospital discharge, medications, operations, etc.) was estimated to be $190.3 billion (Roger et al., 2012). In 2010, it is estimated that 7.6 million people experienced a heart attack, and 125,000 resulted in death (Go et al., 2013). There are many heart-related diseases that cause damage to the cardiac tissue. For example, myocardial infarction (MI or commonly referred as heart attack) can cause necrosis to a large number of cardiac myocytes (heart cells) (Konstantinidis et al., 2012). Myocardial infarction occurs when the blood flow from the

coronary arteries to the heart is obstructed which halts the continuous supply of oxygen to the heart tissue resulting in the death of cardiomyocytes within two minutes of being deprived of oxygen (Randall and Romaine, 2005). Hypertension (high blood pressure) can cause cardiac tissue damage over the course of many years asymptomatically (Mendis et al., 2011). Aging causes cardiac tissue damage via deterioration; nearly 1 gram of cardiac tissue is lost every year even in the absence of heart disease (Olivetti et al., 1991). Upon diagnosis for increased risk of a MI, treatments such as oxygen therapy and ingestion of blood thinners, nitroglycerin, and chest pain relievers are administered. Once the diagnosis of a MI is confirmed, treating the formed plaque is considered based on percentage of blockage (Page, 1999). The most common treatments are "clot-busting" medicines and percutaneous coronary intervention (PCI) (Page, 1999). The patient can reduce the risk of recurrence of heart attacks by following a healthy diet, maintaining a healthy weight and exercise regimen, and curbing habits such as cigarette smoking and drinking alcohol (Page, 1999, Roger et al., 2012, Randall and Romaine, 2005, Mendis et al., 2011, Go et al., 2013). These treatments are preventive measures rather than repairing the damaged region of the heart tissue.

Many parts of the human body including skin and bone can regenerate after a small injury or fracture. Whether cardiac tissue regenerates after major cardiac tissue damage is still a controversial topic, despite some evidence of remodeling activity (Cleutjens et al., 1999). In general, the remodeling process of cardiac tissue is described to occur in four phases (Cleutjens et al., 1999). Phase 1 is the death of cardiac myocytes (also referred as cardiomyocytes) either due to necrosis (characterized by swelling of the cells) or apoptosis (characterized by shrinkage of cells) (Cleutjens et al., 1999). A majority of

apoptotic cells cannot be phagocytized by neighboring cells and remain in the heart tissue, which triggers phase 2, acute inflammation (Cleutjens et al., 1999). This inflammatory response causes migration of granulocytes which are responsible for removing the dead cells from the damaged area. After successful removal of the dead cells, new extracellular matrix proteins are being deposited in the damaged area. Phase 3 is granulation tissue formation, which increases the tensile strength of the damaged area and prevents the cardiac tissue from rupturing (Cleutjens et al., 1999). In addition, the granulation tissue undergoes angiogenesis, which is essential for wound healing. A mature granulation tissue (2-3 weeks old) consists of partly cross-linked collagens, macrophages, blood vessels, and myofibroblasts. Phase 4 is scar formation. At this point the majority of cells, except myofibroblasts, undergo apoptosis and the collagen fibers are fully cross-linked (Cleutjens et al., 1999).

In summary, these remodeling stages do not recruit a large number of new cells, instead they increase the size of the existing cells and increase the amount of stress the individual cell experiences. This puts the patient at a greater risk of developing another heart attack and thus not a very effective and reliable method of injury repair. Many scientists have been working on repairing the damage with additional cells so that the amount of stress on individual cells is reduced and thus lowers the risk of having another heart attack.

2.2 Repairing the damage with cells

Terminally differentiated cells (such as cardiac myocytes) are needed to repair and repopulate a damaged area. Cardiac cells are difficult to harvest and grow in vast quantities. Therefore, due to a limited quantity of terminally differentiated cardiac myocytes, an alternative cell source and type needs to be used. Stem cells are an

intriguing alternative because theoretically, stem cells can differentiate into cardiac cells (Bollini et al., 2011, Young et al., 2011). Stem cells are precursor cells that give rise to different cell lines. The process of which a stem cell converts into a different cell type is called differentiation. In addition to different differentiation capabilities, there are different types of stem cells (Chong et al., 2014, Keefer and Desai, 2011, Hwang et al., 2008, Heng et al., 2004, Dawson et al., 2008). Embryonic stem cells are found in the embryo and are known to be pluripotent, meaning they can differentiate into any type of cell. However, to harvest embryonic stem cells one must destroy the blastocyst, which raises ethical issues on when does life start. Due to ethical issues, many researchers have avoided using human embryonic stem cells.

On the other hand, mesenchymal stem cells (MSCs) have societal acceptance but are not pluripotent and proliferate less than embryonic stem cells (Li et al., 2007, Zuk et al., 2001, Richardson et al., 2008, Lindroos et al., 2011, Elnakish et al., 2012). They can differentiate into lineage-related and also some cell types from different lineage. Obtaining a large number of adult stem cells is difficult (Segers and Lee, 2008), but they can be found in adult tissues, including bone marrow, umbilical cord, and adipose (fat) tissue (Bosi et al., 2005, Menasche, 2011a, Segers and Lee, 2008, Lindroos et al., 2011). Availability of MSCs is abundant due to the prominence of bone marrow registries, but there is concern about immune response and rejection of transplanted cells. Autologous stem cells harvested from the patient being treated can minimize the need for immunosuppression therapies post-implantation. Currently, most FDA approved stem cell based therapies use MSCs derived from the bone marrow (Bosi et al., 2005, Menasche, 2011a, Segers and Lee, 2008, Lindroos et al., 2011). Bone marrow stem cell

isolation is painful and harvest number is low (Kern et al., 2006). As previously mentioned, another source for stem cells is fat tissue (Kern et al., 2006, Young et al., 2011, Zuk et al., 2001, van Dijk et al., 2008, Lindroos et al., 2011, Choi et al., 2010). Due to the advances of plastic surgery, specifically liposuction, harvesting adipocyte stem cells is simple and quick. Adipose tissue derived stem cells were shown to differentiate into various cell types including heart cells (Zuk et al., 2001). Recently, a small population of stem cells residing the heart has been discovered. These stem cells have been called cardiac stem cells (CSCs) (Bearzi et al., 2007). These discovery is still recent and protocols regarding isolation are still being developed. Therefore, for this study, I used human adipocyte stem cells that are commercially available.

Cardiomyogenesis is the process where a stem cell differentiates into a cardiomyocyte. Cardiomyocytes can be differentiated from stem cells and have been explored to regenerate cardiac tissue (Emmert et al., 2014). Differentiation can be induced by a number of conditions including, mechanical stimulus, electrical stimulus, or chemical stimulus (Happe and Engler, 2016, Bollini et al., 2011, Menasche, 2011a, Hidalgo-Bastida et al., 2007, Leor et al., 2005, Guo et al., 2006, Keefer and Desai, 2011, Hwang et al., 2008, Heng et al., 2004, Dawson et al., 2008, Choi et al., 2010). Recently, cardiomyogenesis in hASCs has been investigated with many different techniques and different results. The best technique is the one that produces cells with cardiac receptors and produces beating heart cells. One of the most popular techniques is to culture hASCs with rat neonatal cardiomyocytes (Choi et al., 2010). Within 1 week, hASCs were beating and expressing high levels of cardiac receptors (Choi et al., 2010). The main problem with this technique is the use of animal cells in combination with human cells

and is therefore limited only to a non-clinical setting. Another technique to induced cardiomyogenesis is to expose the cells to 5-azacytidine (AZA) with and without laminin. AZA has successfully induce cardiomyogenesis in both animal and human adipocyte stem cells. However, beating heart cells have not been observed (Choi et al., 2010, Wan Safwani et al., 2012). A research group decided to culture hASCs on top laminin and stimulate them with AZA (van Dijk et al., 2008). While morphological changes were observed, no beating cells were found. Another stimulant that has been investigated for cardiomyogenesis is phorbolmyristate acetate (PMA), a protein kinase C activator (Chang et al., 2012). This research group reported the presence of mRNA that indicated cells underwent cardiomyogenesis in 6 days. However, no results have been published using the mentioned techniques and there is no mention of morphological changes and beating cells. There are many other techniques that claim to induce cardiomyogenesis but they all have disadvantages. I decided to focus on 5-azacytidine due to multiple sources confirming differentiation of hASCs into cardiomyocytes by expression of cardiac markers.

With the increased availability of various cell sources, the focus has shifted towards methods to deliver those cells to the needed area in the heart. Cells that are transplanted into the heart have to integrate with the native tissues and align with the preexisting tissue pattern. In addition to alignment of cells, cell survival and distribution is a major drawback of delivering stem cells alone to the affected area. This is due to the delivery mechanism by which the cells are delivered. Cells are delivered by a syringe, and therefore millions of cells are clustered into a small space. This means that cells will be competing with each other for nutrients and without proper nutrients 90% of cells

transplanted into the area are dead within a week (Behfar et al., 2014, Menasche, 2011a, Segers and Lee, 2008). Since delivering a pellet of cells does not ensure the alignment, survival, and distribution of cells, biomaterials with appropriate properties are needed, which is the focus of the next section.

2.3 Scaffold based tissue engineering

There are four major approaches to delivering cells to the heart: intracoronary, intramyocardial, intravenous, and epicardial attachment (Campbell and Suzuki, 2012). Intracoronary injection induces little inflammatory response but does not allow for cell attachment. Intramyocardial injection allows for adult stem cell delivery to a specific area, but in the process causes inflammation, mechanical injury, and cell clusters. Intravenous injection is the most common route for delivery but location specificity is a concern along with cell attachment. Epicardial attachment of biomaterials allows for better cell attachment than other routes, but limited cell migration is an issue. There is no clear preferred route since each has its own advantages and disadvantages.

Biodegradable scaffolds are used to provide a temporary substrate to seeded cells and support tissue regeneration either *in situ* or *in vitro* (Emmert et al., 2014). Seeded cells adhere and proliferate, migrate, and differentiate (Ratner, 2004). The scaffold transiently degrades, leaving only the necessary healthy tissue. There are two types of scaffolds: naturally occurring and manmade scaffolds, each with advantages and disadvantages. Naturally occurring scaffolds are obtained by decellurizing tissue from human or animal sources with the goal of repopulating them with stem cells (Moroni and Mirabella, 2014). Components of the extracellular matrices are generally conserved among species and are relatively non-immunogenic even by xenogeneic recipients. Therefore, if cellular

components are eliminated from tissues, rejection reactions can be prevented. The main advantage of using decellularized tissue is that it structurally resembles the native tissue and therefore supports regeneration into functional similar tissue. Decellularized scaffolds derived from porcine heart valves, human pericardium, and whole rat hearts have been used for cardiac tissue engineering (Vashi et al., 2015). While this approach has been successful in repairing smaller and less complicated tissues, like the trachea and bladder, it is yet to be successful on larger and more complicated cardiac tissues. Using decellularized tissue is constrained by obtaining reliable, reproducible products in large-scale preparations and is subject to the concerns of heterogeneity in the structural features (Raghavan et al., 2005).

An alternative option is forming manmade matrices with properties similar to the structure of a tissue to be replaced. Manmade scaffolds can be further divided into two categories, preformed scaffolds and hydrogels. Manufacturing preformed porous scaffolds using pure components allows formation of matrices with required features in addition to large scale production (Oh et al., 2009, Madihally and Matthew, 1999a, Kim and Mooney, 2000, Leor et al., 2005, Dawson et al., 2008, Amir et al., 2009). Further, advances in nanotechnology have made possible technology to control the tissue regeneration via delivery of essential factors. Significant advances have been made in fabricating porous scaffolds from biodegradable polymers (Lawrence et al., 2009, Li et al., 2005, Huang et al., 2006). The porous structure may be modified post-fabrication by inclusion of nanoparticles or etching the surface of the matrix. Generating a porous scaffold is done either by additive processes such as bioprintring, and electrospinning, or by reductive processes such as controlled rate freezing and lyophilization, salt leaching,

and gas foaming techniques (Hong and Madihally, 2011). The scaffold's properties can be manipulated via selection of biocompatible materials, solvents used, and processing methods. To recreate the native architecture, scaffolds should guide similar cellular alignment and deposition of *de novo* synthesized matrix components (Happe and Engler, 2016). In summary, biomaterials or delivery of cells alone is not enough to regenerate the tissue. The combination of both biomaterials and stem cells need to combine to regenerate the damaged tissue. Additionally, the delivery route of the implantation of a scaffold needs to be considered. For example, performing an open heart surgery allows the surgeon to transplant the scaffold to the affected area with ease. However, open heart surgery is a complicated surgery and not everyone is able to withstand a major surgery like that. Therefore, another type of scaffold needs to be considered (hydrogels) to increase the population of potential patients that are able to be treated with a therapy that uses both biomaterials and stem cells. The next section will cover hydrogels and how they can be easily transplanted using less complicated surgery.

2.4 Hydrogel fabrication

The main disadvantage of pre-formed scaffolds is the delivery route, which requires the use of major invasive surgery. Injectable hydrogels offer a minimally invasive alternative for arthroscopic surgeries and ease of incorporation of cells and bioactive agents. Hydrogels are water-swollen, cross-linked polymeric structures held together by chemical bonds and/or van der Waals forces (Ratner, 2004, Enderle and Bronzino, 2012, Slaughter et al., 2009). Hydrogels can be specifically designed to respond to different environmental factors such as temperature, radiation, pH, chemical agents, etc. There are three types of hydrogels: natural hydrogels, synthetic hydrogels, and natural and synthetic

blend hydrogels (Rafat et al., 2008, Lawrence et al., 2009, Saha et al., 2007, Hodde, 2002, Dawson et al., 2008). Natural hydrogels are composed of naturally derived polymers such as chitosan, collagen, gelatin, cellulose, fibrinogen, etc. Hydrogels based on natural polymers are biocompatible, biodegradable, have high cell adhesion, and resemble the native ECM structure (Li and Guan, 2011). Disadvantages of using hydrogels based on natural polymers include weak mechanical strength, immune rejection (depending on the source of the polymer), slow gelation, fast degradation, and potential carcinogenic consequences (Li and Guan, 2011). On the other hand, synthetic hydrogels are composed, as the name implies, of synthetic polymers such as polyethylene glycol, polyvinyl alcohol, polyglycolic acid, polylactic acid, etc. Synthetic hydrogels can have fast gelation times and are commonly bio-inert, biocompatible, and easily manipulated to obtain desired mechanical properties (Li and Guan, 2011). Disadvantages of using synthetic hydrogels include low cell adhesion, inability to deliver by injection, toxic crosslinking agents, non-biodegradability, and elastic modulus mismatch (Li and Guan, 2011). In summary, hydrogels are a better alternative because of their delivery method. Both natural and synthetic polymers have their disadvantages, therefore the choice of one over the other is based on what specific challenges are present in the disease that the treatment is for. For cardiac tissue regeneration, natural polymers are a better choice due to their molecular similarity to cardiac tissue. Next, I will be presenting the two polymers I chose as the foundation for the hydrogel investigated in this research project.

2.5 Hydrogel's components: chitosan, gelatin, and other polymers

The polymers chosen as the hydrogel's components are chitosan, gelatin, growth

medium, calcium peroxide, 5-azacytidine, laminin, transglutaminase, and PLGA nanoparticles encapsulating doxycycline hyclate. Chitosan is obtained by deacetylation of chitin (Shigemasa Y, 1994), the second most abundant polymer occurring in nature, it also has other advantages such as low cost, and easy availability (Khor and Lim, 2003). Chitosan exhibits different physicochemical characteristics, i.e., MW, crystallinity, deacetylation and positive charge. It is soluble in weak acids (pH<6.3) and can be easily processed into films and porous scaffolds of desired configuration (Madihally and Matthew, 1999a). Chitosan is metabolized into non-toxic D-glucosamines by lysozymes (Mi et al., 2002, Tomihata and Ikada, 1997) and hence is biodegradable. Lysozyme is an innate non-immunologic antibacterial enzyme and is one of the most structurally well-characterized carbohydrate hydrolases (Kristiansen et al., 1998). The three-dimensional structures of lysozyme in both the complexed and uncomplexed states have been established and the substrate binding sites are also known. The lysozymal hydrolysis of chitosan is an acid catalytic reaction with a peak reaction rate occurring around pH 4.5 to 5.5. Chitosan can be processed into beads, gels, fibers, or films (Aiba S-i, 1987, Hirano S, v, Kikuchi Y, 1976), and has shown promise for a number of tissue engineering applications (Cai et al., 2002, Chung et al., 2002, Lahiji et al., 2000, Mizuno et al., 2003, Zhu et al., 2002).

Chitosan hydrogels can be formed by either pH or temperature changes and by chemically crosslinking polymers. Thermoresponsive hydrogels have been developed by combining a solution of deacetylated chitosan with β-glycerophosphate (Iyer et al., 2012). These hydrogels can be tailored to gel at body temperature while remaining in a liquid state at room temperature. The role of β-glycerophosphate is to lower the surface

electrostatic charge of chitosan and therefore elevate the pH of the solution to biological condition (pH = 7.4) (Riva et al., 2011). The poly-alcohol group of β-glycerophosphate shields the chitosan chain, accelerating the formation of a hydrophilic shell around the chitosan molecule, and thus improving the chitosan chain protective hydration. This prevents chitosan from precipitating out with change in pH at low temperature. However, as the temperature is increased, hydrophilic interactions and hydrogen bonding interactions increase, triggering physical crosslinking throughout the whole solution, and starting the gelation process (Riva et al., 2011). Chemically crosslinked hydrogels can be formed by covalently linking chitosan and another polymer (in this case poly-ethylene glycol, PEG) with the use of a crosslinking agent. Dal Pozzo et al. reported that PEG-dialdehyde diethyl acetals are suitable compounds for the crosslinking of chitosan and partially reacetylated chitosan (Dal Pozzo et al., 2000). This is one of many example crosslinking methods for chitosan based hydrogels and scaffolds reported (Berger et al., 2004, Ravi Kumar, 2000, Riva et al., 2011, Dal Pozzo et al., 2000).

In order to overcome some of the limitations of chitosan, one approach is to blend with highly ductile PCL, along with gelatin, collagen, or other proteins (Table 2.1). These additions function to improve the hydrogel performance by either increasing the mechanical strength, introducing cell binding sites, and/or tailoring the degradation rate. Some of the aforementioned polymers can be found in the extracellular matrix (ECM). ECM is mainly composed of proteoglycans and fibrous proteins. Fibrous proteins found in the ECM include: collagen, elastin, laminin, and fibronectin. Collagen is the most abundant fibrous protein in animals. Collagen's main function is to provide tensile strength and regulate cell adhesion. The protein elastin provides recoil for tissues that

undergo repeated stretching, such as muscle fibers and cardiac tissue. Laminin and fibronectin play key roles in cell differentiation, migration, and adhesion. The most abundant protein in the human body is collagen, which therefore makes this protein an excellent additive for chitosan hydrogels due to natural binding sites and cellular interactions.

Table 2.1. Hydrogels of chitosan in combination with other molecules

Molecule name	**pH neutralization method**
Collagen (Chiu and Radisic, 2011)	PBS and NaOH
Alginate (Deng et al., 2015)	β-glycerophosphate
RoY Peptide (Shu et al., 2015)	β-glycerophosphate
Gold nanoparticles and polyethylene glycol (PEG) (Brondani et al., 2014)	Crosslinked with tetraethylene glycol dialdehyde, glycol dialdehyde diethyl diacetals, or tetraethylene glycol disuccinimidyl disuccinate
Lactose and azidobenzoic acid (Fujita et al., 2005)	Cross-linked by UV
Lactic acid and methacrylic acid (Hong et al., 2007)	Radical polymerization

Gelatin is an inexpensive, nonirritating, biocompatible, and biodegradable protein derived from the hydrolysis of collagen. Gelatin contains a peptide sequence that promotes cell attachment. Gelatin is blended with chitosan via electrostatic interactions without additional chemical cross-linkers and porous scaffolds can be formed. Cells exposed to gelatin-containing chitosan structures also show higher level of MMP-2 MMP-9 (Iyer et al., 2012), leading to premature degradation of the scaffold when higher number of cells are loaded. This could lead to attrition of delivered cells prior to engraftment. Furthermore, in heart failure, MMP-9 plays a major role in the pathological remodeling of ECM (Tyagi and Joshua, 2014). Whether cells are delivered by hydrogel, scaffold, or simply injected directly into the heart, the cell retention is extremely low. When using a

chitosan hydrogel, Hong et al. reported that the cell retention increased to 17.5% (compared to a 10% retention of cells delivered with no hydrogel) one week after implantation, and attributed this to the stability of the hydrogel (Hong et al., 2007).

Premature degradation of scaffolds is one of the most challenging problems when designing cellular therapies to be used in conjunction with biomaterials. One easy way to get around the problem is to use synthetic non-biodegradable materials. However, these materials may not be optimal for some treatments. Therefore, most people choose to use naturally occurring polymers. Naturally occurring polymers generally have better cytocompatability and are easily degrade by the host compared to synthetic polymers. But being easily degradable can be an issue because fast degradation or premature degradation can lead to incomplete treatment and therefore ineffective. The enzymes responsible for premature degradation are called Matrix Metalloproteinase (MMP). MMPs are responsible for degrading proteins mostly present in the extracellular matrix (ECM). While most MMPs target ECM proteins, there are some that are involved in the processing of cytokines, chemokines, hormones, adhesion molecules, and membrane-bound proteins. The involvement of MMPs in the processing of these molecules can lead to changes in normal cellular behavior, cell-cell communication, and tumor progression. There are 26 different MMP enzymes (table 2.2).

Table 2.2. Metallomatrix Proteinase Family.

Metallomatrix Proteinase (MMP) Number	**other names**
MMP-1	Collagenase-1, interstitial collagenase, vertebrate collagenase
MMP-2	Gelatinase A, 3/4 collagenase, 72kDa gelatinase, MMP-5, tissue gelatinase, type IV collagenase
MMP-3	Stromelysin-1, collagenase activating protein, MMP-6, procollagenase activator, proteoglycanse, transin
MMP-7	matrylysin, putative, metalloproteinase-1, uterine metalloendopeptidase
MMP-8	collagenase-2, neutrophil collagenase
MMP-9	Gelatinase B, 92 kDa gelatinase, macrophage gelatinase, neutrophil gelatinase, type IV collagenase, type V collagenase
MMP-10	stromelysin-2, transin-2
MMP-11	stromelysin-3
MMP-12	macrophage elastase, metalloelastase
MMP-13	AgMMP3 (Anopheles gambiense), collagenase 3, rat collagenase
MMP-14	membrane type (MT) MMP-1, MT1-MMP, MTMMP-1
MMP-15	membrane type (MT) MMP-2, MT2-MMP, MTMMP-2, SMCP-2
MMP-16	membrane type (MT) MMP-3, MT3-MMP, MTMMP-3, ovary metalloproteinase
MMP-17	membrane type (MT) MMP-4, MT4-MMP, MTMMP-4, MMP25beta (Brachydanio rerio)
MMP-18	collagenase 4, xCol4 (Xenopus)
MMP-19	RASI-1, RASI-6
MMP-20	enamelysin
MMP-21	XMMP (Xenopus)
MMP-22	CMMP (*Gallus domesticus*), MMP-27 (*Homo sapiens*), matrix metallopeptidase 27
MMP-23A	
MMP-23B	cysteine-array matrix matalloproteinase, CA-MMP, MIFR protein (Homo sapiens), MMP23A g.p. (Homo sapiens), femalysin
MMP-24	membrane type (MT) MMP-5, MT5-MMP, MTMMP-5
MMP-25	membrane type (MT) MMP-6, MT6-MMP, MTMMP-6, leukolysin
MMP-26	endometase, matrilysin-2
MMP-28	epilysin
Matrix Metalloproteinase Like-1	MMPL1

While there are many MMPs, they can be separated into major groups when concerning degradation of biomaterials. One group is called Collagenases (MMP-1, MMP-8, MMP-13, and MMP-19) and degrade fibrillary collagens in their native triple-helical supersecondary structure. Another group is called Gelatinases (MMP-2 and MMP-9) and degrades gelatin are known to be involved in inflammatory processes, tumor progression, and cardiovascular and autoimmune diseases. This section will focus on Collagenases and Gelatinases because the substrates that these groups encase are commonly used in the creation of biomaterials to be used in clinical applications and the inhibitor chosen for this therapy has been shown to reduce the activity of collagenases and gelatinases.

High levels of MMPs can be observed during the process of tissue remodeling in a wound healing environment, especially during cardiac remodeling. (2008). A link has been associated between MMP activity and cardiac remodeling, specifically collagenases and gelatinases (2008). Cells that release these MMPs during cardiac remodeling include but are not limited to cardiomyocytes, cardiac fibroblasts, endothelial cells, vascular smooth muscle cells, neutrophils, and macrophages (2008). No single cell type is responsible for the production or release of all MMPs listed but there is overlap between them. Most biomedical treatments that are being developed will be exposed to MMPs when they are implanted in the body and therefore, be exposed to an environment that can cause the biomaterial to be prematurely degraded.

To overcome premature degradation, two courses of action were taken. First course of action was to inhibit gelatinases, which are responsible for digesting gelatin chains. Second course of action is to naturally crosslink gelatin molecules with transglutaminase to enhance the mechanical stability of the hydrogel. Therefore, to prevent premature

degradation, MMP-2 and MMP-9 activity must be inhibited. Inhibition of matrix metalloproteinases (MMPs) is not an easy task, as matter of fact the Food and Drug Administration (FDA) has only approved one single compound to be used as an MMP inhibitor as a safe and effective treatment. Doxycycline hyclate was approved in 1967 and initially used as an antimicrobial agent. However, in 1989 the FDA approved doxycycline to be used as an inhibitor of collagenase for the treatment of periodontitis. Thus, making doxycycline the first and only MMP inhibitor to be approved by the FDA (Sang et al., 2006, Stechmiller et al., 2010). By no means does this mean that doxycycline is the only MMP inhibitor, in fact we now know the different types of MMP and their structures, activation mechanisms, degradation mechanisms, and functions. Doxycycline, has been shown to inhibit MMP-1, MMP-2, MMP-8, MMP-9, MMP-13 (Smith et al., 1999, Liu et al., 2003). This inhibitor focuses on collagenase and gelatinases. A drawback of doxycycline has a half-life of 18-22 hours and therefore is only a temporary solution. The best solution would be to slowly release doxycycline over a prolonged period of time until the treatment has had enough time to display positive results, such as successful migration of implanted cells, regeneration of tissue, angiogenesis, etc. Extended release of doxycycline has been achieved by encapsulating doxycycline in PLGA-PCL microparticles (Mundargi et al., 2007).

In order to further increase mechanical stability and decrease degradation rate, addition of transglutaminase (TG) was investigated. TG (EC 2.3.2.13) catalyzes Ca^{2+}-dependent transamidation of proteins and formation of protein polymers via protease-resistant covalent isopeptide bonds, which are approximately twenty times stronger than hydrogen and hydrophobic interactions (Zemskov EA, 2006). The catalyzed TG reaction results in

the formation of the amide crosslink from γ-carboxamide and primary amine functionalities (Aeschlimann and Paulsson, 1994). Calcium-independent TG is typically used in the crosslinking in gelatin, yogurt, meat and fish analogues (surimi) (Lim et al., 1999, Joseph et al., 1994). TG containing hydrogels are used as adhesives and for *in vitro* expansion of cells (Jones and Messersmith, 2007). Gelatin cross-linked with TG is used in forming *in situ* gel adhesives and is very promising as a hemostatic surgical sealant for soft tissues (Liu et al., 2009).

The hydrogel in this research project was be exposed to a nutrient and oxygen deficient environment. In order to address the hypoxic environment of the ischemic heart, oxygen releasing molecules such as sodium percarbonate, calcium peroxide, magnesium peroxide, hydrogen peroxide, and fluorinated compounds could be helpful (Camci-Unal et al., 2013). For this project, calcium peroxide was chosen because of the compounds slower release rate of oxygen. Oh et al has shown that cells cultured on a PLGA scaffold with calcium peroxide particles can survive for 10 days in a hypoxic environment (Oh et al., 2009). However, when calcium peroxide is dissolved in acidic conditions (needed to dissolve chitosan), pH changes can occur and the presence of calcium could cause chelation and destabilization of the hydrogel. To supplement this environment with nutrients, powdered growth medium was added. Growth medium is used in *in vitro* conditions to supplement cells with nutrients needed for growth and proliferation.

In summary, for this therapy to be successful, it needs to increase the survival rate of stem cells that are embedded in the hydrogel and implanted in the heart. To do this, we looked at the drawbacks of chitosan and gelatin and addressed them. For example, chitosan has no binding domain therefore gelatin was added. Gelatin increases MMP-2

and MMP-9 activity, therefore doxycycline and TG were added. The environment where the hydrogel was to be implanted was also considered. This environment is high on MMP-2 and MMP-9, and low on nutrients and oxygen. Growth medium and calcium peroxide were added to increase nutrients and oxygen concentration. Finally, to ensure that the embedded stem cells differentiate into cardiomyocytes, a stimulating agent was added into the hydrogel's formulation.

CHAPTER III

IMPROVING THE STABILITY OF CHITOSAN–GELATIN-BASED HYDROGELS FOR CELL DELIVERY USING TRANSGLUTAMINASE AND CONTROLLED RELEASE OF DOXYCYCLINE

3.1 Introduction

In this study, we hypothesize that inhibiting MMP activity during the initial phase of post-cell delivery improves the stability of the chitosan-gelatin (CG) hydrogels, while long term stability and mechanical property can be improved with a slow enzymatic cross-linking using transglutaminase (TG), and adding nutrients to the hydrogel formulation would address nutrient requirements (Broderick et al., 2005, McDermott et al., 2004). TG is found in most living organisms, and its functions include blood clotting and liver detoxification (Greenberg et al., 1991). Calcium-independent microbial TG (mTG) is popularly used in the covalent crosslinking of gelatin between glutamine and lysine residues (Lim et al., 1999, Joseph et al., 1994). mTG containing hydrogels are used in forming *in situ* gel adhesives and for *in vitro* expansion of cells (Jones and Messersmith, 2007).

Published in Journal of Drug Delivery and Translational Research

mTG increases the mechanical strength of gelatin-based hydrogel (Aeschlimann and Paulsson, 1994), and mTG cross-linked gelatin is very promising as a hemostatic surgical sealant for soft tissues (Liu et al., 2009). However, TG in high concentrations is toxic and causes cell death, leading to concerns on cytotoxicity (Broderick et al., 2005). MMP-2 activity in fibroblasts is regulated by the mechanical strength of hydrogels (Tomasek et al., 1997). An overexpression of MMP-2/9 results in premature degradation of the hydrogel and loss of cells. One approach to inhibiting MMP-2/9 activity is using doxycycline (DOX), a member of tetracycline family of drugs known for antibiotic properties. Independent of antibacterial activity, it is tested in numerous conditions associated with elevated ECM degrading enzymes, including arthritis and chronic wounds management (Newby, 2012). Since serum half-life of DOX is 18-22 hours (Agwuh and MacGowan, 2006), we approached encapsulation of DOX in PLGA nanoparticle prior to mixing in the hydrogel. Experiments were performed to evaluate the approach in vitro using fibroblasts. Furthermore, mechanical properties were determined to assess whether TG added in the hydrogel would cross-link gelatin, increase mechanical stability, and thus decreasing the rate of degradation. These results show 2.5 times improvement in cell retention and slow release rate of DOX with TG cross-linked CG hydrogels.

3.2. Materials and methods

3.2.1. Sources for Materials.

Low MW chitosan (50 kDa and 75-85% deacetylation), gelatin type A (300 Bloom), β-glycerophosphate (2GP), 50:50 poly lactic-co-glycolic acid (PLGA, 110 kDa), polyvinyl alcohol (PVA, 30-70 kDa, 87-90% hydrolyzed), Doxycycline hyclate (DOX,

pharmaceutical secondary standard) and bovine serum albumin (BSA) were procured from Sigma Aldrich Co (St. Louis, MO). Phosphate buffer solution (PBS, pH=7.4), 5-(and-6)-carboxyfluorescein diacetate, succinimidyl ester (CFDA-SE) - mixed isomers, and powdered DMEM low glucose were procured from Life Technologies. (Carlsbad, CA). Trypsin/EDTA, DMEM, and FBS, human foreskin fibroblasts (hFF-1) were procured from ATCC (Manassas, VA). MMP-2/MMP-9 substrate I, fluorogenic was procured from Millipore (Billerica, MA). TG (EC 2.3.2.13) was procured from Ajinomoto (Fort Lee, NJ).

3.2.2. DOX-loaded PLGA Nanoparticle preparations.

DOX containing PLGA nanoparticles were prepared using double emulsion technique (Davda and Labhasetwar, 2002, Murakami et al., 1999). In brief, 30% (wt/v) PLGA was dissolved in chloroform and 2% (wt/v) PVA solution was prepared in water containing 0.2% (v/v) chloroform. A 10% DOX solution was prepared and added to the PLGA solution in two portions, vortexing for 1 minute after each addition. The primary emulsion was then added in two portions to the 2% PVA solution with intermittent vortexing, forming the water-in-oil-in-water (w/o/w) emulsion. The particles spontaneously formed with the addition of the PLGA solution to the aqueous 2% PVA solution; emulsion droplets formed and chloroform diffused out from the droplets. The emulsion was sonicated for 5 min using the Sonic Dismembrator Model 500 (Fisher Scientific). The w/o/w emulsion was then stirred overnight to allow for the evaporation of chloroform, allowing the droplets to solidify and form the particles. After evaporation, contents were transferred to 2-mL centrifuge tubes and centrifuged at 14,500 rpm.

Supernatant was removed and particles were washed with deionized water. Contents from all centrifuge tubes were then collected and sonicated for 1 minute. This process was repeated once more to ensure that no DOX was left in the solution.

Particles in solution were lyophilized i) to measure the size of formed nanoparticles using dynamic light scattering (Zeta PALS, Brookhaven Instruments Corporation) and ii) to visualize using scanning electron microscope (Joel JOEL 6360USA Inc., Peabody, MA), similar to a previous publication (Hong and Madihally, 2010). In brief, freeze dried samples were attached to a stub using a double sided conductive tape and sputter-coated with gold for 1 min. Digital micrographs were collected from random locations at 15kV accelerating voltage.

3.2.3. Hydrogel formulation.

Solution of 2% (wt/v) chitosan, 4% (wt/v) gelatin, 2% (wt/v) powdered low glucose DMEM, and 0.003% (wt/v) TG, were prepared in 0.1N HCl (Iyer et al., 2012). The solution was stirred for a minimum of four hours at a temperature of 50°C. After the polymers completely dissolved, 9 mL were transferred to a 50 mL centrifuge tube, placed in an ice bath, and four mL of 0.56 g/mL 2GP was added drop wise under constant stirring. When Dox was added, DOX-PLGA nanoparticle solution was added to the hydrogel solution and mixed thoroughly for samples with DOX.

3.2.4. Mechanical Characterization.

Confined compression testing was performed on hydrogels using an INSTRON 5542 (INSTRON, Canton, MA) and a custom-built anvil, as described previously (Walker and

Madihally, 2014). In brief, hydrogels were prepared in 6-well tissue culture plates by incubating 3 mL of solution for 2 hours at 37°C. Hydrogels were compressed at 1 mm/min crosshead speed at room temperature. Data were exported to MS Excel and compressive modulus was calculated from the slope of the linear portion (20% to 40% strain range) of the stress-strain plot.

Tensile tests were also conducted by applying the load orthogonal to compression testing to ensure uniform cross-linking of the hydrogels, as described previously (Ratakonda et al., 2012). In brief, 20 mL of hydrogel solution was prepared in a 35mm petri dish and incubated for 2 hours. After incubation, 10mm × 14 mm × 3 mm rectangular slices were cut out and loaded to the Instron 5542 and pulled to break at a crosshead speed of 1 mm/min at room temperature. After data collection, stress vs strain was plotted and the slope of the linear region, the elastic modulus, was determined. For all tests, a minimum of three experiments were performed per condition from different preparations.

3.2.5. Doxycycline release from the hydrogels.

Acellular hydrogels were prepared following methods described in Section 2.3 with and without DOX and TG. CG hydrogel prepared without DOX served as the control group. After a 2h incubation period, 2 mL of PBS was added on top of the hydrogel and incubated for 5 days. Every 12 hours, 1 mL of PBS was collected. DOX content was determined using a calibration plot constructed by varying concentrations of DOX solutions (0-24 mg/L) prepared in distilled water. The absorbance of each sample was measured in a spectrophotometer at 375 nm, as published by others (Ramesh et al., 2011). Absorbance at various concentrations were plotted and a linear fit related absorbance to

concentration, which was used to determine unknown DOX concentration.

In order to determine k_d values, DOX concentration was measured by incubating DOX directly in PBS various times until 48 hr. Then a first order decay rate (Costa and Sousa Lobo, 2001) given by

$$\frac{dC_{Dox}}{dt} = -k_d C_{Dox} \quad (1)$$

was used to determine the decay constant k_d [h^{-1}] where C_{DOX} [µg/mL] is the DOX concentration at any time t. This equation was integrated using the limits of integration of when t= 0, C_{DOX}= $C_{DOX,0}$ [µg/mL] and when t= t, C_{DOX}= C_{DOX} to obtain

$$\frac{C_{Dox}}{C_{Dox,0}} = e^{-k_d t} \quad (2)$$

Obtained concentration values were then plotted as a ratio against corresponding time according to the equation. By fitting an exponential decay function, slope value corresponded to the decay constant. In order to determine the DOX release rate K [µg/mL.h] from the hydrogel, a single compartment was assumed. Writing the mass balance gave

$$\frac{dC_{Dox}}{dt} = K - k_d C_{Dox} \quad (3)$$

Equation (3) was rearranged and integrated using t=0, C_{DOX}=0, and t=t, C_{DOX}=C_{DOX} to obtain

$$Ln\left(\frac{K - k_d C_{Dox}}{K}\right) = -k_d t$$

This equation was rearranged to

$$K = \frac{k_d C_{Dox}}{1 - e^{-k_d t}} \quad (4)$$

using which K value at different times were estimated from each experiment. Obtained K values were multiplied by the respective time to get the total concentration released from the hydrogel. For each time point, percentage release was calculated knowing the concentration loaded in the hydrogel (each hydrogel was loaded with DOX at a concentration of 50mg/L). Obtained values were plotted to determine the release profiles. To assess whether the presence of DOX nanoparticles affected the mechanical properties, hydrogels with DOX were submitted to the mechanical tests outlined in section 2.4. To further characterize the mechanical properties of the hydrogels while release of DOX is under way, hydrogels were submerged in PBS and underwent compressive tests at 1, 3 5 and 7 days after initial submersion in PBS. Obtained values were normalized to day zero values in order to understand the stability of the hydrogel in the absence of cells at conditions mimicking cell culture experiments.

3.2.6. Cell culturing in hydrogel.

Human foreskin fibroblasts (hFF-1) were expanded in DMEM supplemented with 15% FBS, following vendors protocol. Cells were maintained at 37°C, 5% CO_2/95% air, and fed with fresh medium every 2-3 days. Once confluent, cells were detached with trypsin/EDTA and then trypsin neutralization solution was added. Cells were centrifuged at 270×g for 5 min and dispersed in growth medium. Viable cells were counted using Trypan blue dye exclusion assay.

hFF-1 between the passages 3-10 were stained with CFDA-SE, and seeded onto hydrogel samples using the procedure previously developed by our group with minor modifications (Iyer et al., 2012). Four conditions of hydrogels were used: CG hydrogel

with and without DOX nanoparticles, and CG with TG (CG-TG) hydrogel with and without DOX nanoparticles. In brief, cells were incubated in growth medium containing 2 μM CFDA-SE at 37°C for 20 min followed by washing the excess stain with growth medium. Then, 0.5×10^6 cells/mL hydrogel were mixed uniformly. One milliliter of mixture was dispensed into the 6-well plate and incubated at 37°C for 2 hours to allow for gelation. Then, growth medium was added. After 24 hours, the growth medium was replaced with fresh medium. This process was repeated every 48 hours until day 5. The spent medium collected was used for viability and MMP-2/MMP-9 analyses.

After five days, cytoplasmic CFDA-SE content was extracted from live cells by three cycles of freeze and thaw, using the procedure previously reported (Iyer et al., 2012). In brief, cell culture medium was replaced with 2mL PBS and placed at -20°C until the PBS froze. After the PBS froze, the plates were thawed at room temperature and the cycle was repeated. Then, the solution was collected and the absorbance was determined using a spectrophotometer Gemini XS spectrofluorometer (MDS technologies, Santa Clara, CA) at the excitation and emission wavelengths of 485 nm and 525 nm, respectively. The CFDA-SE content in the spent medium was also assessed. Obtained fluorescence intensities were converted to number of cells creating a calibration of fluorescence intensity to number of cells obtained as previously described (Iyer et al., 2012), with minor modifications. In brief, cells pre-stained with CFD-SE were seeded at 0.25, 0.40 and 0.50 million/mL CG-TG-DOX solution. Upon gelation, CFD-SE content was extracted by a freeze-thaw cycle similar to that explained above. Hydrogels without cells were used as blanks. A calibration plot was obtained between fluorescence and the number of cells.

Some samples were processed for histology analysis. Samples were fixed using 3.7% formaldehyde for 30 min at room temperature, washed thrice with PBS, stored in ethanol overnight at 4°C, sectioned and stained for Hematoxylin and Eosin (H/E). Digital photomicrographs were captured at representative locations using an inverted microscope.

3.2.7. MMP-2/MMP-9 activity.

In order to understand the effect of DOX on MMP-2/MMP-9 inhibition, the amount of MMP-2/MMP-9 secreted into the growth medium was determined using a fluorogenic substrate (DNP-Pro-Leu-Gly- Met-Trp-Ser-Srg-OH) specific for MMP-2/MMP-9, using protocol described previously (Iyer et al., 2012, Waas et al., 2002). In brief, the absorbance of MMP-2/MMP-9 was recorded at 280 nm excitation wavelength and 360 nm emission wavelength. A 200 μL solution of sampled media and MMP-2/MMP-9 (1mM solution in DMSO) was prepared in a 1:1 ratio. After twenty minutes, the samples were analyzed using a spectrophotometer. The amount of fluorescence was normalized using the total protein content of the samples, measured using a commercially available bicinconic acid assay from Pierce Chemical Company.

3.2.8. Statistical evaluation.

All experiments were repeated three or more times. Significant differences between two groups were evaluated using a one-way analysis of variance (ANOVA) with 95% confidence interval. When $P<0.05$, differences were considered to be statistically significant.

3.3. Results and Discussion

3.3.1. Characterization of DOX-loaded PLGA nanoparticles.

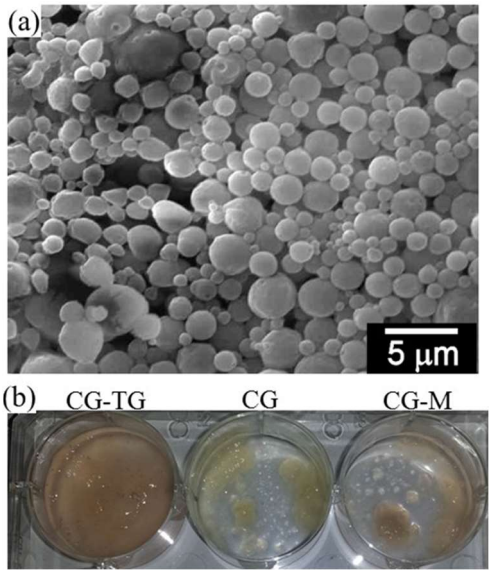

Figure 3.1. Nanoparticles and hydrogel stability. (a) Micrograph of DOX-loaded PLGA nanoparticles. (b) Photograph showing the effect of incubating with the medium on the hydrogel with and without TG.

First, forming DOX-containing particles was evaluated either using PLGA or chitosan. Based on ease of synthesis and uniform shape when observed under a scanning electron microscope, formed PLGA nanoparticles via double emulsion technique were selected for further use. However, SEM analysis (**Figure 3.1a**) indicated a broad size distribution of PLGA nanoparticles. In order to reduce the size distribution, particles were passed through two syringe filters containing 0.45µm and 0.22µm pore diameters. A fraction passed through a 0.22µm filter and were collected and characterized using a dynamic light scattering. These results showed that the PLGA nanoparticles were 260(±12) nm in size. Incorporating DOX to the nanoparticles increased the overall size to 367(±20). These particles were used in subsequent experiments. It is believed that after nano particles were passed through filter the majority of the nanoparticles aggregated to form larger particles than the filter pore size. This aggregation could have been caused during centrifugation or freeze-drying of samples for characterization using a dynamic light scattering.

3.3.2. Effect of TG crosslinking on hydrogel strength.

Previously, we have shown that presence of gelatin in substrates increases gelatinase activity (Iyer et al., 2012). Those experiments were performed using 0.5 % (wt/v) chitosan and 0.5 %(wt/v) gelatin solutions. During preliminary cell experiments (data not shown) using nine times more cells per mL of hydrogel than the previous study (Iyer et al., 2012), hydrogels were found to be unstable. This is attributed to the increased gelatinase and other proteolytic activity due to increased cell number, as this instability was not noticed with reduced cell number even after ten days of culture (Iyer et al., 2012). The concentration of the hydrogel solution was increased to 2 % (wt/v) chitosan and 4 %(wt/v) gelatin to address the stability issue. Increased concentrations of chitosan and gelatin still showed temperature sensitive hydrogel formation. However, any further increase in chitosan along with gelatin caused premature gelation. Hence, TG was added to the hydrogel to increase the hydrogel stability further.

In order to test the effect of these formulation changes, cells were added to the hydrogel and cultured for five days. All formulations gelled at 37°C i.e., changes in the formulation did not affect gelation characteristics. At the end of the experiment, they were exposed to Trypsin/EDTA solution (**Figure 3.1b**). The only hydrogel sample that was stable at the end of the experiment was the hydrogel containing TG.

3.3.3. Effect of DOX and TG on the stability of the hydrogels.

During cell culture experiments, it was noted that CG hydrogels experienced some instability, especially during the first 2-3 days. On the other hand, there was no observable degradation in hydrogels with TG during that same time period. This could

mean that the gelatin crosslinking is completed by within 2-3 days. To determine whether the addition of DOX nanoparticles altered the mechanical properties, the compressive modulus was obtained for hydrogels containing DOX nanoparticles at 33 µL of nanoparticles/L of hydrogel solution. First, values at day zero i.e., without incubation

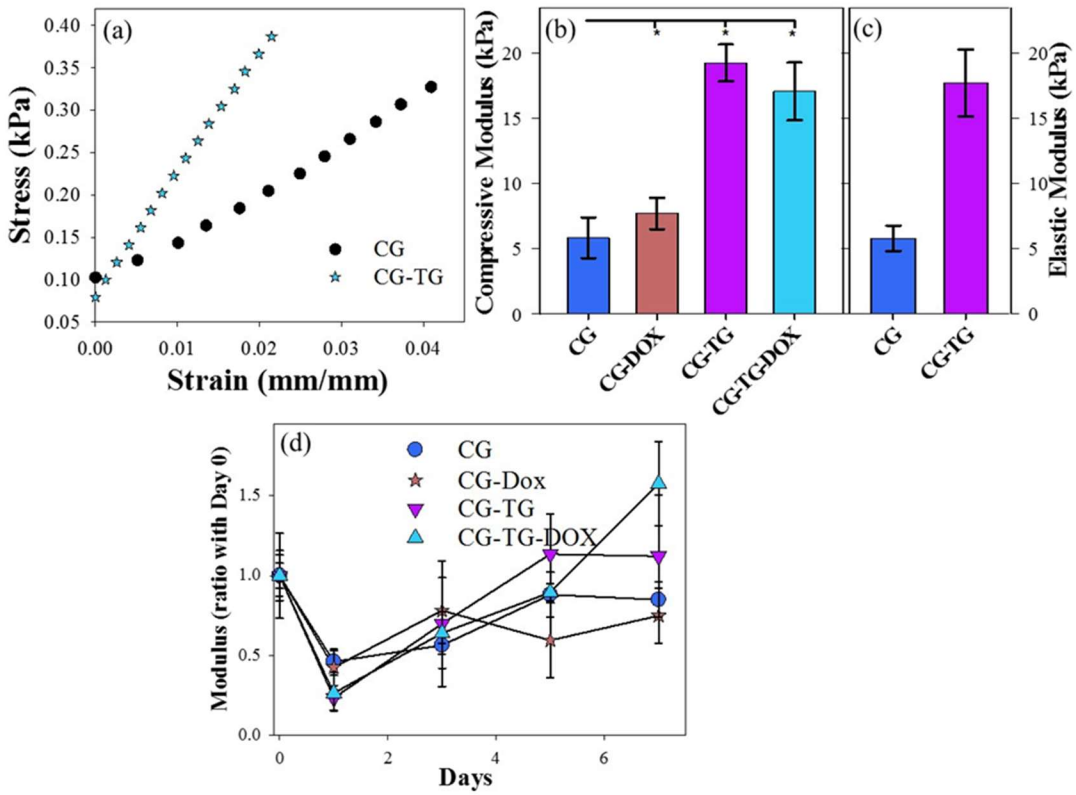

Figure 3.2. Influence of adding DOX Influence of TG crosslinking on the hydrogels. (a) Stress-strain response between the TG with medium added to the CG. (b) Compressive moduli on day zero. Asterisk indicates $p < 0.05$ between the groups indicated. (c) Tensile properties showing the isotropic cross-linking. (d) Changes in compressive moduli with incubation in PBS without cells.

in PBS were evaluated. To measure the effect of crosslinking on mechanical properties, compressive modulus was obtained from the linear region of stress -strain plot (**Figure 3.2a)**. Since the hydrogels were kept at 37°C, TG cross-linking reaction occurred at that temperature which is known to be favorable (Bode et al., 2011). The compressive modulus of 2 % (w/v) chitosan and 4% (w/v) gelatin hydrogel was 5.8 (±1.56) kPa

(**Figure 3.2b**). Addition of DOX-containing PLGA nanoparticles to CG moderately increased the modulus to 7.7 (±1.21) kPa. However, addition of TG to CG without DOX-containing PLGA nanoparticles increased the compressive modulus to 19.3 (±1.41) kPa. This increase is probably due to the addition of growth medium rather than TG, as the cross-linking reaction takes days rather than minutes. A similar increase was noticed in CG-TG samples with DOX-containing PLGA nanoparticles. The modulus marginally reduced to 17.1 (±2.21) kPa.

To ensure that crosslinking was uniform throughout the hydrogel, tensile tests were conducted by stretching the CG hydrogels with TG in the orthogonal direction to that used in compression. Elastic modulus was nearly identical to the compressive modulus, suggesting that the hydrogels are isotropic (**Figure 3.2c**) and TG cross-linking is uniform, as expected due to mixing of TG in the solution prior to gelation. Minor differences between elastic and compressive modulus could be attributed to the differences in experimental setup. Compressive tests were performed in a confined condition while tensile tests were unconfined. Water resistance could add to stiffness in compression, whereas in tensile tests, any water excreted would not add resistance.

In order to understand the stability of the hydrogels better, samples retrieved after incubation in PBS at 37°C were measured by confined compression tests. At day 1 (**Figure 3.2d**), all samples experienced a reduction in compressive modulus, which could be due to removal of 2GP from the hydrogels. Hydrogels containing growth medium experienced more of a reduction in the mechanical properties at day 1. This could be due to growth medium leaching out into PBS and thus weakening the hydrogel. After day 1, samples with DOX nanoparticles and/or TG recovered from the reduced modulus.

However, it is unclear why the addition of DOX nanoparticles helps increase the compressive modulus over time. It is possible that there is some interaction between PLGA and chitosan, and thus increasing its mechanical strength {Chronopoulou, 2013 #552;Schexnailder, 2009 #551;Wang, 2013 #553}. At day 7, the hydrogel containing both TG and DOX nanoparticles was the only sample that showed an increase in compressive modulus. It is evident that the crosslinking of TG starts 24 hours after incubation.

3.3.4. Release profile of DOX in hydrogel embedded with nanoparticles

In order to determine the optimal conditions for DOX release, DOX-containing nanoparticles were dispersed into the CG hydrogel (with and without media and TG) solution and subsequently placed into PBS (pH=7.4) solution. From samples where DOX nanoparticles were directly added to the PBS solution, the decay constant was obtained (**Figure 3.3a**) by fitting the exponential function, following Equation (2). Then the k_d value was found to be 0.0191 h^{-1}. Then, using $t_{1/2} = \frac{Ln2}{k_d}$, the half-life of DOX was calculated which corresponded to 36.3 h. This is somewhat higher than reported in serum (Agwuh and MacGowan, 2006). Others have shown similar profile in PBS, and could be attributed to pH of PBS (Giovagnoli et al., 2010) and absence of enzymes.

Using the calculated k_d values in Equation (4), actual release rate, K, from the hydrogels were assessed. Evaluation of release kinetics showed that much of the DOX release occurred within the first 24h in CG hydrogels (**Figure 3.3b**). Cross-linking CG with TG prolonged the release profile significantly, and nearly 90% of the delivery occurred by 96h. CG hydrogels without DOX were used as controls, which showed no DOX during the study period. Those nanoparticles, which completely encapsulated the DOX could prolong the release of DOX to long term. Further experiments are necessary to understand this scenario.

3.3.5. Influence of DOX and TG on hFF-1 colonization.

In order for CG hydrogel with TG and DOX to be used as a cell carrier, it must support cell culture. To assess the hydrogel's ability to support cell culture, CFDA-SE stained hFF-1s was distributed in the solution and cultured for five days; CFDA-SE is non-toxic and used *in vivo* for visualizing cells or studying uptake of labeled substrates. First, the collected medium was assessed for CFDA-SE fluorescence intensity and the number of

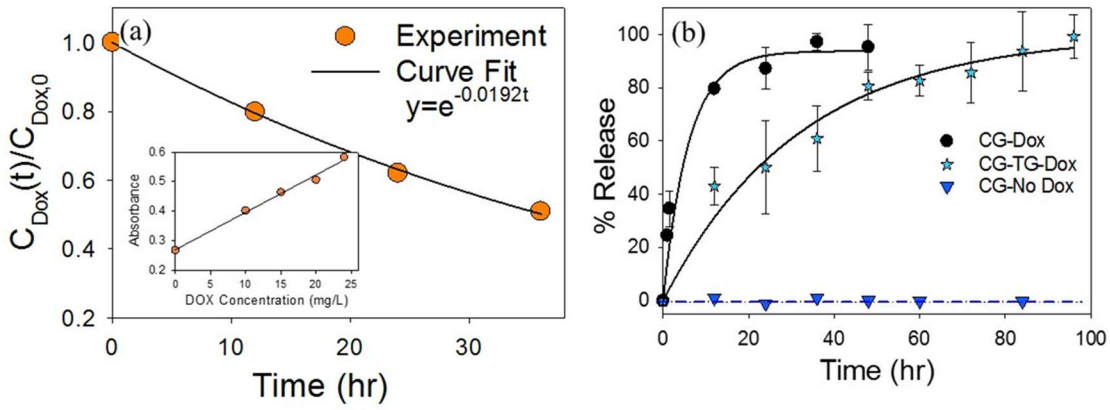

Figure 3.3. DOX release characteristics. (a) Stability of DOX in PBS. Insert is a calibration plot of DOX concentration to absorbance. (b) Percentage of DOX released from the hydrogel. CG-No DOX are actual numbers as they cannot be normalized to the initial concentration. Each data point is an average of 3 samples and error bars correspond to the standard deviations.

dead cells. The highest number of cells (**Figure 3.4a**) were recovered from the CG-TG with DOX nanoparticles. Since there were no significant differences between CG with and without DOX nanoparticles, higher cell death in CG-TG with DOX may not be due to DOX alone. In addition, others have shown that used range of TG concentration is not toxic to cells (Broderick et al., 2005). After five days, cells remaining in the hydrogel were analyzed. Contrary to high cell death, 60% of cells (**Figure 3.4b**) originally seeded in the hydrogel were recovered in the CG-TG hydrogels with DOX nanoparticles. However, only 40-43% cells were recovered from other formulations. DOX helps with cell adhesion and retention (Franco et al., 2006) and cells retrieved from CG with DOX were moderately higher than CG alone, although there was no statistical significance. However, fibroblasts are known to be extensively involved in matrix remodeling after

wound healing. They secrete MMPs more than other cell types. The improved mechanical property of the hydrogel with TG and reduced MMP activity by DOX could be the reason for seeing the improved cell survival in CG-TG and DOX. Other cell types

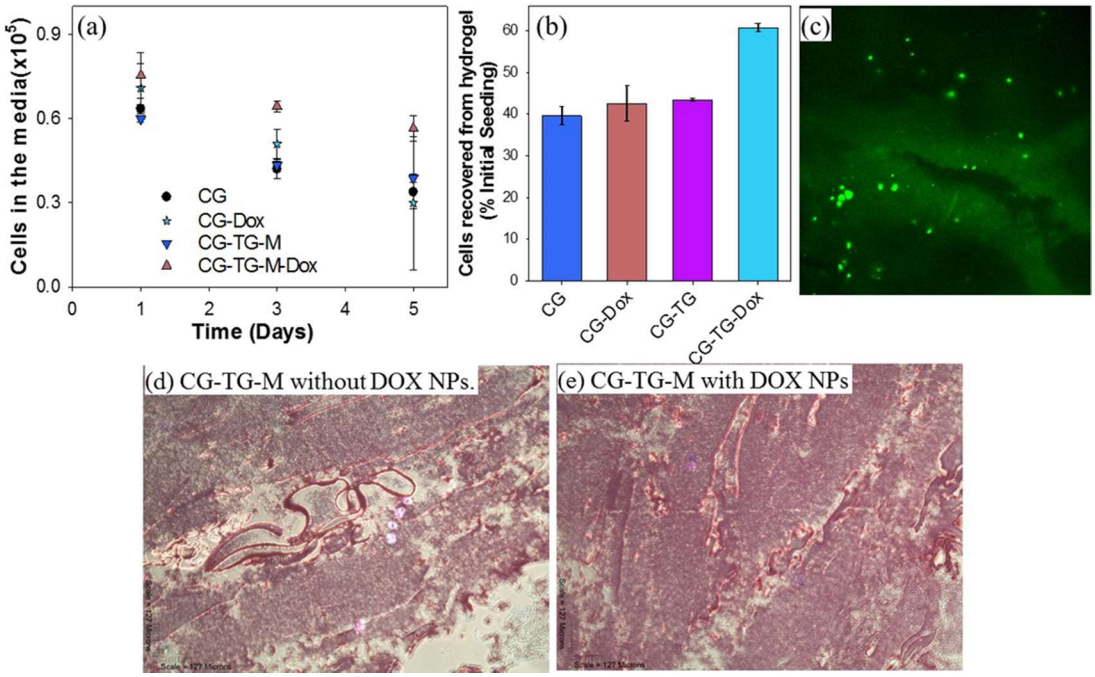

Figure 3.4. Effect on cell retention and survival. (a) Number of dead cells determined indirectly using the amount of CFDA-SE present in the spent medium on days 1, 3 and 5. Asterisk indicates $p < 0.05$ between CG-TG-Dox and CG hydrogels (b) CFDA-SE intensity from the cells were retrieved from the hydrogel on day 5. Asterisk indicates $p < 0.05$ between CG-TG-Dox with other conditions (c) Confocal fluorescent micrographs stained for CFDA-SE. (d and e) H/E stained micrograph showing cell distribution within the matrixes.

have to be tested to understand whether TG cross-linking alone is sufficient to improve viability. The cumulative number of cells i.e., cells in the medium and in the hydrogel were 100% in CG-TG hydrogels with DOX nanoparticles. In other conditions, we could not account for nearly 25-32% of the cells that were initially seeded. The highest number of cell loss was in CG hydrogels, similar to in vivo results where cell attrition is observed. Since the number of cells were mixed together, counted, and divided into four equal parts (one for each condition), alterations in initial seeding could not lead to such variation. Alternatively, when the medium is changed, some floating pieces of hydrogels

and cells are collected. We chose to label the intact cells in those components as dead cells (even though they were still viable), as they will be lost in the *in vivo* scenario. In any case, cross-linking CG with TG and adding DOX nanoparticles significantly improved the retention of cells. Nevertheless, we measured the total fluorescence of CFDA-SE that is initially present in the cells. CFDA-SE is a cytoplasmic stain and equally inherited by the daughter cells during cell division. However, when we quantify CFDA-SE content by spectrophotometry, the total amount of CFDA-SE does not change, due to CFDA being equally divided into daughter cells, compared to initial cytoplasmic content. Hence, cell proliferation could not be tested due to the fixed fluorochrome content during cell culture. We need to do flow cytometry to determine cell growth, similar to our previous studies (Iyer et al., 2012). Despite significant improvement in viable cells, nearly 40% of the cells were dead cells. Hence, one has to further optimize the hydrogel for cell survival by including addition of oxygen releasing molecules and evaluation of the stability of growth medium components.

In order to understand the *in situ* distribution and viability of cells, hydrogels were assessed by confocal fluorescent microscope. These results showed (**Figure 3.4c**) uniform distribution of hFF-1 within the hydrogel. However, cross-linking may decrease the diffusion of nutrients and metabolic products, creating nutrient inefficiency and reduced viability. In order to determine the changes in morphology of the hydrogel, H/E sections were analyzed. These results showed that CG-TG without DOX Nanoparticles (**Figure 3.4d**) appeared less dense compared to CG-TG with DOX nanoparticles (**Figure 3.4e**). This could be an indication of a more crosslinked and stable hydrogel structure. Also, there could be production of ECM elements, which needs to be evaluated. Further

analyses are necessary to better understand the impact of these changes and the need for additional growth medium components.

3.3.6. MMP-2/MMP-9 activity

First, accumulated total protein content in the spent medium was analyzed using bicinchoninic acid (BCA) assay to understand the effect of modifications in the hydrogel. These results (**Figure 3.5**) showed a higher total protein content TCP relative to CG hydrogels on day 1. Trends in total protein contents during the study period were similar in CG and CG-TG hydrogels with DOX. Hydrogel cultures in general had a lower amount of total proteins relative to TCP, probably due to the entrapment of secreted proteins within the hydrogel. In any case, hydrogels without DOX had a higher level of

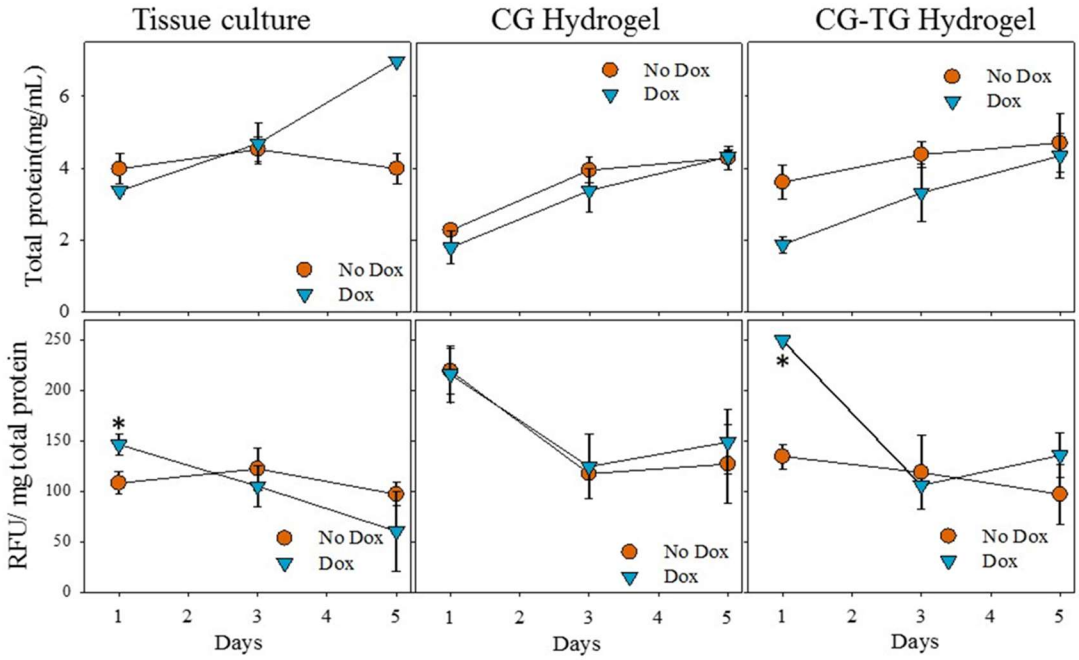

Figure 3.5. MMP secretion into the medium. (a) Total protein content in the spent medium. (b) MMP-2/MMP-9 secreted into the medium. Each data point is an average of at least four pooled samples and error bars correspond to standard deviations. Asterisk indicates $p < 0.05$ between conditions with and without Dox on same day.

total protein content relative to hydrogels with DOX cultures in contrast to the number of cells retrieved on day 5. Previously, we have shown the gelatin is stable in these hydrogels and alterations are not due to increased gelatin leaching (Iyer et al., 2012). Gelatinases are present for a considerable amount of time during the wound repair process (Ravanti et al., 1999). DOX is an inhibitor of MMP2/MMP9 or pro-MMP activation by interacting with the zinc or calcium atoms within their structural center required for stability. Further, TG cross-linked collagen is degraded slowly by MMPs (DM et al., 2006). In order to understand the implication of delivery of DOX and TG cross-linking, MMP2/MMP9 activities were measured. On day 1, there was a significant effect of DOX in TCP cultures (**Figure 3.5**), but not at other time points, probably due to shorter half-life of DOX in the medium. On the contrary, DOX had some effect in CG scaffolds with and without TG on day 3. There was a significant reduction in MMP-2/MMP-9 activity CG-TG hydrogels with DOX on Day 3 relative to day 1. Although part of this reduction could be due to the increased protein content, similar to CG hydrogels, the slope of reduction was attributed to the DOX release. Despite further increase in total protein content on day 5, moderate increase in MMP-2/MMP-9 activity was observed. This could probably be due to an increased amount of nutrients in the hydrogels, which increased the activity of cells in remodeling the activity. On day 5, however, CG hydrogels alone had increased MMP-2/MMP-9 activity, while addition of TG had suppressed MMP-2/MMP-9 activity. This could be related to the stability of the CG hydrogels which may lead to burst release of DOX and then follow the same path as TCP samples. This suggests that DOX delivery through the hydrogel is beneficial in maintaining the stability of DOX.

3.4 SUMMARY

This study demonstrated the possibility of preparing CG injectable hydrogels that can be used to deliver cells. DOX loaded PLGA nanoparticles were then placed in different hydrogels. The release profile analyzed by a single compartment modeling showed that DOX can be released in a controlled manner using CG cross-linked with TG. Addition of TG and media improved the mechanical property of the hydrogels with and without fibroblasts. CG cross-linked with TG showed significant improvement in the retention of human foreskin fibroblasts (hFF-1) cultures at day 5; cells recovered from CG-TG was 2.5 times more than that collected from CG with DOX release. There was inhibition of MMP-2/MMP-9 activity, directly correlating cause and effect of DOX release levels and improvement in hydrogel stability, which further helped cell retention. Cell cultures showed no toxicity from DOX at the proposed concentration, although TG crosslinking had some effect on cytotoxicity. Improved retention of cells holds promise in using the CG-based cell delivery to repair tissues.

CHAPTER IV

IMPROVED CHITOSAN-GELATIN INJECTABLE HYDROGELS FOR ADULT STEM CELL DELIVERY FOR CARDIAC REPAIR

4.1 Introduction

Regeneration of cardiac tissue was investigated by delivering stem cells to damaged cardiac tissue caused by myocardial infarction (Segers and Lee, 2008, Ye et al., 2011). However, 90% of injected cells were dead after one week due to various factors including delivery method and microenvironment of injected cells. Cell death can be attributed to a lack of uniform distribution and a lack of nutrients and oxygen due to the absence of blood flow to the tissue (Kurdi et al., 2010). To address these problems, biomaterials such as hydrogels and scaffold can be applied to cell based therapies (Kurdi et al., 2010, Pascual-Gil et al., 2015). To prevent cells from being lumped and delivered into a small area in the heart, hydrogels or scaffold can be first seeded with the cells and then implanted in the heart. With this method, cells will be distributed among the scaffold or hydrogel and be able to treat a larger area. In addition, both hydrogels and scaffolds can be designed to contain nutrients and oxygen releasing particles to supply the embedded cells with nutrients and oxygen (Camci-Unal et al., 2013, Oh et al., 2009). The preference of a hydrogel over a scaffold depends on the delivery mechanism.

With the use of scaffolds one must conduct an open heart surgery to implant the scaffold to the affected region. However, if one uses a hydrogel, a major complicated surgery approach can be avoided. Hydrogels can be design to respond to environmental changes such as temperature change, and therefore, are an excellent candidate for a non-invasive approach (Chenite et al., 2000). Researchers have shown that short term *in vivo* rat bone marrow derived stem cell survival was increased to 23% at the end of one week with the addition of a type I collagen gel (Simpson et al., 2007). Cell death is still being attributed to lack of nutrients and lack of oxygen. The addition of biomaterials have also brought a new set of problems, including mechanical stability, gelation time, and mechanical property compatibility (Li and Guan, 2011, Ye et al., 2011). Chitosan hydrogels are increasingly being explored to serve as cell carriers for biomedical approaches. This is in part due to their quick thermoresponsive characteristic that allows them to be a liquid at room temperature and solidify at body temperature (Cheng et al., 2010, Chenite et al., 2001, Chenite et al., 2000). Chitosan is obtained by deacetylation of chitin, the second most abundant polymer occurring in nature (Shigemasa Y, 1994). Chitosan is metabolized into non-toxic D-glucosamines by lysozymes (Mi et al., 2002, Tomihata and Ikada, 1997) and hence is biodegradable. In addition to being degradable and easily available, chitosan also shares features similar to glycosaminoglycans present in the extracellular matrix. Chitosan hydrogels can be developed to have a wide range of elastic moduli by simply changing the concentration of chitosan (Cheng et al., 2010, Huang et al., 2006, Mi et al., 2002, Ngoenkam et al., 2010). Chitosan hydrogels have previously been used to regenerate cardiac tissue with limited success during *in vivo* experiments (Hong et al., 2007). Cell death in this study was largely attributed to the degradation and

stability of the hydrogel. As previously mentioned, chitosan is biodegradable and the environment surrounding damaged cardiac tissue is populated with extra cellular matrix degrading enzymes. A disadvantage of using chitosan only hydrogels is that chitosan has no sites for cells to attach. Therefore, a polymer containing binding site is usually combined. In our laboratory, we have previously used gelatin to compliment chitosan hydrogels to be more compatible with cells (Huang et al., 2005, Iyer et al., 2012). Hydrogels containing gelatin are subject to premature degradation caused by an increased activity of matrix metalloproteases, specifically MMP-2 and MMP-9 (Makowski and Ramsby, 1998). However, we have previously shown how to increase the stability of the hydrogel by the addition of PLGA nanoparticles encapsulating doxycycline hyclate (Tormos et al., 2015).

Previously, we developed a chitosan-gelatin hydrogel that were able to withstand hFF-1 culture for 1 week (Tormos et al., 2015). In addition, this hydrogel had mechanical properties that were in the same order as cardiac tissue (Tormos et al., 2015). We were able to increase the mechanical stability of the hydrogel using a two prong strategy (Tormos et al., 2015). First, inhibition of MMP-2 and MMP-9 activity was achieved by exposing cells to doxycycline hyclate (Tormos et al., 2015). Second, the hydrogel's gelatin molecules were crosslinked by using transglutaminase. These two approaches helped increase the stability of the hydrogel both short and long term. In this study, we investigated the effect that different commercially available chitosan and gelatin had on the hydrogel's mechanical properties. Since improvements still felt short of our goal of obtaining a hydrogel with mechanical properties similar to cardiac tissue, we varied the concentration of gelatin from 0-10% (wt/v). Next, we subjected hydrogel from the

optimal conditions to cyclical testing and relax and hold tests to assess the hydrogel's ability to withstand continuous contraction and expansion. Finally, we investigated the hydrogel's ability to support human adipocyte stem cell culture for up to 3 weeks and assessed whether similar mechanical properties and a 3D environment were enough to differentiate human adipocyte stem cells to cardiomyocytes.

4.2 Materials and methods

4.2.1. Sources for Materials.

Low MW chitosan (50 kDa and 75-85% deacetylation), medium (190 - 310 kDa and 75-85% deacetylation), high molecular weight chitosan (310 - 375 kDa and 75-85% deacetylation), gelatin type A (100, 175, and 300 Bloom) and type B (225 Bloom), β-glycerophosphate (2GP), 50:50 poly lactic-co-glycolic acid (PLGA, 110 kDa), polyvinyl alcohol (PVA, 30-70 kDa, 87-90% hydrolyzed), Doxycycline hyclate (DOX, pharmaceutical secondary standard) and bovine serum albumin (BSA) were procured from Sigma Aldrich Co (St. Louis, MO). Phosphate buffer solution (PBS, pH=7.4), 5-(and-6)-carboxyfluorescein diacetate, succinimidyl ester (CFDA-SE) - mixed isomers, StemPro® Human Adipose-Derived Stem Cells, MesenPRO RS™ Medium kit, L-glutamine (200 mM, liquid), and powdered DMEM low glucose were procured from Life Technologies. (Carlsbad, CA). MMP-2/MMP-9 substrate I, fluorogenic was procured from Millipore (Billerica, MA). Food grade Active TI transglutaminase (Enzyme Commission 2.3.2.13) was procured from Ajinomoto (Fort Lee, NJ). Trypsin-EDTA was purchased from American Type Culture Collection (ATCC – Manassas, VA). Fresh porcine hearts were purchased from Ralphs Meat Packing Company located in Perkins,

OK. Anti-GATA4 antibody (catalog no. ab84593) was purchased from Abcam (Cambridge, MA). Purified anti-human CD105 (catalog no. 323202), FITC Donkey anti-rabbit IgG (catalog no. 406403), and PE anti-mouse IgG1 (catalog no. 406607) was obtained from Biolegend (San Diego, CA). DAPI Nucleic Stain (catalog no. D1306) was purchased from Thermo Scientific Pierce (Waltham, MA). 5-azacytidine (catalog no. A1287) and Dulbecco's Modified Eagle's Medium – low glucose (catalog no. D6046) was purchased from Sigma Aldrich (St. Louis, MO). Cultrex® Mouse Laminin I (1 mg/mL) catalog no. 3400-010-01 was purchased from Trevigen (Gaithersburg, MD). Fetal Bovine Serum (catalog no. 30-2020) was purchased from ATCC (Manassas, VA).

4.2.2. Hydrogel formulation.

Hydrogel solution was created by previous methods with minor modification (Tormos et al., 2015). In brief, chitosan, gelatin, powdered low glucose DMEM (cat no. 31600-083), and TG, were prepared in 0.1N HCl according to previous reported methods(Tormos et al., 2015). Solutions were stirred for a minimum of four hours at a temperature of 50-70°C. After the polymers completely dissolved, solution was transferred to a 50 mL centrifuge tube, placed in an ice bath, and 0.56 g/mL 2GP was added drop wise under constant stirring until pH reached biological conditions (7.2-7.4). When Dox was added, DOX-PLGA nanoparticle were filtered through a 0.22μm filter and then added to the hydrogel solution and mixed thoroughly.

4.2.3. Mechanical Characterization.

Compression tests. Unconfined compression testing was performed on hydrogels using an

INSTRON 5542 (INSTRON, Canton, MA) and a custom-built anvil with a diameter of 25mm, as described previously (Tormos et al., 2015). In brief, hydrogels were casted in 6-well tissue culture plates by incubating 3 mL of solution for 2 hours at 37ºC. Hydrogels were compressed at 1 mm/min crosshead speed. Data were exported to MS Excel and compressive modulus was calculated from the slope of the linear portion (20% to 40% strain range) of the stress-strain plot.

Tensile tests. Tensile tests were also conducted by applying the load orthogonal to compression testing to ensure uniform cross-linking of the hydrogels, as described previously (Tormos et al., 2015). In brief, 20 mL of hydrogel solution was prepared in a 35mm petri dish and incubated for 2 hours. After incubation, 10mm × 14 mm × 3 mm rectangular slices were cut out and loaded to the Instron 5542 and pulled to break at a crosshead speed of 1 mm/min at room temperature. After data collection, stress vs strain was plotted and the slope of the linear region, the elastic modulus, was determined. For all tests, a minimum of three experiments were performed per condition from different preparations.

Stress relaxation experiments. Hydrogel samples were prepared similar to tensile tests were used in these experiments and porcine heart tissue samples were prepared as described in section 2.1. These samples were subjected to seven successive steps of ramp and hold tests. Each ramp was stretching to 5% at 2.5%/s of the original length. Each holding was for 20 seconds. Stress was plotted against time. To understand the effect of each stage on the hydrogel, they were normalized by subtracting stress and time elapsed at the beginning of each stage. In addition, reduced relaxation function was calculated to understand the amount of stress relaxed in each stage, similar to our previous publications

(Ratakonda et al., 2012). Porcine hearts were sliced while frozen at a thickness of 3mm using a deli slicer blade.

Cyclical tests. Hydrogel samples were prepared similar to tensile tests and porcine heart tissue samples were prepared as described in section 2.1 were stretched 10% of their length and then returned to their original position. Sample were stretched at a speed of 72 cycles per minute for up to 30 min.

4.2.5. Cell culturing in hydrogel.

Human adipocyte stem cells (hASCs) were expanded in MesenPRO RS™ Medium kit, following vendor's protocol. Cells were maintained at 37°C, 5% CO_2/95% air, and fed with fresh medium every 2-3 days. Once confluent, cells were detached with trypsin-EDTA 1X and then trypsin was neutralized using MesenPRO RS™ Medium. Cells were centrifuged at 210×g for 5 min and dispersed in growth medium. Viable cells were counted using Trypan blue dye exclusion assay.

hASCs between the passages 3-8 were stained with CFDA-SE, and seeded onto hydrogel samples using the procedure previously developed by my laboratory with minor modifications (Tormos et al., 2015). In brief, cells were incubated in growth medium containing 2 μM CFDA-SE at 37°C for 20 min followed by washing the excess stain with growth medium. Cells were added to the hydrogel at 0.5×10^6 cells/mL hydrogel and mixed evenly within the solution. 0.5 mL of mixture was then dispensed into the 6-well plate and incubated at 37°C for until gelation was achieved. Then, 2mL growth medium was added. After 24 hours, the growth medium was collected for viability via CFDA SE

analysis and replaced with fresh growth medium. This process was repeated every 48 hours until completion of experiment.

After completion of experiment, cytoplasmic CFDA SE content was extracted from live cells by three cycles of freeze and thaw, using the procedure previously reported (Tormos et al., 2015). In brief, cell culture medium was replaced with 2mL PBS and placed at -20°C until the PBS froze. After the PBS freezes, the plates were thawed at room temperature and cycle was repeated. Then, the solution was collected and the absorbance was determined using a spectrophotometer Gemini XS spectrofluorometer (MDS technologies, Santa Clara, CA) at the excitation and emission wavelengths of 485 nm and 525 nm, respectively. The CFDA-SE content in the spent medium was also assessed. Obtained fluorescence intensities were converted to number of cells using a calibration of fluorescence intensity to number of cells obtained as previously described (Tormos et al., 2015).

4.2.6. 2D Differentiation protocol.

Differentiation in 2-D culture was carried out in two different ways similar to previous reports (Choi et al., 2010, Wan Safwani et al., 2012, van Dijk et al., 2008, Chang et al., 2012). First, differentiation of hASCs was attempted using Phorbol Myristate Acetate (PMA). In brief, 100,000 hASCs were seeded on each well of a six-well plate. 24 hours after seeding, cells were washed with PBS twice and growth medium containing 10µM PMA was added. Growth medium was changed every three days and the experiment concluded after nine days. On day nine, cells were harvested and stained with antibodies. GATA4 (a transcriptional activator) and cardiac troponin I (cTropI, the inhibitory subunit

of troponin) are genetic markers commonly used to identify cardiomyocytes (Heineke et al., 2007, Wang et al., 2004). The second method was to use laminin and 5-azacytidine as others have previously done (Choi et al., 2010, van Dijk et al., 2008, Wan Safwani et al., 2012). Briefly, for hASCs cultured on laminin, 2mL of a PBS solution containing laminin (concentration 0.42µg/mL) was added to each well. After 30minutes, wells were washed with fresh PBS. 10,000 hASCs were cultured in each well and supplemented with control growth medium (DMEM supplemented with 10% FBS). After 24 hours, cells were washed with phosphate buffer solution (PBS) and growth medium containing 5-azacyidine (9µM) or controlled medium was added. Twenty-four hours after exposure to AZA, cells were washed with PBS and supplemented with controlled growth medium for the duration of the experiment. Growth medium was replaced every three days until completion of the experiment. After 3 weeks culture, hASCs were washed and stained with Endoglin (CD 105), hASC marker, GATA4, cardiac marker, and DAPI, nucleic acid marker (Choi et al., 2010, van Dijk et al., 2008, Wan Safwani et al., 2012).

4.2.6. Immunohistochemistry

After completion of cell culture experiments, some samples were processed for cryosectioning. Samples were submerged in Tissue-Tek® O.C.T. Compound and frozen at -20°C. Samples were sent to Stephenson Cancer Tissue Pathology Core at the University of Oklahoma for cryosectioning. Samples were cut at a thickness of 6µm. After cryosectioning, slides were prepared for immunohistochemistry. First, using a PAP pen a border was drawn around the sample of interest. Next sample was washed with PBS to get rid of any leftover OCT. PBS containing 1% BSA was added in order to

crosslink any non-specific sites and incubated at room temperature for 30 minutes. After 30 minutes, slide was rinsed with PBS and primary antibody was added and incubated for 60 minutes at room temperature. After 60 minutes, slide was rinsed with PBS and secondary antibody was added and incubated for 30 minutes at room temperature. After 30 minutes, slide was rinsed with PBS and either DAB or DAPI was added and incubated at room temperature for 5 minutes. If DAB was added, after 5 minutes, slide was rinsed with PBS and hematoxylin was added and incubated for 15 seconds. After 15 seconds, slide was rinsed thoroughly with PBS. Slide was covered with 2-3 drops of cytoseal and a cover slip and was allowed to dry in a dust free place. Digital photomicrographs were captured at representative locations using a CCD camera connected to an inverted microscope.

4.2.7. RNA expression

RNA expression of CD105 and CD44 was analyzed by qPCR. Cells cultured on 6 well plate were harvested using trypsin. RNA was isolated using RNeasy Mini Kit from Qiagen and following vendor's protocol. After RNA was isolated, RNA concentration was determined by using Nanodrop 1000 (Thermo Scientific). Next, RNA was purified by using DNase I, Amplification Grade (cat No. 18068-015) from ThermoFisher Scientific. After all DNA has been digested, sample is prepared for amplification. RT-PCR was carried out by using SuperScript™ III First-Strand Synthesis SuperMix for qRT-PCR (cat. No. 11752-050) from ThermoFisher Scientific and following their protocol. Amplification was carried out in 0.2mL centrifuge tube with a domed cap from Thermo Scientific Pierce (cat. No. SP-0019). Amplification was carried in the PTC-100

programmable thermal controller (MJ Research, Inc.). Next, qPCR was achieved using SYBR® GreenER™ qPCR SuperMix Universal from ThermoFisher Scientific (cat No. 11762-100) and following vendor's protocol, with minor modifications. Vendor's protocol was modified to account for a smaller volume than recommended (20μL instead of 50μL). Primers' sequence for adipocyte stem cell markers were obtained from Su et al (Su et al., 2014). Custom primers were ordered from Integrated DNA Technologies (Coralville, IA). Primers used are presented in Table 1 along with their sequence. qPCR was carried out in a 96 well plate and using the 7500 Real Time PCR System (Applied Biosystems, Grand Island, NY). Results from qPCR experiment were analyzed using 7500 System Software (Applied Biosystems, Grand Island, NY).

4.2.8. Statistical evaluation.

All experiments were repeated three or more times. Significant differences between two groups were evaluated using a one-way analysis of variance (ANOVA) with 95% confidence interval. When $P<0.05$, differences were considered to be statistically significant.

4.3 Results and discussion

4.3.1. Effect of Gelatin and Chitosan Properties on Compressive properties

We used the previous formulation as the baseline, a chitosan-gelatin hydrogel (CG) with 2%wt and 4%wt, respectively (Su et al., 2014).Using LMW chitosan and type A (acid solubilized gelatin) 300-bloom gelatin (CG) previously, we demonstrated that the addition of growth medium and transglutaminase (TG) improved the mechanical

properties of the hydrogel (Tormos et al., 2015). We performed compression testing on gel specimens at room temperature. Assuming Hook's law, elastic modulus was determined from the linear region. Others have reported that increasing the concentration of chitosan also increases the rate of gelation (Cheng et al., 2010, Ngoenkam et al., 2010). Further, hydrogels showed spongy porosity with open pore architecture, suitable for the diffusion of nutrients to the entrapped cells. Hydrogels containg only chitosan revealed loose, irregular and larger pore diameters wheras, the collagen only based hydrogels exhibited interconnected fibrous network (Wang and Stegemann, 2010, Song et al., 2010). However, the hydrogel's mechanical properties were not similar to porcine cardiac tissue (46.89 ± 5.63 kPa).

Commercially, there are different types of chitosan and gelatin, therefore it is important to characterize and investigate different types of chitosan and gelatin to determine the best formulation for cardiac regeneration therapy. To assess the effect of gelatin's type (either acid solubilized or base solubilized) and bloom number (or MW), we changed the type of gelatin while using the low molecular weight chitosan for all the formulations. We determined the compressive modulus for gelatin type A 100 bloom (CG-100 type A), gelatin type A 175 bloom (CG-175 type A), gelatin type B 225 bloom (CG-225 type B), and gelatin type A 300 bloom (CG, the baseline and previously used formulation). In **figure 4.1a**, the stress and the strain from the different samples was plotted and a line was fitted through, the resulting slope is the compressive modulus of the sample. In **figure 4.1b**, the hydrogel with the highest compressive modulus was CG, the baseline, with a compressive modulus of 6.84 ± 0.70 kPa when looking at the different types of gelatin. There was a significant difference between CG and the other different gelatin

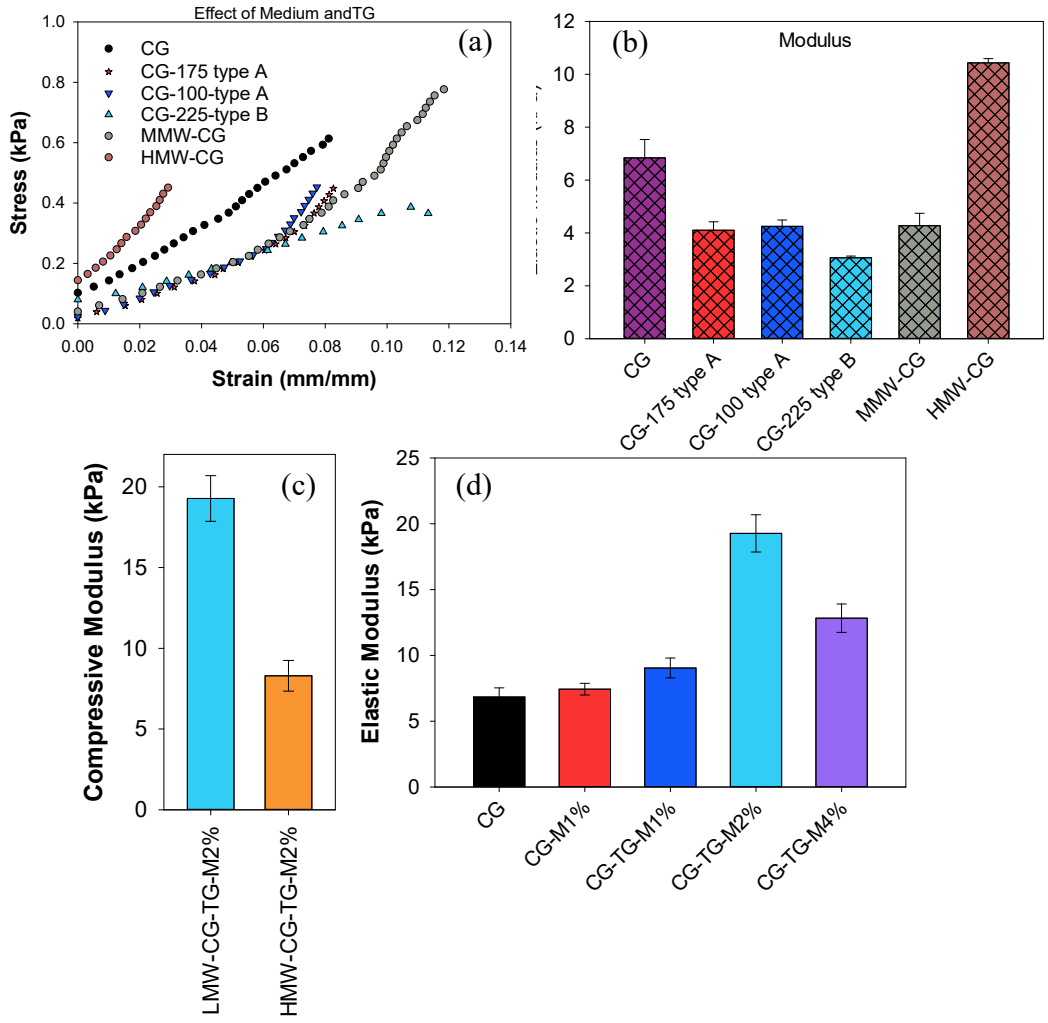

Figure 4.1. Effect of MW of Chitosan and Gelatin on linear compressive properties. (a) Stress-strain curves of various samples. (b) Effect of chitosan molecular weight on compressive modulus. (b) Changes in the compressive modulus. (c) Effect of MW of chitosan on compressive modulus with gelatin type A 300 bloom, TG and 2% media. (d) Effect of powdered growth medium concentration with LMW chitosan, gelatin type A 300 bloom.

formulations but no significant difference was found between the other gelatin formulations. Further, to assess the effect of chitosan's molecular weight on the hydrogel's compressive modulus, we used gelatin type A 300 bloom for all different chitosan molecular weights. We determined the compressive modulus for low molecular weight (CG), medium molecular weight (MMW), and high molecular weight chitosan (HMW). In **figure 4.1b**, the hydrogel with the highest compressive modulus was HMW.

This compressive modulus 10.43 ± 0.16 kPa were as our baseline was 6.84 ± 0.70 kPa. Previously, we have used low molecular weight chitosan and type A 300 bloom gelatin with 2% (w/v) growth medium and 0.003% (w/v) transglutaminase. Using high molecular weight chitosan (in the absence of media and TG) resulted in a higher compressive modulus than low molecular weight chitosan. Therefore, we compared our previously obtained data with high molecular weight chitosan with type A 300 bloom gelatin, 2% (w/v) media, and 0.003% TG (w/v). The addition of media and TG hindered the compressive modulus of the hydrogel (**figure 4.1c**). There was a significant difference between the two formulations. Our previous formulation had a compressive modulus of 19.27 ± 1.41 kPa and the new formulation had a compressive modulus of 8.30 ± 0.95 kPa.

Next, we determined the effect of powdered growth medium concentration in the hydrogel's formulation (**Figure 4.1d**). We tested two different formulations and compared them with our previous results. The hydrogel's compressive modulus was higher at 2% (w/v). Higher (4% w/v) and lower (1%w/v) concentrations resulted in lower compressive modulus.

4.3.2. Effect of Gelatin Concentration on Compressive properties

So far we've determined the best type of gelatin, type of chitosan, and amount of growth medium. However, we are still not close to the compressive modulus of cardiac tissue 46.89 ± 5.63 kPa. Therefore, we wanted to further manipulate the formulation in order to obtain a hydrogel with a higher modulus. Similar to what we did with growth medium, we looked at changing the concentration on either chitosan or gelatin. Our lab has

previously shown the benefits of gelatin in terms of cell attachment and spreading. For cardiac application, we want cells to be able to spread, therefore, it would be beneficial to have more gelatin than chitosan. In our next experiment, we varied the concentration of

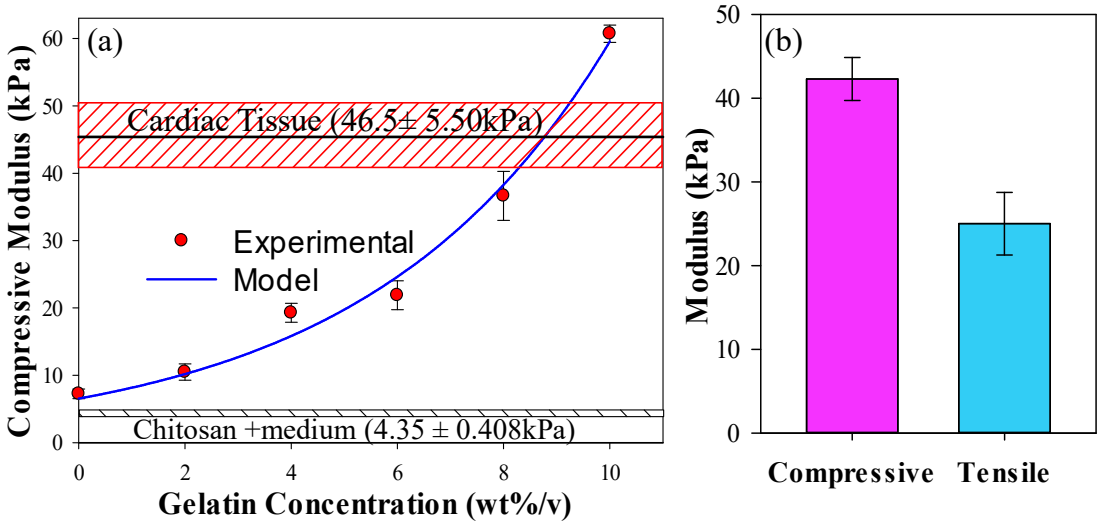

Figure 4.2. Effect of gelatin concentration and TG cross-linking on mechanical properties. (a) Compressive properties and used the model is Modulus=$6.54e^{0.221C}$ where c is the concentration in Weight%/volume. (b) Effect of tensile testing in the orthogonal direction relative to compressive property.

gelatin from 0% (w/v) to 10% (w/v), concentrations higher than 10% (w/v) had premature gelation problems (**Figure 4.2a**). These formulations were created with low molecular weight chitosan (2% w/v), growth medium (2% w/v), and TG (0.003 % w/v). The closest compressive modulus to that of cardiac tissue was the formulation with 8% w/v gelatin. This formulation had a compressive modulus of 36.64 ± 3.64 kPa. The next higher concentration (10 %w/v) had a compressive modulus of 60.72 ± 1.28 kPa. Since a concentration of 8% w/v is closer to cardiac tissue than 10% w/v, we decided to use 8% w/v gelatin for further experiments.

Compressive tests only evaluate the properties of the material in one direction. Therefore, we wanted to evaluate the properties of the hydrogel in another direction. Next, we submitted hydrogel samples to tensile tests (**Figure 2b**). The Tensile modulus

was 25.02 ± 3.74 kPa. Since the mechanical properties vary along with the direction at which the force is applied, this hydrogel formulation can be considered anisotropic, which is similar to cardiac tissue. Since chitosan chain length could show steric hindrance to the cross-linking reaction of gelatin with TG, the effect of MW was tested. Low MW chitosan (**Figure 4.2a**) had higher strength than high MW chitosan in the presence of growth media and TG. Tensile tests were also performed by connecting the hydrogels in the orthogonal direction to that of the compressive directions. Analyzed properties (**Figure 4.2b**) were similar to that of compressive condition, suggesting hydrogels are isotropic and different components are uniformly distributed including the chemical cross-linking reaction of TG.

4.3.3. Comparison of viscoelastic behavior of the hydrogel.

Cardiac tissue is stretched in different directions and in a cyclical fashion and behaves like viscoelastic materials which store and dissipate energy within the complex molecular structure, producing hysteresis and allowing creep and stress relaxation to occur (Ratakonda et al., 2012, Chen et al., 2008). Thus, a full description of the mechanical analysis requires nonlinear viscoelastic behavior. For this purpose, we performed experiments with new formulation and compared with porcine cardiac tissue. Also, one stage is not sufficient to understand the relaxation behavior as the accumulated stress levels in each stage is different, hence samples were subjected to 7 stages of ramp-and hold experiments with load limits predetermined by the linear portion of the stress–strain curves obtained under tensile testing. First, a stress vs time plot showed (**Figure 4.3a**) that the hydrogel was able to withstand less stress in the tensile mode while compression

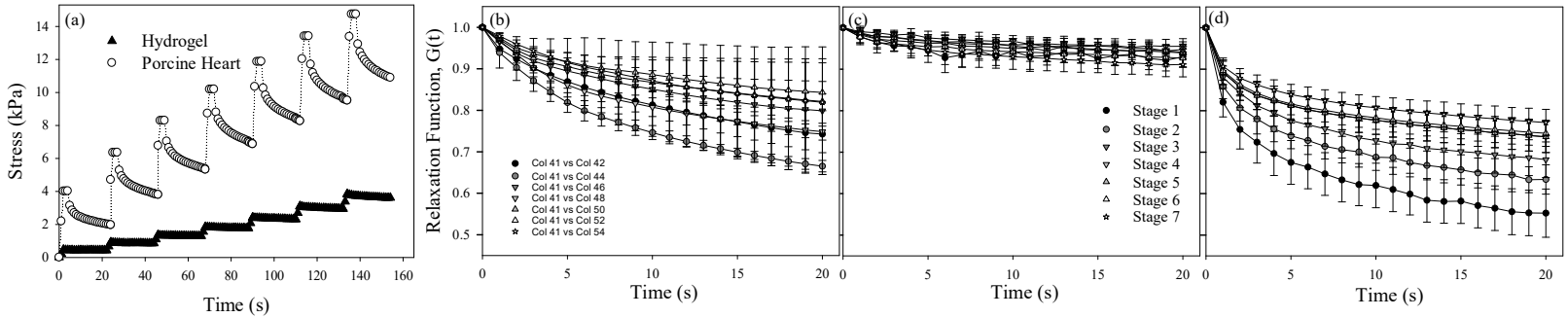

Figure 4.3. Comparison of stress-relaxation behavior between porcine pericardium and hydrogel. (a). Effect of ramp and hold on stress relaxation. (b) Reduced relaxation function for different stages in the 2%8% CG hydrogel with TG. (c). reduced relaxation function for porcine pericardium.

conditions were similar to the cardiac tissue. The initial stress accumulated in the first cycle varied from 2.5 kPa to 4 kPa in the cardiac tissue. The percentage relaxation in the first stage was 45% in the first stage which decreased to 23% in the cardiac tissue. In tensile mode, the relaxation in the CG hydrogel varied from 5% to 10%. In compressive mode relaxation varied from 7% to 15%. This is unlike the CG porous scaffolds prepared by freeze-drying which showed nearly 90% relaxation in successive stages. Interestingly, the cross-linked samples showed strain hardening characteristics similar to natural tissues including cardiac tissue; the more the material is stretched, the stiffer it gets. This is unlike CG porous scaffolds which showed no effect of ramp and hold on the stiffness characteristics of materials. This suggests the TG cross-linking changes the properties of the matrixes and there may be a

post-translation modification of the matrixes by TG. To verify this point, the stress and time were normalized so that each cycle can be accurately compared. **Figure 4.3b-c** also shows that hydrogel stabilizes faster than cardiac tissue during the hold of the material, whereas cardiac tissue takes more time to stabilize.

4.3.4. Comparison of cyclical behavior of the hydrogel.

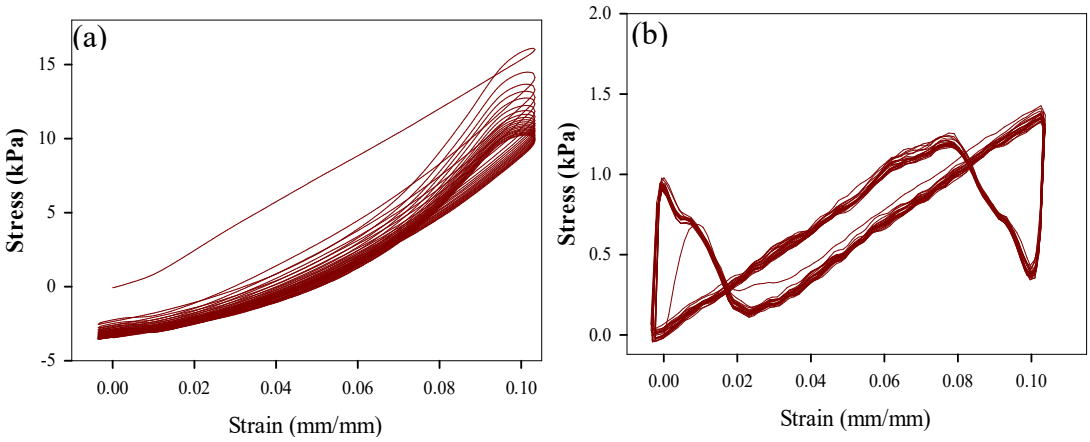

Figure 4.4. Cyclical behavior between porcine pericardium and hydrogel. (a) Porcine pericardium. (b) 2%8%CG hydrogel with TG and medium. Shown are the first 20 cycles in each sample.

Cardiac tissue is stretched 10% of its length repetitively in cyclical form and the injected matrix has to support the process until maturation of the tissue (Lee and Boughner, 1985). Therefore, we wanted to test whether the hydrogel can withstand repeated contraction and expansion just as the heart tissue experiences. We conducted cyclical test on 2%8% hydrogel where we took the hydrogel and stretched and contracted it 10% of its length for various times at a frequency of 72 cycles per minute (**Figure 4.4**). We observed two things: the first being that after 30 minutes of continues cycles the hydrogel did not break and no tears were observed. Second, we quantified the stress and strain and compared it to porcine cardiac tissue. Except the first cycle, the rest of the cycles were identical.

Hence, only first thirty cycles are shown (Figure 1g). These results show that hydrogels to be used have appropriate mechanical properties for use in cardiac tissue regeneration. The hydrogel is able to sustain less stress than that of cardiac tissue.

4.3.5. Retention of adipocyte stem cells.

Apart from mechanical property similarity, an important characteristic of this hydrogel is cell culture compatibility. To assess the hydrogel's ability to support stem cell culture, stem cells stained with CFDA-SE were seeded in the hydrogel and cultured for 1,2, or 3 weeks. Previously we have used CFDA-SE to determine *in vitro* retention of fibroblast embedded in hydrogels (Tormos et al., 2015). The amount of retention of live cells in the hydrogel varied from 84.09±4.02% to 79.57±2.10%, with highest viability at 1 week and the lowest at 3 weeks (**Figure 4.5a**).

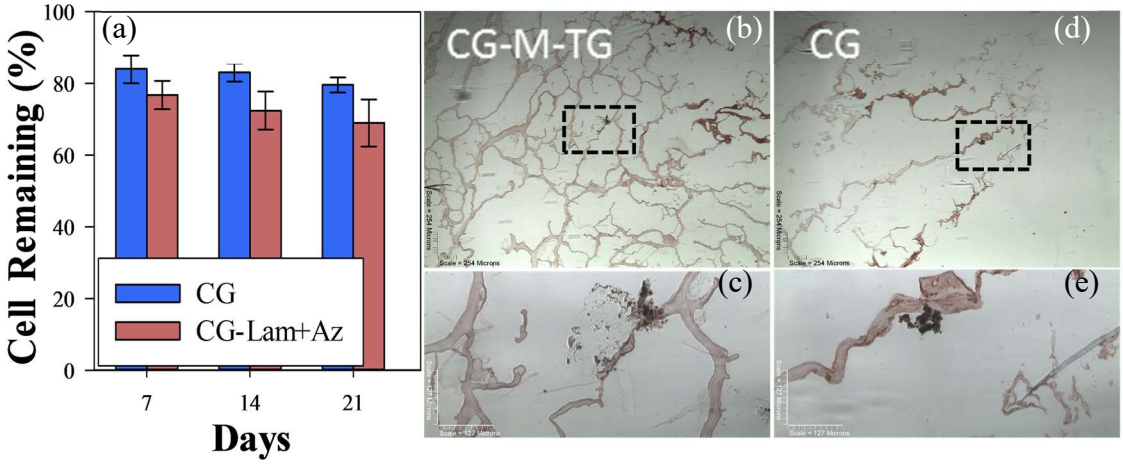

Figure 4.5. hASC retention and distribution after 21 days in culture. (a) Cells recovered. (b) CG-M-TG hydrogel after 7 days stained with CD105-HRP (red) conjugate and counterstained with hematoxylin for nucleic stain (black) at 4X magnification. (c) 20X magnification of insert in (b). (d) CG hydrogel after 7 days stained with CD105-HRP (red) conjugate and counterstained with hematoxylin for nucleic stain (black) at 4X magnification. (e) 20X magnification of insert in (d).

These decrease in cell viability is small and probably due to degradation of scaffold. Still,

at all time points, we have surpasses our previous cell viability percentage which was at 60% for a seven day period (Tormos et al., 2015). In addition to viability, some hydrogel samples were cryosectioned and stained for H&E. This comparison of CG and TG hydrogels shows the benefits of crosslinking gelatin molecules with TG. As it is seen in Figure 5b-c, TG containing hydrogels appear to have a more interconnected network, whereas non TG hydrogels are less connected and more prone to degradation and destabilization.

4.3.5. Status of adipocyte stem cells.

Another goal of the hydrogel was to serve as a differentiation vessel for stem cells into cardiomyocytes. To test whether stem cells retain their genomic profile, qPCR, flow cytometry, and immunohistochemistry was conducted on cells seeded on TCP and hydrogel samples. hASCs are routinely characterized by detecting CD105 (or endoglin, a type I integral transmembrane glycoprotein) and STRO-1 (a 75kd surface protein) (Zannettino et al., 2008, Pierelli et al., 2001). To confirm whether the commercially purchased hASC maintained these markers in extended tissue culture, I evaluated them by flow cytometry. hASCs were harvested (100,000 cells) with TrypLE proteolytic

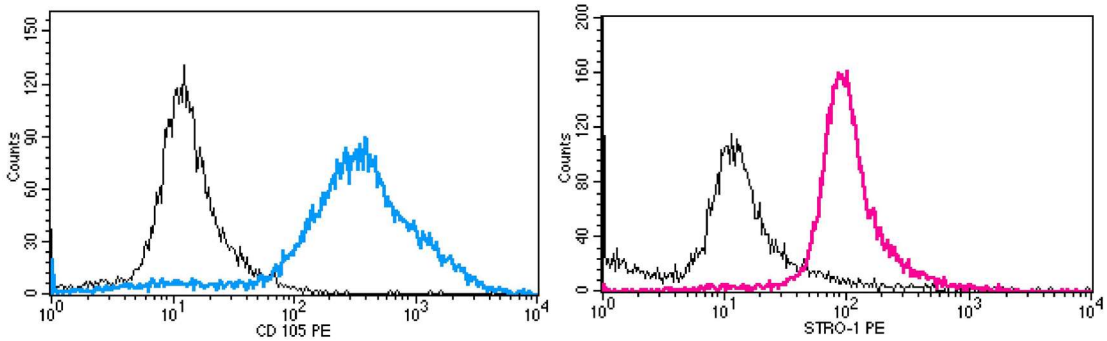

Figure 4.6. Presence of hASC markers a) Histogram plot for CD105. b) Histogram plot for STRO-1.

enzyme and stained with antibodies and respective isotype controls. The cell population was divided into three groups. First group, negative control group and black line in **Figure 4.6**, contained no antibody stain. The two other groups were stained with CD 105 and STRO-1 separately. After analyzing these samples using the flow cytometer, I obtained histogram plots for all groups (**Figure 4.6**). These plots show the hASCs were positive for both CD105 and STRO-1.

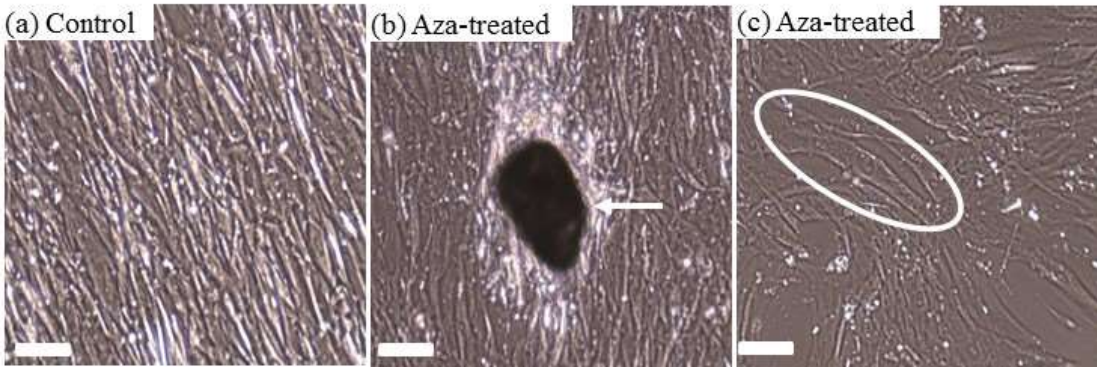

Figure 4.7. Morphological changes of hASCs after exposure to 5-Azacytidine after 2

First differentiating hASCs into cardiomyocytes was investigated using PMA because the differentiation protocol calls for shorter duration (9 days instead of 21 days for other methods) of incubation. However, no morphological changes were observed on the final day of experiment. PMA was substituted by 5-azacytidine and laminin similar to previous reports (van Dijk et al., 2008). To verify what 5-azacytidine and laminin were a viable option for cardiac differentiation, hASCs were exposed to 5-azacytidine and cultured on laminin coated plates. Similar to previous reports, morphological changes were observed at 2 weeks (**Figure 4.7**). To characterize the genetic profile qPCR and immunohistochemistry were conducted at the end of 3 weeks. qPCR methods outlined on section 4.2.8 were followed for hASCs cultured on TCP for 21 days. qPCR methods

showed that there was no genotypic change for hASCs cultured on TCP for 3 week (**Figure 4.8**). For immunohistochemistry, methods outlined on section 4.2.7 were followed on TCP samples that have been cultured for 21 days. Immunohistochemistry images shows that hASCs markers (CD105 and CD144) are present in the absence of 5-azacytidine and laminin. On the contrary, presence of hASC markers decrease and cardiac markers start to appear when exposed to 5-azacytidine and laminin. For some unknown reason, cardiac markers were visible using immunohistochemistry but not on qPCR. Since these experiments were conducted on different samples, it is possible that samples used for qPCR did not differentiate. This is a plausible reason since differentiation by 5-azacytidine is somewhat inconsistent (Wan Safwani et al., 2012). Furthermore, immunohistochemistry was conducted on hydrogels embedded with hASCs and cultured for 3 weeks. From these results we can conclude that neither the media nor the hydrogel's mechanical properties are enough to cause differentiation of hASCs.

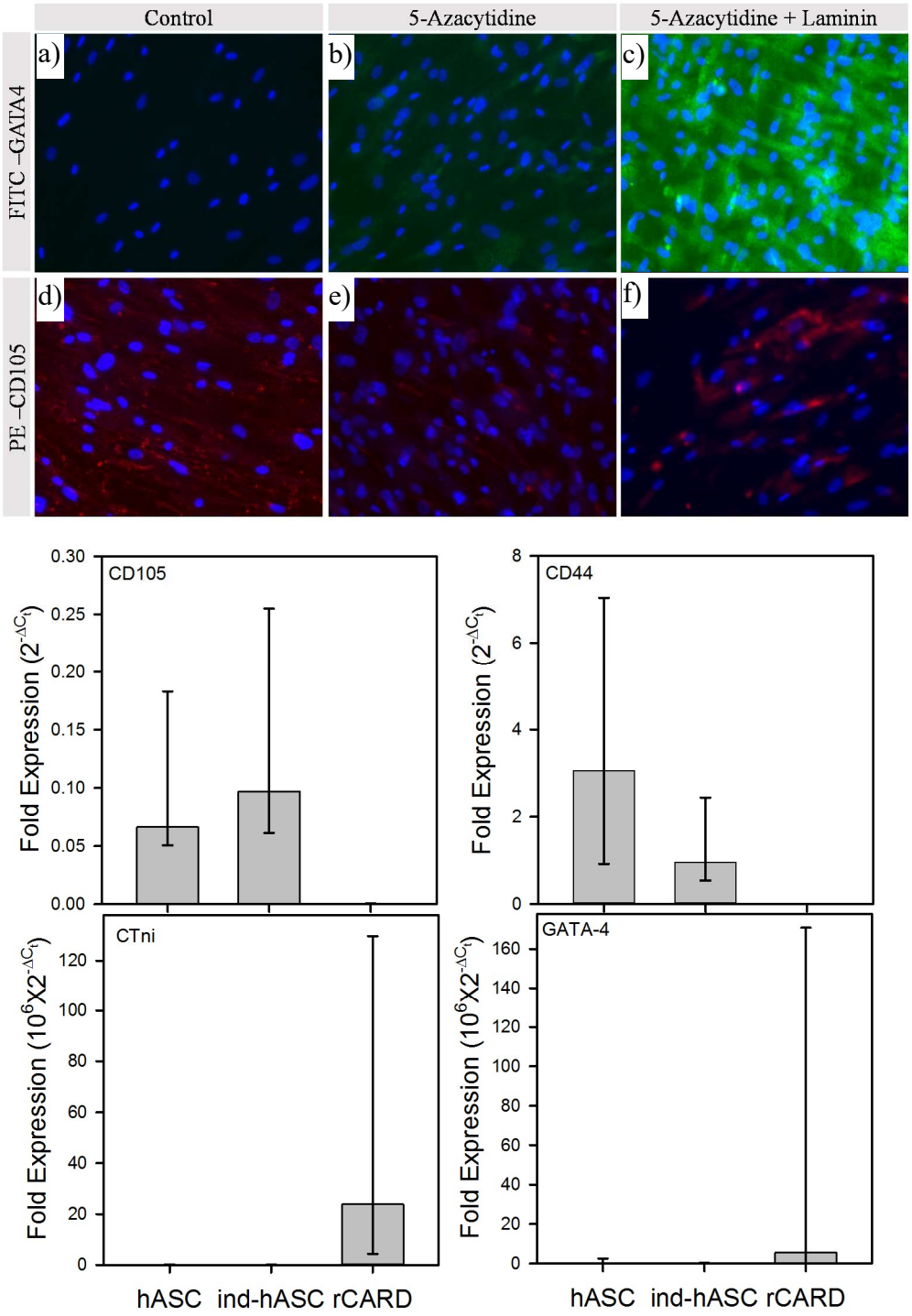

Figure 4.8. Effect of laminin coating and 5-Azacytidine in 2D cultures. Green fluorescence color (a-c) represents FITC tagged GATA4 antibody, red fluorescence color (d-f) represents PE tagged CD105 antibody. Control images show no green color and a lot of red (a, d). This is expected as those cells were not exposed to 5-azacytidine nor laminin. 5-azacytidine cells showed both markers, meaning some differentiation is taking place but not very effectively (b, e). 5-Azacytidine and laminin treated cells showed a high amount of green color, meaning GATA4 expression is high, and low red color, meaning CD105 expression is low (c, f).

The addition of a stimulant must be included for cells to differentiate. Previously, we presented an injectable hydrogel that had mechanical properties similar to cardiac, was able to support hASC culture for three weeks without significant cell loss, and was able to withstand premature enzymatic degradation. Immunological staining showed that mechanical properties and a 3D culture environment were not enough to differentiate hASCs into cardiomyocytes. Therefore, we decided to include into the hydrogel 5-azacytidine and laminin to induce cardiac differentiation. Van Dijk et. al showed that hASCs cultured on laminin and exposure of 5-azacytidine for 24 hours induced differentiation after 3 weeks (van Dijk et al., 2008). We repeated the experiments and got similar results (**Figure 4.9**). However, similar to previous reports, no beating cells were observed.

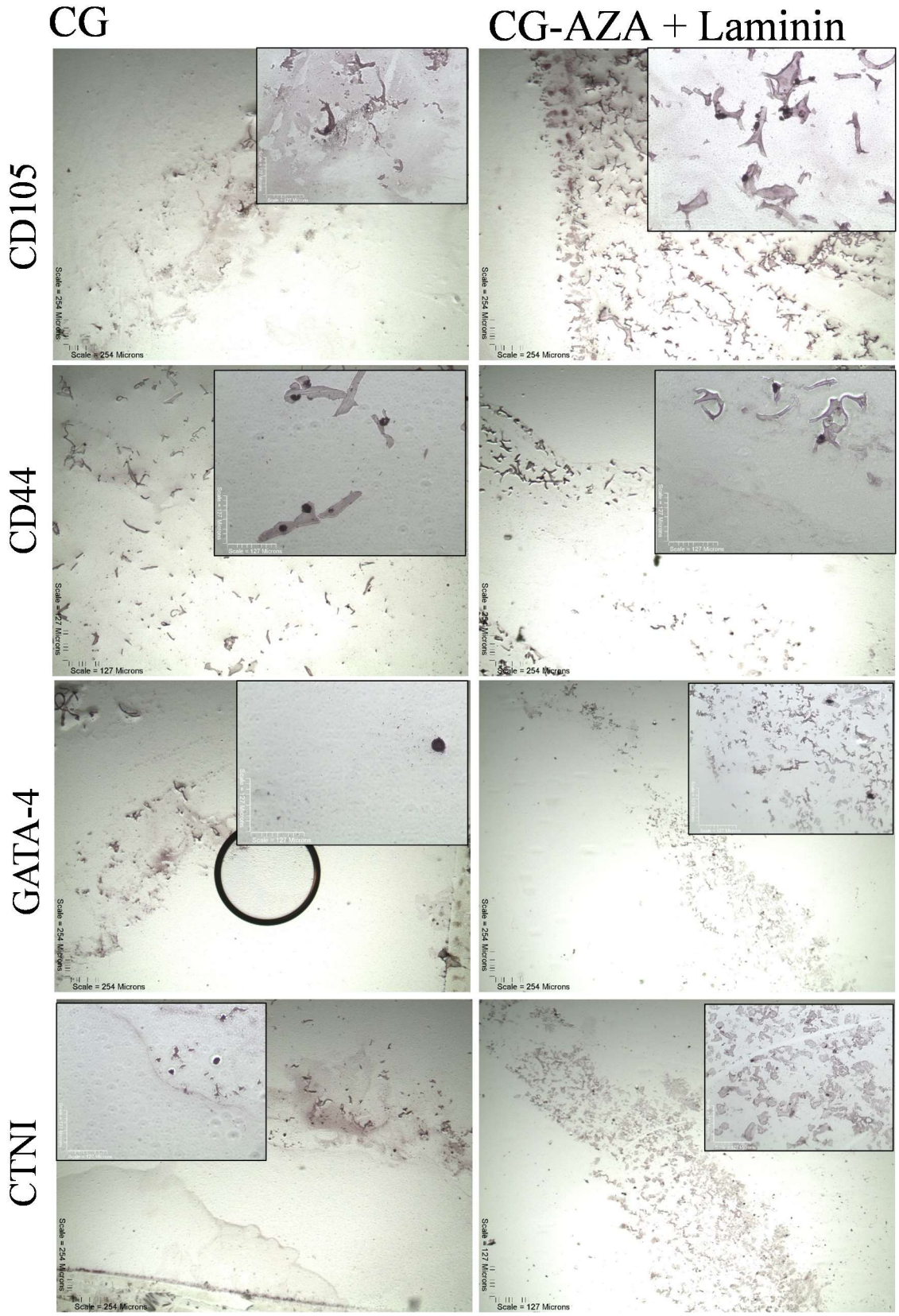

Figure 4.9. Immunohistochemical images of CG hydrogels containing TG with or without exposure of laminin and 5-azacytidine.

4.6. SUMMARY

In this study, I evaluated the possibility of improving the mechanical properties of an injectable hydrogel to be used for cardiac regeneration therapy. The optimal formulation for cardiac regeneration therapy by investigating the effects that different molecular weights of chitosan, gelatin, different types of gelatin, and growth medium concentration had on the hydrogel's mechanical properties. The condition with the most significant effect on mechanical properties was the concentration of gelatin. I found that the amount of gelatin can be altered to obtain different mechanical properties without sacrificing the injectable hydrogel main characteristics. In addition to determining mechanical properties, we also evaluated the hydrogel in activities that the cardiac tissue experiences. During cycle tension test, we realized that while hydrogel and cardiac tissue have similar profiles, cardiac tissue remains more elastic than the injectable hydrogel. During the relax and hold test, we found that another similarity that this injectable hydrogel has with cardiac tissue is that both hardened with increased amount of stretching. Not only did we observed mechanical improvements but improvements were also observed during cell culture experiments. Previously, we had a 60% cell viability after 1 week of cell culture and now we can surpass that even at 3 weeks. H&E staining further supports the notion that TG crosslinking makes the hydrogel more stable by showing a more interconnected material than hydrogels without TG. Finally, we determined that media nor mechanical property similarity can differentiate hASCs into cardiomyocytes. Therefore, for future studies, we will look into the possibility of adding a chemical stimulant known to differentiate hASCs into cardiomyocytes.

.

CHAPTER V

AN INJECTABLE OXYGEN RELEASING CHITOSAN-GELATIN HYDROGEL FOR CARDIAC TISSUE ENGINEERING

5.1. Introduction

For years, heart disease has been the leading cause of death in the United States (Mendis et al., 2011, Roger et al., 2012, Writing Group et al., 2010, Go et al., 2013, Members et al., 2012, Kochanek et al., 2011). Myocardial infarction, otherwise known as heart attack, affects millions of Americans every year. For years, patients who have been diagnosed with experiencing a heart attack have relied on preventative treatments, meaning these treatments focused of reducing the risk of enduring another heart attack. Thanks to advances in the field of tissue engineering, there is a dim light of hope for patients with damaged cardiac tissue (Segers and Lee, 2008, Ye et al., 2011). Researchers are utilizing stem cells to repair and regenerate the cardiac tissue. Researchers have seeded millions of stem cells in the damaged region and have had limited success. This attrition of cells is believed to be due to the lack of blood supply to the damaged tissue which exposes the implanted cells to a nutrient and oxygen deprived environment (Kurdi et al., 2010). Another problem is the lack of cellular distribution, however, researchers have overcome this challenge by incorporating biomaterials to the cell based therapy.

The addition of biomaterials introduce a number of challenges that must be addressed if this therapy is to be successful. These challenges include a compatibility between cardiac tissue and scaffold, addition of nutrients and oxygen, and mechanical stability of the scaffold (Kurdi et al., 2010, Pascual-Gil et al., 2015). Previous studies from our group have focused on developing and optimizing an injectable hydrogel with nutrients, mechanical properties similar to cardiac tissue, and prolonged stability of the material (Tormos et al., 2015). This study will focus on delivering oxygen to cells embedded in the damaged tissue. Oxygen generating materials are centralized over the production of hydrogen peroxide because with the production of two hydrogen peroxide molecules it will further react to produce two molecules of water and a molecule of oxygen (Equation 1) (Camci-Unal et al., 2013).

$$2H_2O_2 \rightarrow O_2 + 2H_2O$$

Solid inorganic peroxides, such as calcium peroxide (CaO_2), magnesium peroxide (MgO_2), and sodium percarbonate (Na_2CO_2), are the primary candidates for the production of hydrogen peroxide. This is because upon the reaction of solid inorganic peroxides and water, hydrogen peroxide will be formed. For instance, take calcium peroxide as an example (Equation 2).

$$2CaO_2 + 4H_2O \rightarrow 2CaOH + 3H_2O_2$$

However, the drawbacks of solid inorganic peroxides are due to their solubility limitations. Calcium peroxide has a solubility of 1.65g/L and due to the production of calcium hydroxide the pH of the environment were calcium peroxide dissolves will rise.

This change in pH can be a problem especially for tissue engineering applications where pH change can cause cell death.

The next part of this study is to assess differentiation on a 3D environment. Previously, we have shown that the adipocyte stem cells embedded in the hydrogel were not able to differentiate into cardiomyocytes. This supports the idea that while mechanical cues are important for differentiation, embedding stem cells in a tissue with mechanical properties similar to cardiac tissue is not enough. Therefore, chemical stimulants, 5-azacytidine and laminin, were added to the hydrogel formulation and differentiation was assessed. Previous research groups have achieved differentiation of human adipocyte stem cells into non-beating cardiomyocytes by culturing hASCs in laminin coated wells and exposure to 5-azacytidine. This method of differentiation was selected due to the simplicity of this method and smooth incorporation into our hydrogel.

In this study we have investigated the addition of calcium peroxide as a possible candidate for *in situ* oxygen release. Additionally, we investigated the addition of laminin and 5-azacytidine in order to differentiate the human adipocyte stem cells embedded in the hydrogel into cardiomyocytes.

5.2. Materials and Methods

5.2.1. Sources for Materials.

Low MW chitosan (50 kDa and 75-85% deacetylation), gelatin type A (100, 175, and 300 Bloom), β-glycerophosphate (2GP), 50:50 poly lactic-co-glycolic acid (PLGA, 110 kDa), polyvinyl alcohol (PVA, 30-70 kDa, 87-90% hydrolyzed), Doxycycline hyclate (DOX, pharmaceutical secondary standard), CaO_2, 5-azacytidine (catalog no. A1287), Dulbecco's Modified Eagle's Medium – low glucose (catalog no. D6046), and bovine

serum albumin (BSA) were procured from Sigma Aldrich Co (St. Louis, MO). Phosphate buffer solution (PBS, pH=7.4), 5-(and-6)-carboxyfluorescein diacetate, succinimidyl ester (CFDA-SE) - mixed isomers, StemPro® Human Adipose-Derived Stem Cells, MesenPRO RS™ Medium kit, L-glutamine (200 mM, liquid), and powdered DMEM low glucose were procured from Life Technologies. (Carlsbad, CA). Food grade Active TI transglutaminase (Enzyme Commission 2.3.2.13) was procured from Ajinomoto (Fort Lee, NJ). Fetal Bovine Serum (catalog no. 30-2020) and Trypsin-EDTA was purchased from American Type Culture Collection (ATCC – Manassas, VA). Fresh porcine hearts were purchased from Ralphs Meat Packing Company located in Perkins, OK. Anti-GATA4 antibody (catalog no. ab84593) was purchased from Abcam (Cambridge, MA). Purified anti-human CD105 (catalog no. 323202), FITC Donkey anti-rabbit IgG (catalog no. 406403), and PE anti-mouse IgG1 (catalog no. 406607) was obtained from Biolegend (San Diego, CA). DAPI Nucleic Stain (catalog no. D1306) was purchased from Thermo Scientific Pierce (Waltham, MA). Cultrex® Mouse Laminin I (1 mg/mL) catalog no. 3400-010-01 was purchased from Trevigen (Gaithersburg, MD).

5.2.2. Hydrogel formulation.

Hydrogel solution was created by previous methods with minor modification (Tormos et al., 2015). In brief, chitosan, gelatin, powdered low glucose DMEM (cat no. 31600-083), calcium peroxide, and TG, were prepared in 0.1N HCl (Tormos et al., 2015) according to various required conditions. Solutions were stirred for a minimum of four hours at a temperature of 60°C. After the polymers completely dissolved, solution temperature was lowered to 37°C and was transferred to a 50 mL centrifuge tube, and 0.56 g/mL of cold

2GP (4°C) was added drop wise under constant stirring until pH reached biological conditions (7.2-7.4). When Dox was added, DOX-PLGA nanoparticle were filtered through a 0.22µm filter and then added to the hydrogel solution and mixed thoroughly.

5.2.3. Mechanical Characterization.

Compression tests. Unconfined compression testing was performed on hydrogels using an INSTRON 5542 (INSTRON, Canton, MA) and a custom-built anvil with a diameter of 25mm, as described previously (Tormos et al., 2015). In brief, hydrogels were casted in 6-well tissue culture plates by incubating 3 mL of solution until complete gelation was achieved at 37°C (**Figure 5.1**). Hydrogels were compressed at 1 mm/min crosshead speed. Data were exported to MS Excel and compressive modulus was calculated from the slope of the linear portion (20% to 40% strain range) of the stress-strain plot.

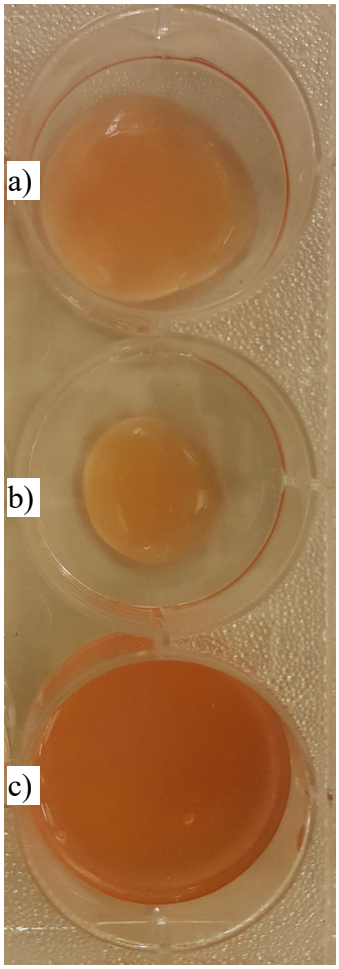

Figure 5.1. Hydrogel samples after gelation. A) 1mL of hydrogel. B) 0.5mL of hydrogel. C) 3 mL of hydrogel.

Tensile tests. Tensile tests were also conducted by applying the load orthogonal to compression testing to ensure uniform cross-linking of the hydrogels, as described previously (Tormos et al., 2015). In brief, 20 mL of hydrogel solution was prepared in a 35mm petri dish and incubated until complete gelation was achieved at 37°C. After incubation, 10mm × 14 mm × 3 mm rectangular slices were cut out and loaded to the Instron 5542 and pulled to break at a crosshead

speed of 1 mm/min at room temperature. After data collection, stress vs strain was plotted and the slope of the linear region, the elastic modulus, was determined. For all tests, a minimum of three experiments were performed per condition from different preparations.

Stress relaxation experiments. Hydrogel samples were prepared similar to tensile tests were used in these experiments and porcine heart tissue samples were prepared as described previously. Similar dimension (10mm × 14 mm × 3 mm) of porcine heart tissues were sliced from the posterior side of the right ventricle while frozen using Chef's Choice® 610. These samples were subjected to seven successive steps of ramp and hold tests. Each ramp was stretching to 5% at 2.5%/s of the original length. Each holding was for 20 seconds. Stress was plotted against time. To understand the effect of each stage on the hydrogel, they were normalized by subtracting stress and time elapsed at the beginning of each stage. In addition, reduced relaxation function was calculated to understand the amount of stress relaxed in each stage, similar to our previous publications (Ratakonda et al., 2012).

Cyclical tests. Hydrogel samples and porcine heart tissue samples were prepared similar to ramp and hold tests described above. Samples were stretched 10% of their length at a speed of 72 cycles per minute and cycles were repeated for 30 min.

Adhesion tests. In order for this treatment to be successful, the hydrogel must attach to the cardiac tissue. To test adhesion to cardiac tissue, porcine cardiac tissue harvested from the left ventricle was used. Hydrogel was added on top of cardiac tissue, followed by another identical piece of cardiac tissue (sandwich-like configuration) and allowed to gel (**Figure 5.2a**). The cardiac tissues were glued to petri dishes to prevent any movement of tissue during incubation for gelation of the hydrogel at 37°C and testing.

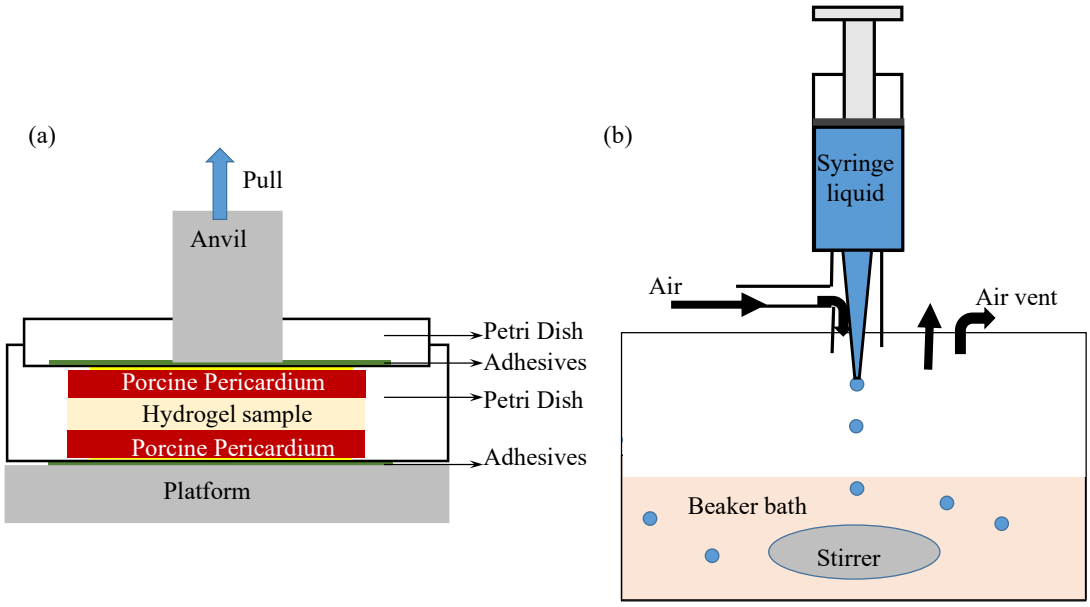

Figure 5.2. Schematics of experimental setup. (a). Assembly used for the peel test. (b) Forming chitosan encapsulated CaO_2 particles.

After hydrogel solidified, photographs were taken and the strength of adhesion was determined using tensile testing where the top petri dish was taped to an anvil and stretched at a speed of 1 mm/min. Three samples per condition were tested. After data was collected, stress vs strain was determined as before.

5.2.4. 3-D cell culture.

Human adipocyte stem cells (hASCs) were expanded in MesenPRO RS™ Medium kit, following vendor's protocol. Cells were maintained at 37°C, 5% CO_2/95% air, and fed with fresh medium every 2-3 days. Once confluent, cells were detached with trypsin-EDTA 1X and then trypsin was neutralized using MesenPRO RS™ Medium. Cells were centrifuged at 210×g for 5 min and dispersed in growth medium. Viable cells were counted using Trypan blue dye exclusion assay.

hASCs between the passages 3-8 were stained with CFDA-SE, and seeded onto hydrogel samples using the procedure previously developed by my laboratory with minor

modifications(Tormos et al., 2015). In brief, cells were incubated in growth medium containing 2 μM CFDA-SE at 37°C for 20 min followed by washing the excess stain with growth medium. Cells were added to the hydrogel at 0.5×10^6 cells/mL hydrogel and mixed evenly within the solution. 0.5 mL of mixture was then dispensed into the 6-well plate and incubated at 37°C for until gelation was achieved. Then, 2mL growth medium was added. After 24 hours, the growth medium was collected for viability via CFDA SE analysis and replaced with fresh growth medium. This process was repeated every 48 hours until completion of experiment.

After completion of experiment, cytoplasmic CFDA SE content was extracted from live cells by three cycles of freeze and thaw, using the procedure previously reported (Tormos et al., 2015). In brief, cell culture medium was replaced with 2mL PBS and placed at -20°C until the PBS froze. After the PBS freezes, the plates were thawed at room temperature and cycle was repeated. Then, the solution was collected and the absorbance was determined using a spectrophotometer Gemini XS spectrofluorometer (MDS technologies, Santa Clara, CA) at the excitation and emission wavelengths of 485 nm and 525 nm, respectively. The CFDA-SE content in the spent medium was also assessed. Obtained fluorescence intensities were converted to number of cells using a calibration of fluorescence intensity to number of cells obtained as previously described (Tormos et al., 2015).

5.2.5. 3-D Differentiation

hASCs (P2-P3) were embedded in hydrogels containing 9μM 5-azacytidine and 2μg of laminin per mL of hydrogel solution at a concentration of 500,000cells per mL of

hydrogel solution. Each well on a six-well plate contained 0.5mL of hydrogel and cells. The hydrogel was allowed to gel and supplemented with growth medium. After 24 hours, growth medium was replaced with fresh medium, this was repeated every 48 hours until the termination of the experiment at 21 days. At the end of the experiment samples were prepared for immunohistochemistry (described in the next section).

5.2.6. Immunohistochemistry

After completion of cell culture experiments, some samples were processed for cryosectioning. Samples were submerged in Tissue-Tek® O.C.T. Compound and frozen at -20°C. Samples were sent to Stephenson Cancer Tissue Pathology Core at the University of Oklahoma for cryosectioning. Samples were cut at a thickness of 6µm. After cryosectioning, slides were prepared for immunohistochemistry. First, using a PAP pen a border was drawn around the sample of interest. Next sample was washed with PBS to get rid of any leftover OCT. PBS containing 1% BSA was added in order to crosslink any non-specific sites and incubated at room temperature for 30 minutes. After 30 minutes, slide was rinsed with PBS and primary antibody was added and incubated for 60 minutes at room temperature. After 60 minutes, slide was rinsed with PBS and secondary antibody was added and incubated for 30 minutes at room temperature. After 30 minutes, slide was rinsed with PBS and either DAB or DAPI was added and incubated at room temperature for 5 minutes. If DAB was added, after 5 minutes, slide was rinsed with PBS and hematoxylin was added and incubated for 15 seconds. After 15 seconds, slide was rinsed thoroughly with PBS. Slide was covered with 2-3 drops of cytoseal and a cover slip and was allowed to dry in a dust free place. Digital photomicrographs were

captured at representative locations using a CCD camera connected to an inverted microscope.

5.2.7. Forming encapsulated particles of calcium peroxide.

Embedding of CaO_2 was attempted with different protocols listed in Table 1. Typical experimental setup used for the formation of the particles (**Figure 5.2b**) consisted of syringe placed inside an annular area supplied with pressurized air (Madihally and Matthew, 1999b). A list of attempted test conditions is shown in **Table 5.1.** In the first test, chitosan solution was prepared similar to Section 2.2 and once chitosan was dissolved, CaO_2 was added. Chitosan solution was added in a drop-wise manner to the bath of NaOH solution. The second test was similar to the first test except location of chitosan solution and NaOH were interchanged; 100 mg of calcium peroxide was added into 10 mL of sodium hydroxide solution (2N) and in a drop-wise manner add it to a static chitosan solution (variable concentration). Third and fourth tests were the replacement of NaOH with sodium tripolyphosphate (TPP, 25mg/mL) and deionized water (DI water), respectively, at different stirring speeds (300 and 1000RPM).

Table 5.1. List of conditions for formation of CaO2 encapsulated particles.

Liquid dispensed from the Syringe	**Liquid bath in the beaker**
Chitosan with calcium peroxide	Sodium hydroxide
Sodium hydroxide with calcium peroxide	Chitosan
TPP with calcium peroxide	Chitosan
Water with calcium peroxide	chitosan

5.2.8. Statistical evaluation.

All experiments were repeated three or more times. Significant differences between two groups were evaluated using a one-way analysis of variance (ANOVA) with 95% confidence interval. When $P<0.05$, differences were considered to be statistically significant.

5.3. Results and discussion

5.3.1. Impact of calcium peroxide on hydrogel formulation

As previously stated, it is believed that the lack of oxygen is one of the factors that can play a role in the death of cells embedded in the scaffold. The goal of this study is to include an oxygen releasing compound to our previously developed hydrogel formulation. Calcium peroxide was the chosen oxygen releasing compound in this study. However, very quickly it was realized that addition of calcium peroxide would not be easy. First it was noticed right away (thanks to the phenol red present in DMEM), that addition of calcium peroxide sharply increased the pH of the solution. Since chitosan can only dissolve in an acidic environment, an optimal condition was found were calcium peroxide was present and did not hinder chitosan from dissolving. That amount was 100 mg of calcium peroxide for every 100mL of hydrogel solution. While both chitosan and calcium peroxide were able to dissolve, it was observed that small oxygen bubbles was occurring upon dissolution of calcium peroxide. This is due to the oxygen being released as soon as calcium peroxide dissolved. This indicates that calcium peroxide will dissolve quickly if the conditions are adequate. This causes a problem because chitosan takes 4 hours to fully dissolve, therefore, it is believed that by the time the hydrogel solution is used to form a hydrogel, most of the oxygen has already been released. Nevertheless, we

continued forward with the addition of calcium peroxide and determined the impact that the addition of calcium peroxide had on the hydrogel formulation methods. The pH of hydrogel solutions with and without calcium peroxide was monitored upon small amounts of β-glycerophosphate (2GP) being added. As demonstrated on Table 2, the amount of 2GP was decreased by half to reach biological pH (7.2 – 7.4).

Table 5.2. Effect of addition of 2GP on pH of CG solution.

Amount of 2GP added (mL)	pH of 2% chitosan – 8% gelatin – 2% media with TG	pH of 2% chitosan – 8% gelatin – 2% media with TG and CaO2
0	5.46 ± 0.06	5.98 ± 0.06
1	6.47 ± 0.09	6.87 ± 0.06
2	6.85 ± 0.05	7.27 ± 0.03
3	7.10 ± 0.02	
4	7.23 ± 0.03	

5.3.2. Mechanical properties of hydrogels with calcium peroxide

I found that the addition of CaO_2 increased the strength of the hydrogel compared to a hydrogel without CaO_2 (**Figure 5.3**). Its compressive modulus increased from 35.1 ± 2.10 kPa to 41.6 ± 4.07 kPa. This increase in compressive modulus is probably due to less β-glycerophosphate (2GP) solution used to adjust the pH of the solution. Therefore, the concentration of polymers are less diluted.

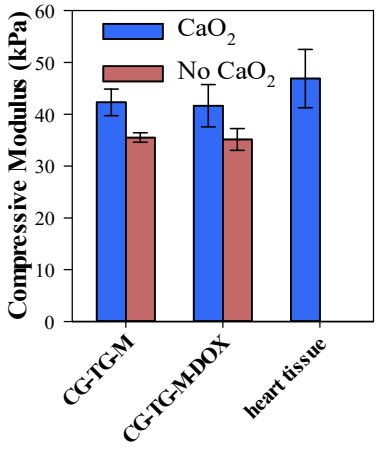

Figure 5.3. Effect of CaO2 addition on hydrogel property.

Similar to my previous formulations, I conducted relax and hold tests to understand the relaxation characteristics. First, a stress vs time plot showed (**Figure 5.4a**) that the hydrogel was able to withstand the same stress in the tensile mode similar to the cardiac

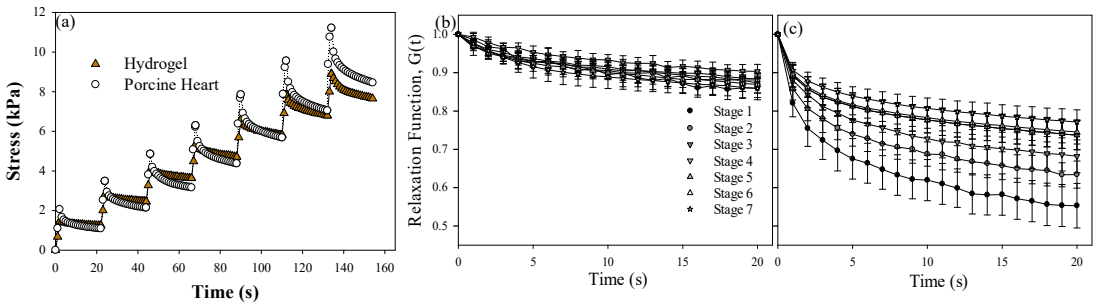

Figure 5.4. Comparison of stress-relaxation behavior between porcine pericardium and hydrogel. (a). Effect of ramp and hold on stress relaxation. (b) Reduced relaxation function for different stages in the 2%8% CG hydrogel with TG and CaO_2. (c). Reduced relaxation function for porcine pericardium.

tissue. This is a significant improvement relative to the hydrogels without CaO_2, which showed less stress accumulation than the cardiac tissue in the tensile mode. Without CaO_2, the hydrogel was able to resist less stress and therefore not be as elastic as cardiac tissue. On the other hand, the hydrogel with CaO_2 was able to produce more stress and

have a ramp profile similar to cardiac tissue. Then the relaxation in each stage was compared. In tensile mode, the relaxation in the CG hydrogel varied from 10% to 15%, still significantly less compared to cardiac tissue; the percentage relaxation in the first stage was 45% in the first stage which decreased to 23% in the cardiac tissue. The CaO_2 containing samples retained the strain hardening characteristics similar to natural tissues including cardiac tissue; the more the material is stretched, the stiffer it gets.

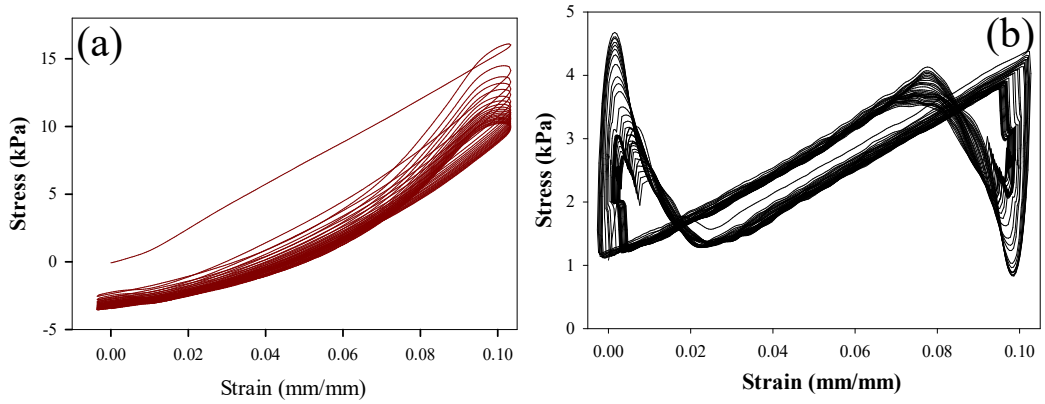

Figure 5.5. Cyclical behavior between porcine pericardium and hydrogel. (a) Porcine pericardium. (b) 2%8%CG hydrogel with TG and medium. Shown are the first 20 cycles in each sample.

During the cyclical test, it was confirmed that the hydrogel is able to resist more force and produce more stress but it was not close to cardiac tissue (**Figure 5.5**). This difference in cyclical profile could be due to the hydrogel having randomly aligned fibers, whereas cardiac tissue has an aligned structure.

5.3.4. Peel Test results

When hydrogel is injected, it needs to attach to the native tissue. Hence, I wanted to understand the adhesive strength of the hydrogel to the cardiac tissue. A standard peel test (ASTM D903) is used in testing the adhesive strength. My initial experiments used those protocols and tested the samples. However, during the preparation of those samples, one has to use a hook that connects to the cross-head of the tensile testing

machine. This significantly weakened the test sample. Hence, I designed a new system that required no hook to be used. Maximum stress was 1.45 ± 0.19 kPa, which is slightly stronger that the commercially available fibrin adhesive (Tisseel®) (McDermott et al., 2004) (**Figure 5.6**). This suggests that the hydrogel could be used in the cardiac regeneration. If additional strength is required, one could increase the concentration of TG, as currently used concentration of TG in the hydrogel is 10X less than the recommended level (Broderick et al., 2005).

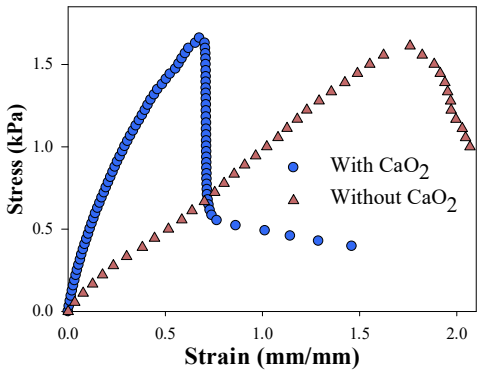

Figure 5.6. Strength of adhesion of hydrogel to the pericardium. Stress-strain curve showing the break point.

This adhesion test was conducted on a static harvested sample where as an *in vivo* setting other variables need to be considered. I attempted to attach this hydrogel to a rat's heart in an *ex vivo* setting. The heart was kept beating by pumping calcium buffer through the heart. However, the flow of the buffer caused a boundary layer outside the heart and the hydrogel could not attach. There is a chance that the hydrogel might still attach while in an *in vivo* setting due to chitosan being a blood clotting agent. On the other hand, depending on the formation of blood clots can lead to further complication.

5.3.5. Viability of hASCs with CaO_2

First, viability of stem cells after three weeks was assessed due to long-term exposure of 5-azacytidine, which reports have shown to be

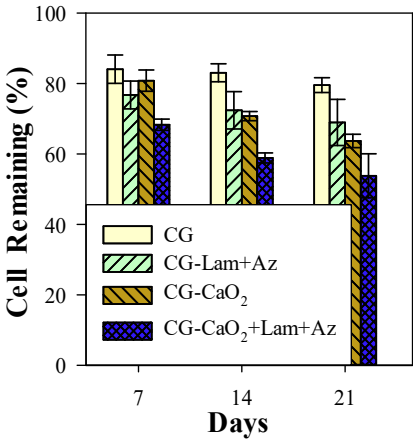

Figure 5.7. Effect of additives on hASC recovery from the hydrogel during 21-day cultures.

toxic at high and prolonged concentrations. Hydrogels containing TG showed an approximate 10% decrease in cell viability for all time periods. This could be a direct result of long term exposure to 5-azacytidine. Furthermore, addition of calcium peroxide seemed to decrease viability even more. **Figure 5.7** shows that the addition of calcium peroxide alone decreases viability to 60% at the end of three weeks. The combinations of calcium peroxide and 5-azacytidine further decrease the viability to 50%. This loss in cell viability could be due to chelation. Chelation of calcium ions may reduce TG crosslinking between chitosan chains, ultimately decreasing the stability of the hydrogel.

5.3.6. 3D Differentiation

qPCR was expected to be used to support immunohistochemical evidence of however, hydrogels were not able to degrade and isolation of quality cell and/or RNA was not achieved. As previously shown, exposure to proteolytic enzyme Trypsin, did not degrade the hydrogels (Tormos et al., 2015). 5-azacytidine and laminin were included in the hydrogel formulation to assess whether differentiation can occur in a 3D environment. At the end of 21 days, presence of hASC markers confirm that hASCs did not differentiate regardless if they were exposed to 5-azacytidine and laminin or not (**Figure 5.8**). Furthermore, lack of cardiac markers also confirm that differentiation did not occur. In addition, structure of hydrogels is clearly very different than as observed on Chapter IV. While TG and doxycycline improved stability by increased crosslinking, at the end of 21 days most of that structure is degraded.

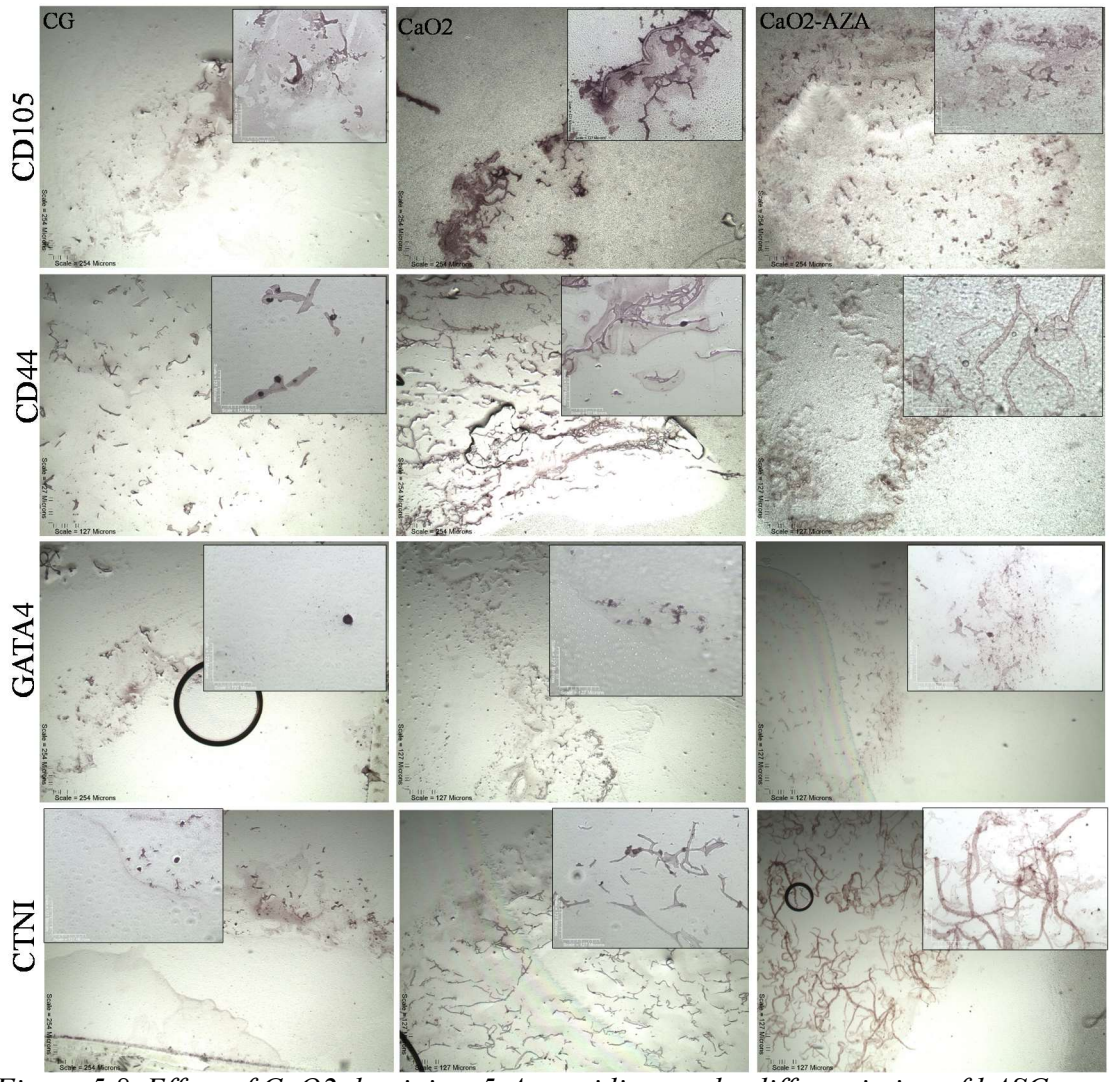

Figure 5.8. Effect of CaO2, laminin +5-Azacytidine on the differentiation of hASCs after 21 days. Inset are the higher magnification images from locations with cells

5.3.7. Formation of particles

It is believed that most of the oxygen is being burst-released prior to *in vitro* experiments. Therefore, similar to our controlled release of doxycycline, calcium peroxide was entrapped in chitosan nanoparticles. PLGA nanoparticles have a slow degradation rate, therefore a polymer that degrades faster was chosen. Chitosan particles have been previously used to entrap proteins and their release is applicable to our needs. Back on table 1, different conditions were listed for the formation of chitosan particles embedding

calcium peroxide. First, a larger amount of calcium peroxide (1 gram compared to 100 mg) was added to 100mL of a 2% (w/v) chitosan solution. The calcium peroxide that was added formed a "blob" of chitosan peroxide and would not dissolve or even spread out in the chitosan solution (**Figure 5.9a**). Even when added as a high concentrated solution, calcium peroxide did not spread and dissolve (**Figure 5.9b**). Therefore, it was decided to switch the experimental setup and have basic solution with calcium peroxide being added to chitosan solution. Addition of a 1% (w/v) of calcium peroxide in sodium hydroxide (2N) to a 2% (w/v) chitosan solution was attempted (**Figure 5.9a**). This resulted in large particles (6.44 ± 0.57 mm) with an inside diameter of 4.41 ± 0.24 mm that are not able to precipitate. While particles were obtained, isolation was not possible. If particles were centrifuged, they would lose their shape and flatten out. If particles were scooped out using a spatula, they also lost their shaped upon removal from chitosan solution. It was then decided that sodium hydroxide might not be the optimal condition for making chitosan particles. Next, sodium hydroxide was replaced with sodium tripolyphosphate (TPP) at a concentration of 25mg/mL. TPP has been previously used to make chitosan nanoparticles. Due the lack of detail provided on methods including chitosan and TPP,

Figure 5.9 Addition of calcium peroxide to chitosan solution. (a) In powder form. (b) In solution.

several experimental conditions were attempted. First, a 1% CaO_2 solution in TPP was added to a 2% chitosan solution with no stirring. No precipitation was observed for these conditions. Next, chitosan was diluted to 1% (w/v) and while precipitation was observed

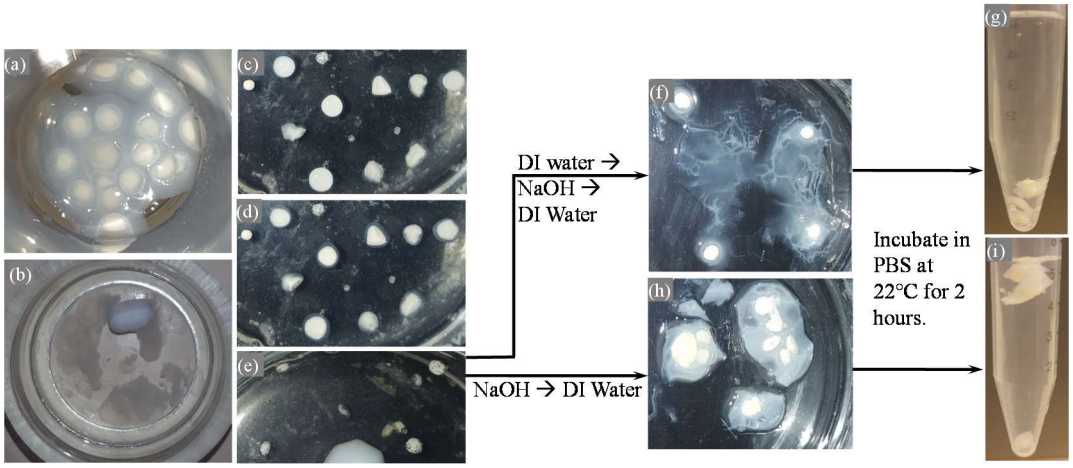

Figure 5.10. Effect of encapsulation process on particle formation. **(**a) Condition #2. A 10 mL syringe was loaded with a 1% solution of calcium peroxide (w/v) in sodium hydroxide (1M) and a 14 gage needle was used to release the solution in a drop-wise manner to a 2%chitosan solution (w/v). (b) Condition #3, a 10 mL syringe was loaded with a 1% solution of calcium peroxide in TPP (25mg/mL) (w/v) and a 14 gage needle was used to release the solution in a drop-wise manner to a 0.25% chitosan solution (w/v). (c) Condition #4, a 10 mL syringe was loaded with a 1% solution of calcium peroxide (w/v) in deionized water and a 14 gage needle was used to release the solution in a drop-wise manner to a 2.0 %chitosan solution (w/v). (d) Condition #4 after 10 minutes. (e) Condition #4 after 24 hours. (f) Condition #4 upon addition of DI to wash excess chitosan, followed by addition of NaOH (2M) and 5 minutes of incubation at room temperature, followed by 3 washes of DI water to wash off any excess NaOH. (g) Incubation of chitosan particles in PBS at room temperature after 2 hours. (h) Condition #4 upon addition of sodium hydroxide (2M), followed by 3 washes of DI water. (i) Incubation of chitosan particles in PBS at room temperature after 2 hours.

particle formation was not instant and therefore the CaO_2 spread all over the solution forming blobs similar to previous experiments. Chitosan was further diluted but the same problem persisted (**Figure 5.10b**). Then we decided to take advantage of the blob formation and use it to surround the CaO_2 with chitosan and then expose it to NaOH to create a precipitation layer encapsulating the CaO_2. Addition of 1% (w/v) CaO_2 in DI

water was done without stirring due to aggregation of droplets (**Figure 5.10c**). CaO_2 droplets were dispersed in a petri dish containing 2% (w/v) chitosan solution. Initially, no distinction could be made from an inner and outer diameter, however, after 10 minutes the distinction became clear (**Figure 5.10d**). After 24 hours, the DI water had dispersed and only spherical aggregates of CaO_2 remained (**Figure 5.10e**). Aggregates were submerged to ensure complete chitosan engulfing. With a spatula, CaO_2 aggregates were isolated and placed in a clean petri dish. Next, 2 paths were taken. First the aggregates were washed with DI water to remove excess chitosan, followed by an addition of 2N NaOH for 5 minutes (to induce precipitation), and finally 3 washes of DI water to neutralize any NaOH present (**Figure 5.10f-g**). The other path was similar except there was no removal of excess chitosan (**Figure 5.10h-i**). While both path resulted in chitosan particles, those without the pre-wash of DI water released oxygen faster, evident by floating particles.

5.4 Summary

In this study, the addition of calcium peroxide to the hydrogel formulation to serve as the oxygen releasing compound was investigated. The addition of CaO_2 had positive and negative effects on the hydrogel's performance. On the positive side, CaO_2 increased linear mechanical properties and brought the mechanical properties of the hydrogel similar to cardiac tissue. In addition, it improved the cyclical properties of the hydrogel however, it is still far away from cardiac tissue. On the negative side, CaO_2 decreases hASC viability. Cell viability is incredibly critical and therefore any changes in hydrogel formulation that decreases viability should be eliminated. Furthermore, the addition of CaO_2 did not induce differentiation as seen by presence of hASC markers at the end of 21

days regardless of whether the cells were exposed to 5-azacytidine and laminin. Since oxygen is limited in a necrotic environment, encapsulation of CaO_2 was investigated. Encapsulation of CaO_2 was unsuccessful despite various and different encapsulation methods. This is believed to be due to the gelation method of the encapsulation methods attempted. The gelation method or formation of particles of these methods are slow and take time, which gives enough time for CaO_2 to dissolve and release the oxygen. Therefore, it is recommended for other encapsulation methods to be attempted as long as particle formation occurs instantaneously and calcium peroxide is dispersed in an organic solvent to prevent dissolution of CaO_2.

.

CHAPTER VI

CONCLUSION AND RECOMMENDATIONS

6.1 CONCLUSIONS

The goal of this study was to investigate a chitosan-gelatin hydrogel as a suitable candidate for cardiac tissue repair and regeneration for patients who have experienced a heart attack. Researchers are working on developing cells based therapies to repair the damage using stem cells (Behfar et al., 2014, Campbell and Suzuki, 2012, Garbern and Lee, 2013, Segers and Lee, 2008). However, stem cells alone cannot repair the tissue alone. Studies have shown that an injection of stem cells to the damaged region is not successful because the majority of the implanted cells (~90%) die within 1 week (Behfar et al., 2014, Menasche, 2011a, Segers and Lee, 2008). Cell death is hypothesized to be caused by lack distribution of cells, lack of nutrients, and lack of oxygen. However, even with the addition of biomaterials, improvement in cell survival upon delivery was minimal (Hong et al., 2007). While the addition of biomaterials resolved the issue of lack of distribution, it added more problems. Problems that are associated with the addition of biomaterials include: stability of material, immune reaction by the host, and mechanical property compatibility. The focus of this study was to develop a cell based therapy that

addresses the issues of lack of nutrients, lack of oxygen, material stability, mechanical property compatibility, and immune reaction by the host. To address these challenges I decided to split the project into three aims. Aim 1 was to investigate the behavior of the developed hydrogel when exposed to forces similar to what cardiac tissue experiences. Results addressing this aim are presented in Chapter III and Chapter IV and a conclusion regarding this aim is available on section 6.1.1 Aim 2: was to improve the survival of hASCs after application. Results addressing this aim are presented in Chapter IV and Chapter V and a conclusion of this aim is available on section 6.1.2. Aim 3 was to evaluate cardiomyogenesis of hASCs in a 3-D environment. Results addressing this aim are presented in Chapter IV and Chapter V and a conclusion regarding this aim is available on section 6.1.3.

6.1.1 Aim 1: To develop hydrogel that can withstand wound healing environment and improve cell survival

I explored the possibility of stabilizing the chitosan-gelatin (CG) injectable hydrogels using i) controlled release of doxycycline (DOX) to prevent premature degradation due to increased gelatinase activity (MMP-2 and MMP-9), and ii) transglutaminase (TG) to *in situ* cross-link gelatin to improve the mechanical stability.

The release profile analyzed by a single compartment modeling showed that 90% of DOX released from cross-linked CG hydrogels after four days, unlike CG hydrogels where 90% of DOX was released within the first day.

Addition of TG enhanced the CG hydrogel stability significantly. DOX can be released in a controlled manner using CG cross-linked with TG. Addition of TG and media improved the mechanical property of the hydrogels with and without fibroblasts.

CG cross-linked with TG showed significant improvement in the retention of human foreskin fibroblasts (hFF-1) cultures at day 5; cells recovered from CG-TG was 2.5 times more than that collected from CG with DOX release. There was inhibition of MMP-2/MMP-9 activity, directly correlating cause and effect of DOX release levels and improvement in hydrogel stability, which further helped cell retention. More than 60% of seeded fibroblasts were recovered from the CG-TG hydrogels at day 5, unlike 40% recovered from CG-hydrogels. Inhibition of MMP-2/MMP-9 were observed. Improved retention of cells holds promise in using the CG-based cell delivery to repair tissues.

6.1.2 Aim 2: To improve the survival of hASCs after application and evaluate 3D differentiation.

I determined the optimal hydrogel formulation by exploring different types of gelatin and chitosan, and by varying the concentration of gelatin, growth medium, and transglutaminase. The optimal concentration was determined by comparison of mechanical properties between hydrogel and porcine cardiac tissue. The optimal formulation included 2% (w/v) chitosan, 8% (w/v) gelatin, 2% (w/v) growth medium, 0.03% (w/v) transglutaminase, and 0.1% (w/v) calcium peroxide. With this formulation, compressive modulus of the hydrogel was the closest to porcine cardiac tissue. In terms of cyclical properties, this formulation was also optimal for cardiac tissue regeneration. During the relax and hold test, the optimal hydrogel had similar relaxation profile to cardiac tissue. On the other hand, cyclical profile did not appear similar but hydrogel was able to withstand up to 30 minutes of continuous testing.

Differentiation of hASCs into cardiomyocytes was first attempted in 2-D and then transitioned to a 3-D environment. Differentiation was successful using laminin and 5-

azacytidine for 21 days, while exposure to PMA for 9 days was not successful. Laminin and 5-azacytidine was included in the hydrogel formulation to induce differentiation.

More than 80% of seeded hASC were recovered from the CG-TG hydrogels at day 21. However, evaluated differentiation markers suggested that hASCs did not differentiate. Presence of Laminin and 5-azacytidine decreased cell viability.

6.1.3 Aim 3: To add oxygen releasing component in hydrogel formulation and investigate hydrogel's differentiation ability and mechanical properties.

Calcium peroxide (CaO_2), an oxygen releasing molecule was added to the hydrogel formulation to further increase cell viability. Optimal hydrogel formulation was explored by altering CaO_2 and 2-glycerolophosphate, which is used to adjust pH required for thermosensitive gelation of chitosan hydrogel. The mechanical properties were improved by addition of calcium peroxide both linear and nonlinear properties.

With this formulation, mechanical properties of the hydrogel improved further, reaching that of porcine cardiac tissue. In terms of cyclical properties, this formulation was also optimal for cardiac tissue regeneration. During the relax and hold test, the optimal hydrogel had similar relaxation profile to cardiac tissue. However, stress-strain profiles in cyclical conditions did not appear similar but hydrogel was able to withstand up to 30 minutes of continuous testing.

Most of the oxygen was released prior to cell culture experiment and cell viability decreased. Since direct addition of CaO_2 resulted in burst release of oxygen, I attempted to encapsulate CaO_2 in chitosan particles. Encapsulation was unsuccessful due to several problems outlined in Chapter V.

Differentiation of hASCs was assessed and evidence of differentiation was not found. Presence of CaO2 decreased cell viability. However, evaluated differentiation markers suggested that hASCs did not differentiate.

6.2 Future Studies

Based on the experience of these findings, I believe few of the relevant issues listed below should be addressed to advance this research.

6.2.1. Time of gelation

Valid production of 2 % (wt/v) chitosan and 8% (wt/v) gelatin hydrogels is somewhat inconsistent and prone to premature gelation. This is believed to be due to the high content of gelatin. Gelatin starts to gel at room temperature, resulting in premature gelation. To counter this problem, one could explore two options:

i) decrease gelatin content and increase chitosan content, and

ii) substitute gelatin for decellularized cardiac tissue.

Addition of more binding domains such as addition of RGD peptide. Modification of chitosan by adding RGD peptide to backbone of chitosan.

6.2.2. Differentiation of hASCs in a 3D environment

Differentiation of human adipocyte stem cells is somewhat inconsistent. As presented in chapter 4, different methods were attempted but only one succeeded. Even 5-azacytidine (the method that succeeded) was inconsistent at times similar to previous reports (Wan Safwani et al., 2012). I recommend to explore additional stimulation in order to provide a more consistent differentiation protocol. For example, mechanical contraction of scaffold while cells are embedded could provide for a more natural environment and

induce differentiation (Black et al., 2009, Happe and Engler, 2016). Another stimulation that can be investigated is the presence of electrical pulses similar to what the cardiac tissue experiences (Pijnappels et al., 2008). An additional option, is to induce differentiation of hASCs by inhibition of mRNA. Another option is to culture primary human cardiomyocytes on tissue culture plates, collect the waste media, and use the waste media to feed hASCs. This media can even be freeze dried into a powder and used as a replacement for DMEM in the hydrogel formulation. The idea behind this experiment is that by culturing cardiomyocytes they will secrete signals to promote growth and proliferation which for stem cells might be signals for differentiation. Finally, another recommendation is to co-culture human cardiomyocytes with hASCs and assess whether differentiation occurred (Bollini et al., 2011, Choi et al., 2010, Hussain et al., 2013).

6.2.3. Use of other stem cell sources

Alternatively, one could explore another source of stem cells or cardiomyocytes. For example, recently a population of cardiac stem cells has been discovered (Bearzi et al., 2007). While protocols for successful isolation and a high yield percentage are still being discovered, this source could become a much better option and might need very little stimulation to differentiate into cardiac cells. Another source of stem cells is to use induced pluripotent stem cells and differentiate them into cardiomyocytes like others have done (Fujiwara et al., 2011). Finally, there is a commercially available source of cardiomyocytes derived from induced pluripotent stem cells (cellulardynamics.com).

6.2.4 Further delivery of oxygen and nutrients

Calcium peroxide encapsulation was unsuccessful with the protocols listed on Chapter V. However, that doesn't mean that it can't be done. I believe that encapsulation of calcium peroxide can be successful using a hydrophobic solvent and with a particle formation that is instantaneous. When particles are form instantaneous it doesn't allow for calcium peroxide to precipitate nor to dissolve while the particle is forming. Using the current formulation the hydrogel must be tested in an *in vivo* setting and assess how fast do blood vessel start to form. The DMEM provided in the hydrogel will not last long and cells need a constant source of nutrients which can be provided be the newly formed blood vessels. If blood vessel formation is to slow, I suggest adding growth factors such as FGF, VEGF, Ang1, Ang2, PDGF, etc.

6.2.5 Co-culture of stem cells with endothelial, smooth vascular, myofibroblasts

One could investigate whether this hydrogel can support multiple cell lines including cardiomyocytes, endothelial cells, smooth vascular cells, and myofibroblasts (Menasche, 2011b). Furthermore, it will be beneficial to investigate whether this hydrogel supports co-culture of the different cell lines previously mentioned.

REFERENCES

2008. *Matrix metalloproteinases in tissue remodelling and inflammation,* Basel : [London, Basel : Birkhäuser

London : Springer, distributor.

AESCHLIMANN, D. & PAULSSON, M. 1994. Transglutaminases: Protein cross-linking enzymes in tissues and body fluids. *Thromb Haemost,* 71.

AGWUH, K. N. & MACGOWAN, A. 2006. Pharmacokinetics and pharmacodynamics of the tetracyclines including glycylcyclines. *J Antimicrob Chemother,* 58**,** 256-65.

AIBA S-I, M. N., TAGUCHI K, FUJIWARA 1987. Covalent immobilization of chitosan derivatives onto polymeric film surfaces with the use of a photosensitve hetero-bifunctional crosslinking reagent. *Biomaterials,* 8**,** 481-488.

AMIR, G., MILLER, L., SHACHAR, M., FEINBERG, M. S., HOLBOVA, R., COHEN, S. & LEOR, J. 2009. Evaluation of a peritoneal-generated cardiac patch in a rat model of heterotopic heart transplantation. *Cell Transplant,* 18**,** 275-82.

BEARZI, C., ROTA, M., HOSODA, T., TILLMANNS, J., NASCIMBENE, A., DE ANGELIS, A., YASUZAWA-AMANO, S., TROFIMOVA, I., SIGGINS, R. W., LECAPITAINE, N., CASCAPERA, S., BELTRAMI, A. P., D'ALESSANDRO, D. A., ZIAS, E., QUAINI, F., URBANEK, K., MICHLER, R. E., BOLLI, R., KAJSTURA, J., LERI, A. & ANVERSA, P. 2007. Human cardiac stem cells. *Proc Natl Acad Sci U S A,* 104**,** 14068-73.

BEHFAR, A., CRESPO-DIAZ, R., TERZIC, A. & GERSH, B. J. 2014. Cell therapy for cardiac repair--lessons from clinical trials. *Nat Rev Cardiol,* 11**,** 232-46.

BERGER, J., REIST, M., MAYER, J. M., FELT, O., PEPPAS, N. A. & GURNY, R. 2004. Structure and interactions in covalently and ionically crosslinked chitosan hydrogels for biomedical applications. *European Journal of Pharmaceutics and Biopharmaceutics,* 57**,** 19-34.

BLACK, L. D., 3RD, MEYERS, J. D., WEINBAUM, J. S., SHVELIDZE, Y. A. & TRANQUILLO, R. T. 2009. Cell-induced alignment augments twitch force in fibrin gel-based engineered myocardium via gap junction modification. *Tissue Eng Part A,* 15**,** 3099-108.

BODE, F., DA SILVA, M. A., DRAKE, A. F., ROSS-MURPHY, S. B. & DREISS, C. A. 2011. Enzymatically cross-linked tilapia gelatin hydrogels: physical, chemical, and hybrid networks. *Biomacromolecules,* 12**,** 3741-52.

BOLLINI, S., POZZOBON, M., NOBLES, M., RIEGLER, J., DONG, X., PICCOLI, M., CHIAVEGATO, A., PRICE, A. N., GHIONZOLI, M., CHEUNG, K. K., CABRELLE, A., O'MAHONEY, P. R., COZZI, E., SARTORE, S., TINKER, A., LYTHGOE, M. F. & DE COPPI, P. 2011. In vitro and in vivo cardiomyogenic differentiation of amniotic fluid stem cells. *Stem Cell Rev,* 7**,** 364-80.

BOSI, A., BARTOLOZZI, B. & GUIDI, S. 2005. Allogeneic stem cell transplantation. *Transplant Proc,* 37**,** 2667-9.

BRODERICK, E. P., O'HALLORAN, D. M., ROCHEV, Y. A., GRIFFIN, M., COLLIGHAN, R. J. & PANDIT, A. S. 2005. Enzymatic stabilization of gelatin-based scaffolds. *J Biomed Mater Res B Appl Biomater,* 72**,** 37-42.

BRONDANI, D., PIOVESAN, J. V., WESTPHAL, E., GALLARDO, H., FIREMAN DUTRA, R. A., SPINELLI, A. & VIEIRA, I. C. 2014. A label-free electrochemical immunosensor based on an ionic organic molecule and chitosan-stabilized gold nanoparticles for the detection of cardiac troponin T. *Analyst,* 139**,** 5200-8.

CAI, K., YAO, K., CUI, Y., LIN, S., YANG, Z., LI, X., XIE, H., QING, T. & LUO, J. 2002. Surface modification of poly (D,L-lactic acid) with chitosan and its effects on the culture of osteoblasts in vitro. *J Biomed Mater Res,* 60**,** 398-404.

CAMCI-UNAL, G., ALEMDAR, N., ANNABI, N. & KHADEMHOSSEINI, A. 2013. Oxygen Releasing Biomaterials for Tissue Engineering. *Polym Int,* 62**,** 843-848.

CAMPBELL, N. G. & SUZUKI, K. 2012. Cell delivery routes for stem cell therapy to the heart: current and future approaches. *J Cardiovasc Transl Res,* 5**,** 713-26.

CHANG, W., LIM, S., SONG, B. W., LEE, C. Y., PARK, M. S., CHUNG, Y. A., YOON, C., LEE, S. Y., HAM, O., PARK, J. H., CHOI, E., MAENG, L. S. & HWANG, K. C. 2012. Phorbol myristate acetate differentiates human adipose-derived mesenchymal stem cells into functional cardiogenic cells. *Biochem Biophys Res Commun,* 424**,** 740-6.

CHEN, Q. Z., BISMARCK, A., HANSEN, U., JUNAID, S., TRAN, M. Q., HARDING, S. E., ALI, N. N. & BOCCACCINI, A. R. 2008. Characterisation of a soft elastomer poly(glycerol sebacate) designed to match the mechanical properties of myocardial tissue. *Biomaterials,* 29**,** 47-57.

CHENG, Y. H., YANG, S. H., SU, W. Y., CHEN, Y. C., YANG, K. C., CHENG, W. T., WU, S. C. & LIN, F. H. 2010. Thermosensitive chitosan-gelatin-glycerol phosphate hydrogels as a cell carrier for nucleus pulposus regeneration: an in vitro study. *Tissue Eng Part A,* 16**,** 695-703.

CHENITE, A., BUSCHMANN, M., WANG, D., CHAPUT, C. & KANDANI, N. 2001. Rheological characterisation of thermogelling chitosan/glycerol-phosphate solutions. *Carbohydrate Polymers,* 46**,** 39-47.

CHENITE, A., CHAPUT, C., WANG, D., COMBES, C., BUSCHMANN, M. D., HOEMANN, C. D., LEROUX, J. C., ATKINSON, B. L., BINETTE, F. & SELMANI, A. 2000. Novel injectable neutral solutions of chitosan form biodegradable gels in situ. *Biomaterials,* 21**,** 2155-61.

CHIU, L. L. & RADISIC, M. 2011. Controlled release of thymosin beta4 using collagen-chitosan composite hydrogels promotes epicardial cell migration and angiogenesis. *J Control Release,* 155**,** 376-85.

CHOI, Y. S., DUSTING, G. J., STUBBS, S., ARUNOTHAYARAJ, S., HAN, X. L., COLLAS, P., MORRISON, W. A. & DILLEY, R. J. 2010. Differentiation of human adipose-derived stem cells into beating cardiomyocytes. *J Cell Mol Med,* 14**,** 878-89.

CHONG, J. J., YANG, X., DON, C. W., MINAMI, E., LIU, Y. W., WEYERS, J. J., MAHONEY, W. M., VAN BIBER, B., COOK, S. M., PALPANT, N. J., GANTZ, J. A., FUGATE, J. A., MUSKHELI, V., GOUGH, G. M., VOGEL, K. W., ASTLEY, C. A., HOTCHKISS, C. E., BALDESSARI, A., PABON, L., REINECKE, H., GILL, E. A., NELSON, V., KIEM, H. P., LAFLAMME, M. A. & MURRY, C. E. 2014. Human embryonic-stem-cell-derived cardiomyocytes regenerate non-human primate hearts. *Nature,* 510**,** 273-7.

CHUNG, T. W., YANG, J., AKAIKE, T., CHO, K. Y., NAH, J. W., KIM, S. I. & CHO, C. S. 2002. Preparation of alginate/galactosylated chitosan scaffold for hepatocyte attachment. *Biomaterials,* 23**,** 2827-34.

CLEUTJENS, J. P., BLANKESTEIJN, W. M., DAEMEN, M. J. & SMITS, J. F. 1999. The infarcted myocardium: simply dead tissue, or a lively target for therapeutic interventions. *Cardiovasc Res,* 44**,** 232-41.

COSTA, P. & SOUSA LOBO, J. M. 2001. Modeling and comparison of dissolution profiles. *Eur J Pharm Sci,* 13**,** 123-33.

DAL POZZO, A., VANINI, L., FAGNONI, M., GUERRINI, M., DE BENEDITTIS, A. & MUZZARELLI, R. A. A. 2000. Preparation and characterization of poly(ethylene glycol)-crosslinked reacetylated chitosans. *Carbohydrate Polymers,* 42**,** 201-206.

DAVDA, J. & LABHASETWAR, V. 2002. Characterization of nanoparticle uptake by endothelial cells. *Int J Pharm,* 233**,** 51-9.

DAWSON, E., MAPILI, G., ERICKSON, K., TAQVI, S. & ROY, K. 2008. Biomaterials for stem cell differentiation. *Adv Drug Deliv Rev,* 60**,** 215-28.

DENG, B., SHEN, L., WU, Y., SHEN, Y., DING, X., LU, S., JIA, J., QIAN, J. & GE, J. 2015. Delivery of alginate-chitosan hydrogel promotes endogenous repair and preserves cardiac function in rats with myocardial infarction. *J Biomed Mater Res A,* 103**,** 907-18.

DM, O. H., COLLIGHAN, R. J., GRIFFIN, M. & PANDIT, A. S. 2006. Characterization of a microbial transglutaminase cross-linked type II collagen scaffold. *Tissue Eng,* 12**,** 1467-74.

ELNAKISH, M. T., HASSAN, F., DAKHLALLAH, D., MARSH, C. B., ALHAIDER, I. A. & KHAN, M. 2012. Mesenchymal stem cells for cardiac regeneration: translation to bedside reality. *Stem Cells Int,* 2012**,** 646038.

EMMERT, M. Y., HITCHCOCK, R. W. & HOERSTRUP, S. P. 2014. Cell therapy, 3D culture systems and tissue engineering for cardiac regeneration. *Advanced Drug Delivery Reviews,* 69–70**,** 254-269.

ENDERLE, J. D. & BRONZINO, J. D. 2012. *Introduction to biomedical engineering,* Amsterdam ; Boiston, Elsevier/Academic Press.

FRANCO, C., HO, B., MULHOLLAND, D., HOU, G., ISLAM, M., DONALDSON, K. & BENDECK, M. P. 2006. Doxycycline alters vascular smooth muscle cell adhesion, migration, and reorganization of fibrillar collagen matrices. *Am J Pathol,* 168**,** 1697-709.

FUJITA, M., ISHIHARA, M., MORIMOTO, Y., SIMIZU, M., SAITO, Y., YURA, H., MATSUI, T., TAKASE, B., HATTORI, H., KANATANI, Y., KIKUCHI, M. & MAEHARA, T. 2005. Efficacy of photocrosslinkable chitosan hydrogel containing fibroblast growth factor-2 in a rabbit model of chronic myocardial infarction. *J Surg Res,* 126**,** 27-33.

FUJIWARA, M., YAN, P., OTSUJI, T. G., NARAZAKI, G., UOSAKI, H., FUKUSHIMA, H., KUWAHARA, K., HARADA, M., MATSUDA, H., MATSUOKA, S., OKITA, K., TAKAHASHI, K., NAKAGAWA, M., IKEDA, T., SAKATA, R., MUMMERY, C. L., NAKATSUJI, N., YAMANAKA, S., NAKAO, K. & YAMASHITA, J. K. 2011. Induction and enhancement of cardiac cell differentiation from mouse and human induced pluripotent stem cells with cyclosporin-A. *PLoS One,* 6**,** e16734.

GARBERN, J. C. & LEE, R. T. 2013. Cardiac stem cell therapy and the promise of heart regeneration. *Cell Stem Cell,* 12**,** 689-98.

GIOVAGNOLI, S., TSAI, T. & DELUCA, P. P. 2010. Formulation and release behavior of doxycycline-alginate hydrogel microparticles embedded into pluronic F127 thermogels as a potential new vehicle for doxycycline intradermal sustained delivery. *AAPS PharmSciTech,* 11**,** 212-20.

GO, A. S., MOZAFFARIAN, D., ROGER, V. L., BENJAMIN, E. J., BERRY, J. D., BORDEN, W. B., BRAVATA, D. M., DAI, S., FORD, E. S., FOX, C. S., FRANCO, S., FULLERTON, H. J., GILLESPIE, C., HAILPERN, S. M., HEIT, J. A., HOWARD, V. J., HUFFMAN, M. D., KISSELA, B. M., KITTNER, S. J., LACKLAND, D. T., LICHTMAN, J. H., LISABETH, L. D., MAGID, D., MARCUS, G. M., MARELLI, A., MATCHAR, D. B., MCGUIRE, D. K., MOHLER, E. R., MOY, C. S., MUSSOLINO, M. E., NICHOL, G., PAYNTER, N. P., SCHREINER, P. J., SORLIE, P. D., STEIN, J., TURAN, T. N., VIRANI, S. S., WONG, N. D., WOO, D., TURNER, M. B., AMERICAN HEART ASSOCIATION STATISTICS, C. & STROKE STATISTICS, S. 2013. Heart disease and stroke statistics--2013 update: a report from the American Heart Association. *Circulation,* 127**,** e6-e245.

GREENBERG, C. S., BIRCKBICHLER, P. J. & RICE, R. H. 1991. Transglutaminases: multifunctional cross-linking enzymes that stabilize tissues. *FASEB J,* 5**,** 3071-7.

GUO, X. M., ZHAO, Y. S., CHANG, H. X., WANG, C. Y., E, L. L., ZHANG, X. A., DUAN, C. M., DONG, L. Z., JIANG, H., LI, J., SONG, Y. & YANG, X. J. 2006. Creation of engineered cardiac tissue in vitro from mouse embryonic stem cells. *Circulation,* 113**,** 2229-37.

HAPPE, C. L. & ENGLER, A. J. 2016. Mechanical Forces Reshape Differentiation Cues That Guide Cardiomyogenesis. *Circ Res,* 118**,** 296-310.

HEINEKE, J., AUGER-MESSIER, M., XU, J., OKA, T., SARGENT, M. A., YORK, A., KLEVITSKY, R., VAIKUNTH, S., DUNCAN, S. A., ARONOW, B. J., ROBBINS, J., CROMBLEHOLME, T. M. & MOLKENTIN, J. D. 2007. Cardiomyocyte GATA4 functions as a stress-responsive regulator of angiogenesis in the murine heart. *J Clin Invest,* 117**,** 3198-210.

HENG, B. C., CAO, T., HAIDER, H. K., WANG, D. Z., SIM, E. K. & NG, S. C. 2004. An overview and synopsis of techniques for directing stem cell differentiation in vitro. *Cell Tissue Res,* 315**,** 291-303.

HIDALGO-BASTIDA, L. A., BARRY, J. J., EVERITT, N. M., ROSE, F. R., BUTTERY, L. D., HALL, I. P., CLAYCOMB, W. C. & SHAKESHEFF, K. M. 2007. Cell adhesion and mechanical properties of a flexible scaffold for cardiac tissue engineering. *Acta Biomater,* 3**,** 457-62.

HIRANO S, M. C., YAMAGUCHI R, MIURA O v. Formation of the Polyelectrolyte Complexes of Some Acidic Glycoasaminoglycans with partially N -Acetylated Chitosans. *Biopolymers,* 17**,** 805-810.

HODDE, J. 2002. Naturally occurring scaffolds for soft tissue repair and regeneration. *Tissue Eng,* 8**,** 295-308.

HONG, J. K. & MADIHALLY, S. V. 2010. Three-dimensional scaffold of electrosprayed fibers with large pore size for tissue regeneration. *Acta Biomaterialia,* 6**,** 4734-4742.

HONG, J. K. & MADIHALLY, S. V. 2011. Next generation of electrosprayed fibers for tissue regeneration. *Tissue Eng Part B Rev,* 17**,** 125-42.

HONG, Y., SONG, H., GONG, Y., MAO, Z., GAO, C. & SHEN, J. 2007. Covalently crosslinked chitosan hydrogel: properties of in vitro degradation and chondrocyte encapsulation. *Acta Biomater,* 3**,** 23-31.

HUANG, Y., ONYERI, S., SIEWE, M., MOSHFEGHIAN, A. & MADIHALLY, S. V. 2005. In vitro characterization of chitosan-gelatin scaffolds for tissue engineering. *Biomaterials,* 26**,** 7616-27.

HUANG, Y., SIEWE, M. & MADIHALLY, S. V. 2006. Effect of spatial architecture on cellular colonization. *Biotechnol Bioeng,* 93**,** 64-75.

HUSSAIN, A., COLLINS, G., YIP, D. & CHO, C. H. 2013. Functional 3-D cardiac co-culture model using bioactive chitosan nanofiber scaffolds. *Biotechnol Bioeng,* 110**,** 637-47.

HWANG, N. S., VARGHESE, S. & ELISSEEFF, J. 2008. Controlled differentiation of stem cells. *Adv Drug Deliv Rev,* 60**,** 199-214.

IACOBELLIS, G. 2009. *Obesity and cardiovascular disease,* Oxford ; New York, Oxford University Press.

IYER, P., WALKER, K. J. & MADIHALLY, S. V. 2012. Increased matrix synthesis by fibroblasts with decreased proliferation on synthetic chitosan-gelatin porous structures. *Biotechnol Bioeng,* 109**,** 1314-25.

JONES, M. E. R. & MESSERSMITH, P. B. 2007. Facile coupling of synthetic peptides and peptide-polymer conjugates to cartilage via transglutaminase enzyme. *Biomaterials,* 28**,** 5215-5224.

JOSEPH, D., LANIER, T. C. & HAMANN, D. D. 1994. Temperature and pH affect transglutaminase-catalyzed "setting" of crude fish actomyosin. *Journal of Food Science,* 59**,** 1018-1023, 1036.

KEEFER, C. L. & DESAI, J. P. 2011. Mechanical phenotyping of stem cells. *Theriogenology,* 75**,** 1426-30.

KERN, S., EICHLER, H., STOEVE, J., KLUTER, H. & BIEBACK, K. 2006. Comparative analysis of mesenchymal stem cells from bone marrow, umbilical cord blood, or adipose tissue. *Stem Cells,* 24**,** 1294-301.

KHOR, E. & LIM, L. 2003. Implantable applications of chitin and chitosan. *BIOMATERIALS,* 24**,** 2339-2349.

KIKUCHI Y, N. A. 1976. Polyelectrolyte Complexes of Heparin with Chitosan. *J Applied Polymer Science,* 20**,** 2561-2563.
KIM, B. S. & MOONEY, D. J. 2000. Scaffolds for engineering smooth muscle under cyclic mechanical strain conditions. *J Biomech Eng,* 122**,** 210-5.
KOCHANEK, K. D., XU, J., MURPHY, S. L., MINIÑO, A. M. & KUNG, H.-C. 2011. National vital statistics reports. *National Vital Statistics Reports,* 59**,** 1.
KONSTANTINIDIS, K., WHELAN, R. S. & KITSIS, R. N. 2012. Mechanisms of cell death in heart disease. *Arterioscler Thromb Vasc Biol,* 32**,** 1552-62.
KRISTIANSEN, A., VARUM, K. M. & GRASDALEN, H. 1998. The interactions between highly de-N-acetylated chitosans and lysozyme from chicken egg white studied by 1H-NMR spectroscopy. *Eur J Biochem,* 251**,** 335-42.
KURDI, M., CHIDIAC, R., HOEMANN, C., ZOUEIN, F., ZGHEIB, C. & BOOZ, G. W. 2010. Hydrogels as a platform for stem cell delivery to the heart. *Congest Heart Fail,* 16**,** 132-5.
LAFLAMME, M. A. & MURRY, C. E. 2011. Heart regeneration. *Nature,* 473**,** 326-35.
LAHIJI, A., SOHRABI, A., HUNGERFORD, D. S. & FRONDOZA, C. G. 2000. Chitosan supports the expression of extracellular matrix proteins in human osteoblasts and chondrocytes. *J Biomed Mater Res,* 51**,** 586-95.
LAWRENCE, B. J., MAASE, E. L., LIN, H. K. & MADIHALLY, S. V. 2009. Multilayer composite scaffolds with mechanical properties similar to small intestinal submucosa. *J Biomed Mater Res A,* 88**,** 634-43.
LEE, J. M. & BOUGHNER, D. R. 1985. Mechanical properties of human pericardium. Differences in viscoelastic response when compared with canine pericardium. *Circ Res,* 57**,** 475-81.
LEOR, J., AMSALEM, Y. & COHEN, S. 2005. Cells, scaffolds, and molecules for myocardial tissue engineering. *Pharmacol Ther,* 105**,** 151-63.
LI, X., YU, X., LIN, Q., DENG, C., SHAN, Z., YANG, M. & LIN, S. 2007. Bone marrow mesenchymal stem cells differentiate into functional cardiac phenotypes by cardiac microenvironment. *Journal of Molecular and Cellular Cardiology,* 42**,** 295-303.
LI, Z. & GUAN, J. 2011. Hydrogels for Cardiac Tissue Engineering. *Polymers,* 3**,** 740-761.
LI, Z., RAMAY, H. R., HAUCH, K. D., XIAO, D. & ZHANG, M. 2005. Chitosan-alginate hybrid scaffolds for bone tissue engineering. *Biomaterials,* 26**,** 3919-28.
LIM, L.-T., MINE, Y. & TUNG, M. A. 1999. Barrier and tensile properties of transglutaminase cross-linked gelatin films as affected by relative humidity, temperature, and glycerol content. *Journal of Food Science* 64**,** 616-622.
LINDROOS, B., SUURONEN, R. & MIETTINEN, S. 2011. The potential of adipose stem cells in regenerative medicine. *Stem Cell Rev,* 7**,** 269-91.
LIU, J., XIONG, W., BACA-REGEN, L., NAGASE, H. & BAXTER, B. T. 2003. Mechanism of inhibition of matrix metalloproteinase-2 expression by doxycycline in human aortic smooth muscle cells. *J Vasc Surg,* 38**,** 1376-83.
LIU, Y., KOPELMAN, D., WU, L. Q., HIJJI, K., ATTAR, I., PREISS-BLOOM, O. & PAYNE, G. F. 2009. Biomimetic sealant based on gelatin and microbial transglutaminase: An initial in vivo investigation. *Journal of Biomedical Materials Research Part B: Applied Biomaterials,* 91B**,** 5-16.

MADIHALLY, S. & MATTHEW, H. 1999a. Porous chitosan scaffolds for tissue engineering. *BIOMATERIALS,* 20**,** 1133-1142.
MADIHALLY, S. V. & MATTHEW, H. W. 1999b. Porous chitosan scaffolds for tissue engineering. *Biomaterials,* 20**,** 1133-42.
MAKOWSKI, G. S. & RAMSBY, M. L. 1998. Identification and partial characterization of three calcium- and zinc-independent gelatinases constitutively present in human circulation. *Biochem Mol Biol Int,* 46**,** 1043-53.
MCDERMOTT, M. K., CHEN, T., WILLIAMS, C. M., MARKLEY, K. M. & PAYNE, G. F. 2004. Mechanical properties of biomimetic tissue adhesive based on the microbial transglutaminase-catalyzed crosslinking of gelatin. *Biomacromolecules,* 5**,** 1270-9.
MEMBERS, W. G., ROGER, V. L., GO, A. S., LLOYD-JONES, D. M., BENJAMIN, E. J., BERRY, J. D., BORDEN, W. B., BRAVATA, D. M., DAI, S., FORD, E. S., FOX, C. S., FULLERTON, H. J., GILLESPIE, C., HAILPERN, S. M., HEIT, J. A., HOWARD, V. J., KISSELA, B. M., KITTNER, S. J., LACKLAND, D. T., LICHTMAN, J. H., LISABETH, L. D., MAKUC, D. M., MARCUS, G. M., MARELLI, A., MATCHAR, D. B., MOY, C. S., MOZAFFARIAN, D., MUSSOLINO, M. E., NICHOL, G., PAYNTER, N. P., SOLIMAN, E. Z., SORLIE, P. D., SOTOODEHNIA, N., TURAN, T. N., VIRANI, S. S., WONG, N. D., WOO, D. & TURNER, M. B. 2012. Heart Disease and Stroke Statistics—2012 Update: A Report From the American Heart Association. *Circulation,* 125**,** e2-e220.
MENASCHE, P. 2011a. Cardiac cell therapy: lessons from clinical trials. *J Mol Cell Cardiol,* 50**,** 258-65.
MENASCHE, P. 2011b. [The heart]. *Bull Acad Natl Med,* 195**,** 1669-76.
MENDIS, S., PUSKA, P., NORRVING, B., WORLD HEALTH ORGANIZATION., WORLD HEART FEDERATION. & WORLD STROKE ORGANIZATION. 2011. *Global atlas on cardiovascular disease prevention and control,* Geneva, World Health Organization in collaboration with the World Heart Federation and the World Stroke Organization.
MI, F. L., TAN, Y. C., LIANG, H. F. & SUNG, H. W. 2002. In vivo biocompatibility and degradability of a novel injectable-chitosan-based implant. *Biomaterials,* 23**,** 181-91.
MIZUNO, K., YAMAMURA, K., YANO, K., OSADA, T., SAEKI, S., TAKIMOTO, N., SAKURAI, T. & NIMURA, Y. 2003. Effect of chitosan film containing basic fibroblast growth factor on wound healing in genetically diabetic mice. *J Biomed Mater Res,* 64**,** 177-81.
MORONI, F. & MIRABELLA, T. 2014. Decellularized matrices for cardiovascular tissue engineering. *Am J Stem Cells,* 3**,** 1-20.
MUNDARGI, R. C., SRIRANGARAJAN, S., AGNIHOTRI, S. A., PATIL, S. A., RAVINDRA, S., SETTY, S. B. & AMINABHAVI, T. M. 2007. Development and evaluation of novel biodegradable microspheres based on poly(d,l-lactide-co-glycolide) and poly(epsilon-caprolactone) for controlled delivery of doxycycline in the treatment of human periodontal pocket: in vitro and in vivo studies. *J Control Release,* 119**,** 59-68.

MURAKAMI, H., KOBAYASHI, M., TAKEUCHI, H. & KAWASHIMA, Y. 1999. Preparation of poly(DL-lactide-co-glycolide) nanoparticles by modified spontaneous emulsification solvent diffusion method. *Int J Pharm,* 187**,** 143-52.

NEWBY, A. C. 2012. Matrix metalloproteinase inhibition therapy for vascular diseases. *Vascul Pharmacol,* 56**,** 232-44.

NGOENKAM, J., FAIKRUA, A., YASOTHORNSRIKUL, S. & VIYOCH, J. 2010. Potential of an injectable chitosan/starch/beta-glycerol phosphate hydrogel for sustaining normal chondrocyte function. *International Journal of Pharmaceutics,* 391**,** 115-24.

OH, S. H., WARD, C. L., ATALA, A., YOO, J. J. & HARRISON, B. S. 2009. Oxygen generating scaffolds for enhancing engineered tissue survival. *Biomaterials,* 30**,** 757-62.

OLIVETTI, G., MELISSARI, M., CAPASSO, J. M. & ANVERSA, P. 1991. Cardiomyopathy of the aging human heart. Myocyte loss and reactive cellular hypertrophy. *Circ Res,* 68**,** 1560-8.

PAGE, J. P. 1999. Heart attack treatments. *JAMA,* 282.

PASCUAL-GIL, S., GARBAYO, E., DÍAZ-HERRÁEZ, P., PROSPER, F. & BLANCO-PRIETO, M. J. 2015. Heart regeneration after myocardial infarction using synthetic biomaterials. *Journal of Controlled Release,* 203**,** 23-38.

PIERELLI, L., BONANNO, G., RUTELLA, S., MARONE, M., SCAMBIA, G. & LEONE, G. 2001. CD105 (endoglin) expression on hematopoietic stem/progenitor cells. *Leuk Lymphoma,* 42**,** 1195-206.

PIJNAPPELS, D. A., SCHALIJ, M. J., RAMKISOENSING, A. A., VAN TUYN, J., DE VRIES, A. A., VAN DER LAARSE, A., YPEY, D. L. & ATSMA, D. E. 2008. Forced alignment of mesenchymal stem cells undergoing cardiomyogenic differentiation affects functional integration with cardiomyocyte cultures. *Circ Res,* 103**,** 167-76.

RAFAT, M., LI, F., FAGERHOLM, P., LAGALI, N. S., WATSKY, M. A., MUNGER, R., MATSUURA, T. & GRIFFITH, M. 2008. PEG-stabilized carbodiimide crosslinked collagen–chitosan hydrogels for corneal tissue engineering. *Biomaterials,* 29**,** 3960-3972.

RAGHAVAN, D., KROPP, B. P., LIN, H. K., ZHANG, Y., COWAN, R. & MADIHALLY, S. V. 2005. Physical characteristics of small intestinal submucosa scaffolds are location-dependent. *J Biomed Mater Res A,* 73**,** 90-6.

RAMESH, V. M., BINGHAM, S. E. & WEBBER, A. N. 2011. A simple method for chloroplast transformation in Chlamydomonas reinhardtii. *Methods Mol Biol,* 684**,** 313-20.

RANDALL, O. S. & ROMAINE, D. S. 2005. *The encyclopedia of the heart and heart disease,* New York, NY, Facts on File.

RATAKONDA, S., SRIDHAR, U. M., RHINEHART, R. R. & MADIHALLY, S. V. 2012. Assessing viscoelastic properties of chitosan scaffolds and validation with cyclical tests. *Acta Biomater,* 8**,** 1566-75.

RATNER, B. D. 2004. *Biomaterials science : an introduction to materials in medicine,* Amsterdam ; Boston, Elsevier Academic Press.

RAVANTI, L., HEINO, J., LOPEZ-OTIN, C. & KAHARI, V.-M. 1999. Induction of Collagenase-3 (MMP-13) Expression in Human Skin Fibroblasts by Three-

dimensional Collagen Is Mediated by p38 Mitogen-activated Protein Kinase. *J. Biol. Chem.,* 274**,** 2446-2455.
RAVI KUMAR, M. N. V. 2000. A review of chitin and chitosan applications. *Reactive and Functional Polymers,* 46**,** 1-27.
RICHARDSON, S. M., HUGHES, N., HUNT, J. A., FREEMONT, A. J. & HOYLAND, J. A. 2008. Human mesenchymal stem cell differentiation to NP-like cells in chitosan-glycerophosphate hydrogels. *Biomaterials,* 29**,** 85-93.
RIVA, R., RAGELLE, H., DES RIEUX, A., DUHEM, N., JÉRÔME, C. & PRÉAT, V. 2011. Chitosan and Chitosan Derivatives in Drug Delivery and Tissue Engineering. *In:* JAYAKUMAR, R., PRABAHARAN, M. & MUZZARELLI, R. A. A. (eds.) *Chitosan for Biomaterials II.* Springer Berlin Heidelberg.
ROGER, V. L., GO, A. S., LLOYD-JONES, D. M., BENJAMIN, E. J., BERRY, J. D., BORDEN, W. B., BRAVATA, D. M., DAI, S., FORD, E. S., FOX, C. S., FULLERTON, H. J., GILLESPIE, C., HAILPERN, S. M., HEIT, J. A., HOWARD, V. J., KISSELA, B. M., KITTNER, S. J., LACKLAND, D. T., LICHTMAN, J. H., LISABETH, L. D., MAKUC, D. M., MARCUS, G. M., MARELLI, A., MATCHAR, D. B., MOY, C. S., MOZAFFARIAN, D., MUSSOLINO, M. E., NICHOL, G., PAYNTER, N. P., SOLIMAN, E. Z., SORLIE, P. D., SOTOODEHNIA, N., TURAN, T. N., VIRANI, S. S., WONG, N. D., WOO, D., TURNER, M. B., COMM, A. H. A. S. & SUBCOMM, S. S. 2012. Heart Disease and Stroke Statistics-2012 Update A Report From the American Heart Association. *Circulation,* 125**,** E2-E220.
SAHA, K., POLLOCK, J. F., SCHAFFER, D. V. & HEALY, K. E. 2007. Designing synthetic materials to control stem cell phenotype. *Curr Opin Chem Biol,* 11**,** 381-7.
SANG, Q. X., JIN, Y., NEWCOMER, R. G., MONROE, S. C., FANG, X., HURST, D. R., LEE, S., CAO, Q. & SCHWARTZ, M. A. 2006. Matrix metalloproteinase inhibitors as prospective agents for the prevention and treatment of cardiovascular and neoplastic diseases. *Curr Top Med Chem,* 6**,** 289-316.
SEGERS, V. F. & LEE, R. T. 2008. Stem-cell therapy for cardiac disease. *Nature,* 451**,** 937-42.
SHIGEMASA Y, S. K., SASHIWA H, SAIMOTO H 1994. Enzymatic degradation of chitins and partially deacetylated chitins. *Int J Biol Macromol,* 16**,** 43-49.
SHU, Y., HAO, T., YAO, F., QIAN, Y., WANG, Y., YANG, B., LI, J. & WANG, C. 2015. RoY peptide-modified chitosan-based hydrogel to improve angiogenesis and cardiac repair under hypoxia. *ACS Appl Mater Interfaces,* 7**,** 6505-17.
SIMPSON, D., LIU, H., FAN, T. H., NEREM, R. & DUDLEY, S. C., JR. 2007. A tissue engineering approach to progenitor cell delivery results in significant cell engraftment and improved myocardial remodeling. *Stem Cells,* 25**,** 2350-7.
SLAUGHTER, B. V., KHURSHID, S. S., FISHER, O. Z., KHADEMHOSSEINI, A. & PEPPAS, N. A. 2009. Hydrogels in regenerative medicine. *Adv Mater,* 21**,** 3307-29.
SMITH, G. N., JR., MICKLER, E. A., HASTY, K. A. & BRANDT, K. D. 1999. Specificity of inhibition of matrix metalloproteinase activity by doxycycline: relationship to structure of the enzyme. *Arthritis Rheum,* 42**,** 1140-6.

SONG, K., QIAO, M., LIU, T., JIANG, B., MACEDO, H. M., MA, X. & CUI, Z. 2010. Preparation, fabrication and biocompatibility of novel injectable temperature-sensitive chitosan/glycerophosphate/collagen hydrogels. *J Mater Sci Mater Med,* 21**,** 2835-42.

STECHMILLER, J., COWAN, L. & SCHULTZ, G. 2010. The role of doxycycline as a matrix metalloproteinase inhibitor for the treatment of chronic wounds. *Biol Res Nurs,* 11**,** 336-44.

SU, J., CHEN, X., HUANG, Y., LI, W., LI, J., CAO, K., CAO, G., ZHANG, L., LI, F., ROBERTS, A. I., KANG, H., YU, P., REN, G., JI, W., WANG, Y. & SHI, Y. 2014. Phylogenetic distinction of iNOS and IDO function in mesenchymal stem cell-mediated immunosuppression in mammalian species. *Cell Death Differ,* 21**,** 388-96.

TOMASEK, J. J., HALLIDAY, N. L., UPDIKE, D. L., AHERN-MOORE, J. S., VU, T. K., LIU, R. W. & HOWARD, E. W. 1997. Gelatinase A activation is regulated by the organization of the polymerized actin cytoskeleton. *The Journal of biological chemistry,* 272**,** 7482-7.

TOMIHATA, K. & IKADA, Y. 1997. In vitro and in vivo degradation of films of chitin and its deacetylated derivatives. *Biomaterials,* 18**,** 567-75.

TORMOS, C. J., ABRAHAM, C. & MADIHALLY, S. V. 2015. Improving the stability of chitosan-gelatin-based hydrogels for cell delivery using transglutaminase and controlled release of doxycycline. *Drug Deliv Transl Res,* 5**,** 575-84.

TYAGI, S. C. & JOSHUA, I. G. 2014. Exercise and nutrition in myocardial matrix metabolism, remodeling, regeneration, epigenetics, microcirculation, and muscle. *Can J Physiol Pharmacol,* 92**,** 521-3.

VAN DIJK, A., NIESSEN, H. W., ZANDIEH DOULABI, B., VISSER, F. C. & VAN MILLIGEN, F. J. 2008. Differentiation of human adipose-derived stem cells towards cardiomyocytes is facilitated by laminin. *Cell Tissue Res,* 334**,** 457-67.

VASHI, A. V., WHITE, J. F., MCLEAN, K. M., NEETHLING, W. M. L., RHODES, D. I., RAMSHAW, J. A. M. & WERKMEISTER, J. A. 2015. Evaluation of an established pericardium patch for delivery of mesenchymal stem cells to cardiac tissue. *Journal of Biomedical Materials Research Part A,* 103**,** 1999-2005.

WAAS, E. T., LOMME, R. M., DEGROOT, J., WOBBES, T. & HENDRIKS, T. 2002. Tissue levels of active matrix metalloproteinase-2 and -9 in colorectal cancer. *Br J Cancer,* 86**,** 1876-83.

WALKER, K. J. & MADIHALLY, S. V. 2014. Anisotropic temperature sensitive chitosan-based injectable hydrogels mimicking cartilage matrix. *J Biomed Mater Res B Appl Biomater*.

WAN SAFWANI, W. K. Z., MAKPOL, S., SATHAPAN, S. & CHUA, K. 2012. 5-Azacytidine Is Insufficient For Cardiogenesis In Human Adipose-Derived Stem Cells. *Journal of Negative Results in BioMedicine,* 11**,** 3.

WANG, H. S., HUNG, S. C., PENG, S. T., HUANG, C. C., WEI, H. M., GUO, Y. J., FU, Y. S., LAI, M. C. & CHEN, C. C. 2004. Mesenchymal stem cells in the Wharton's jelly of the human umbilical cord. *Stem Cells,* 22**,** 1330-7.

WANG, L. & STEGEMANN, J. P. 2010. Thermogelling chitosan and collagen composite hydrogels initiated with beta-glycerophosphate for bone tissue engineering. *Biomaterials,* 31**,** 3976-85.

WRITING GROUP, M., LLOYD-JONES, D., ADAMS, R. J., BROWN, T. M., CARNETHON, M., DAI, S., DE SIMONE, G., FERGUSON, T. B., FORD, E., FURIE, K., GILLESPIE, C., GO, A., GREENLUND, K., HAASE, N., HAILPERN, S., HO, P. M., HOWARD, V., KISSELA, B., KITTNER, S., LACKLAND, D., LISABETH, L., MARELLI, A., MCDERMOTT, M. M., MEIGS, J., MOZAFFARIAN, D., MUSSOLINO, M., NICHOL, G., ROGER, V. L., ROSAMOND, W., SACCO, R., SORLIE, P., ROGER, V. L., THOM, T., WASSERTHIEL-SMOLLER, S., WONG, N. D., WYLIE-ROSETT, J., AMERICAN HEART ASSOCIATION STATISTICS, C. & STROKE STATISTICS, S. 2010. Heart disease and stroke statistics--2010 update: a report from the American Heart Association. *Circulation,* 121**,** e46-e215.

YE, Z., ZHOU, Y., CAI, H. & TAN, W. 2011. Myocardial regeneration: Roles of stem cells and hydrogels. *Adv Drug Deliv Rev,* 63**,** 688-97.

YOUNG, D. A., DEQUACH, J. A. & CHRISTMAN, K. L. 2011. Human cardiomyogenesis and the need for systems biology analysis. *Wiley Interdiscip Rev Syst Biol Med,* 3**,** 666-80.

ZANNETTINO, A. C., PATON, S., ARTHUR, A., KHOR, F., ITESCU, S., GIMBLE, J. M. & GRONTHOS, S. 2008. Multipotential human adipose-derived stromal stem cells exhibit a perivascular phenotype in vitro and in vivo. *J Cell Physiol,* 214**,** 413-21.

ZEMSKOV EA, J. A., HANG J, WAGHRAY A, BELKIN AM. 2006. The role of tissue transglutaminase in cell-matrix interactions. *Front Biosci,* 1**,** 1057-76.

ZHU, H., JI, J., LIN, R., GAO, C., FENG, L. & SHEN, J. 2002. Surface engineering of poly(D,L-lactic acid) by entrapment of chitosan-based derivatives for the promotion of chondrogenesis. *J Biomed Mater Res,* 62**,** 532-9.

ZUK, P. A., ZHU, M., MIZUNO, H., HUANG, J., FUTRELL, J. W., KATZ, A. J., BENHAIM, P., LORENZ, H. P. & HEDRICK, M. H. 2001. Multilineage cells from human adipose tissue: implications for cell-based therapies. *Tissue Eng,* 7**,** 211-28.

VITA

Christian Jose Tormos

Candidate for the Degree of

Doctor of Philosophy

Thesis: IMPROVED STEM CELL RETENTION AND MECHANICAL STABILITY IN A CHITOSAN-GELATIN HYDROGEL

Major Field: Chemical Engineering

Biographical:

Personal data: Born on July 17, 1990 in San Juan, Puerto Rico
Married on July 28, 2012

Education:

Completed the requirements for the Doctor of Philosophy in Chemical Engineering at Oklahoma State University, Stillwater, Oklahoma in July, 2016.

Completed the requirements for the Bachelor of Science in Chemical Engineering at Iowa State University Ames, Iowa in May 2012.

Experience:

Teaching Assistant, Oklahoma State University 2012-2016
Undergraduate Research Assistant, Iowa State University 2009-2012
Research experience for undergraduate scholar, University of Massachusetts Amherst 2009

Professional Memberships:

Tissue Engineering & Regenerative Medicine International Society
Society for Biomaterials
American Institute of Chemical Engineers
Omega Chi Epsilon Honorary Society, Mu Chapter.